Temporal development of the contaminant mass discharge at the Østergade transect in Skuldelev

Lemaire, Grégory Guillaume; Bjerg, Poul Løgstrup

Publication date:
2017

Document Version
Publisher's PDF, also known as Version of record

DTU Environment

Temporal development of the contaminant mass discharge at the Østergade transect in Skuldelev

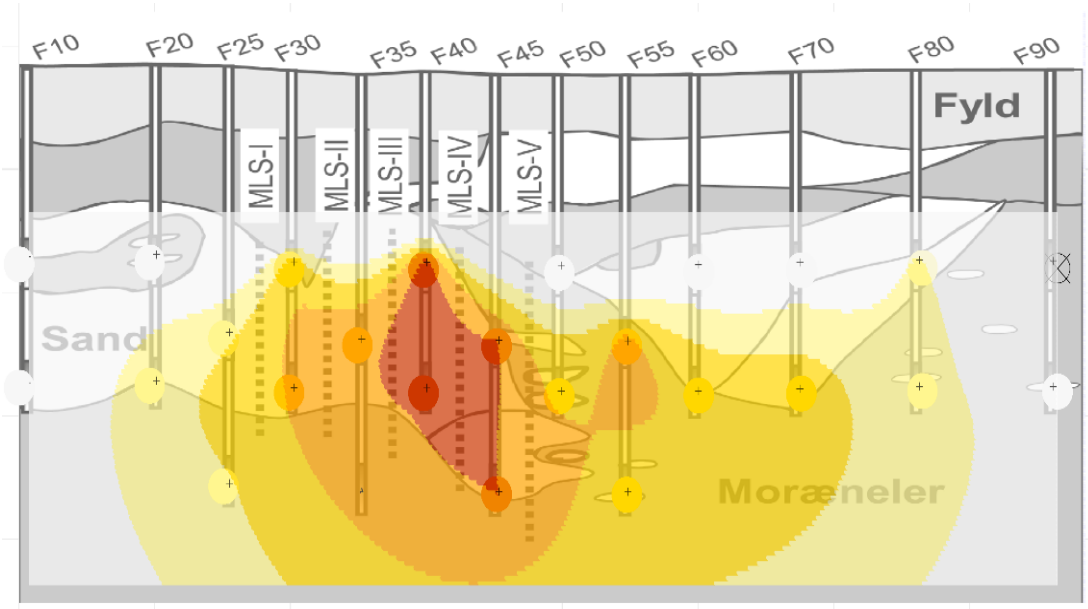

Gregory Lemaire

Poul L. Bjerg

2017

Report
2017

By: Gregory Lemaire
Poul. L. Bjerg

Published by: Department of Environmental Engineering, Bygningstorvet
Request report from: www.sara.env.dtu.dk

Preface

On behalf of Region Hovedstaden, DTU Environment performed an evaluation and contaminant mass discharge determination at Østergade in Skuldelev. The calculation is based on a coherent and systematic use of the chemical and hydrogeological data collected since 2008 by the consulting company, NIRAS, DTU Environment and Region Hovedstaden.

The main objective of this study was to give a coherent estimation of the evolution of the contaminant mass discharge in the upper aquifer for the period 2008-2016. The effect of the different remediation activities in the source area on the plume and the resulting mass discharge is of particular interest.

The following people have participated in the elaboration of this report:
Grégory Lemaire
Poul L. Bjerg

The following people from The Capital Region of Denmark have participated in the steering committee for the project or assisted in the correction of this report:
Henriette Kerrn-Jespersen
Katerina Hantzi
Anne Sivertsen

Finally the following persons have contributed and assisted in collecting the measurement data and information available, for which we are grateful:
Maria H. Hansen, from NIRAS.

Content

Summary

The site of Skuldelev in Denmark is a highly contaminated site, with groundwater pollution by chlorinated solvent originating from multiple hotspots. This site has been investigated for more than ten years now and undergone substantial remedial activities. The study presented here aimed at giving a status of the available data, and a coherent estimation of the evolution of the contaminant mass discharge (CMD) for the period 2008-2016 at the Østergade transect in Skuldelev monitoring the contaminant in the upper aquifer. The calculation is based on a coherent and systematic use of the chemical and hydrogeological data collected since 2008 by different companies and institutions.

For consistency, a standard calculation based on the estimated of Darcy's velocity combined to concentration and discretization of the Østergade transect was proposed for all datasets available for the denominated "F-wells" and "F+MLS" combined. A second method using a data interpolation by kriging method was also performed to ensure that the spatial variations of the concentration data in the transect were accounted for.

The methods are in good agreement and the following conclusions are made:

- A reduction of the contaminant mass discharge is observed at the Østergade transect, especially important during the period 2008-2011 (PCE equivalent). The methods used for this study estimate a 45% to 55% reduction of chlorinated solvents mass discharge between 2009 and 2012.
- This general reduction is observed as a result of the mass reduction achieved in the source area originating from different remediation activities starting in 2006.
- The spatial distribution of the compounds in the transect certainly evolved after 2008 and especially for PCE and TCE. These variations are very likely caused by the remediation in the source area.
- The mass discharge and ratio of chlorinated compounds in the plume also evolved between 2008 and 2016. While PCE and TCE were significantly reduced (and their spatial distribution altered), DCE exhibit a more subtle reduction in mass, while vinyl chloride actually increased steadily. The most recent estimated values are presented in the following table:

Compound	Mass discharge range * February 2016
PCE	[0.02-0.26] kg/year
TCE	[0.05-0.17] kg/year
cisDCE	[0.54-0.79] kg/year
VC	[0.09-0.15] kg/year

*: *dependent on the method and dataset used*

Despite extensive datasets, some of the observations and statements made cannot be fully explained as most of the data collected focused on the source area. Particularly, the evaluation and evolution of redox conditions in the plume and a more thorough water table monitoring

would facilitate the interpretation and the assessment of the variation of contaminant discharge at Østergade.

1. Introduction

1.1 Background

The site of Skuldelev in Denmark is a highly contaminated site, with groundwater pollution by chlorinated solvent originating from multiple hotspots. This site has been investigated for more than 10 years now and undergone substantial remedial activities. In the source area, different remediation technologies have been tested for the different hotspots, mostly by the company NIRAS from 2006. DTU was also involved in the remediation of one hotspot by use of ZVI clay mixing methodology (Fjordboege et al., 2012). Beyond the source area, a contaminant plume formed in the upper aquifer. This plume has also been monitored to evaluate the evolution of the Contaminant Mass Discharge (CMD) and to test different methodologies and devices to estimate this quantity (NIRAS, 2016a). The first contaminant mass discharge evaluation was carried out by DTU on behalf of Region Hovedstaden in 2008 and 2009 (Lange et al., 2011; Troldborg et al., 2012) and was more recently assessed by NIRAS in 2015 and 2016 (Dyreborg and Christensen, 2016).

1.2 Objective of the study

The main objective of the study is to give a status of the data available, and a coherent estimation of the evolution of the contaminant mass discharge for the period 2008-2016 at the Østergade transect in Skuldelev. The effect of the different remediation activities in the source area on the plume and the resulting mass discharge is of particular interest.

1.3 Presentation of the site

Skuldelev is located approximately 5 km west of Roskilde fjord in Denmark. During the period 1968 to 1983, the activities of a metal industry on site resulted in a severe PCE contamination, mostly by disposal through the sewer system. The numerous investigations on site revealed that this contamination is distributed over a total of 6 identified hotpots on site (
Figure 1), and caused severe groundwater contamination as well as indoor air issues in the surrounding dwellings (Figure 1).

The pollution with chlorinated compound reached both the upper and lower aquifer. The general flow direction for the groundwater is east towards Roskilde fjord in both aquifers. The pollution in the upper aquifer resulted in the formation of a contaminant plume extending at least 250 m downgradient from the source. The evolution of the contaminant mass discharge through this upper aquifer is monitored via two transects of monitoring wells, approximately 70 and 200 m downstream. More details and site description can be found in the different consulting reports (NIRAS, 2010; 2016a).

The transect of interest for the evaluation of the contaminant mass discharge is the Østergade transect, visible on
Figure **1** below.

1.4 Presentation of the investigated transect

The investigated transect is located approximately 70 m east of the hotspot areas. It extends in a north-south direction along Østergade over a distance of approximately 80 m. Several types of monitoring wells have been installed over the period 2008-2016 with the associated screens located at elevations ranging from -2 to 4 m (DVR90): F-wells with 1 m long screens, multilevel samplers (0.25 m span between wells), and S-wells with 0.2 m long screens. For this project, only the F-wells and MLS as shown on Figure 2 will be used as the S wells were installed relatively recently and therefore could not provide useful data in the early years.

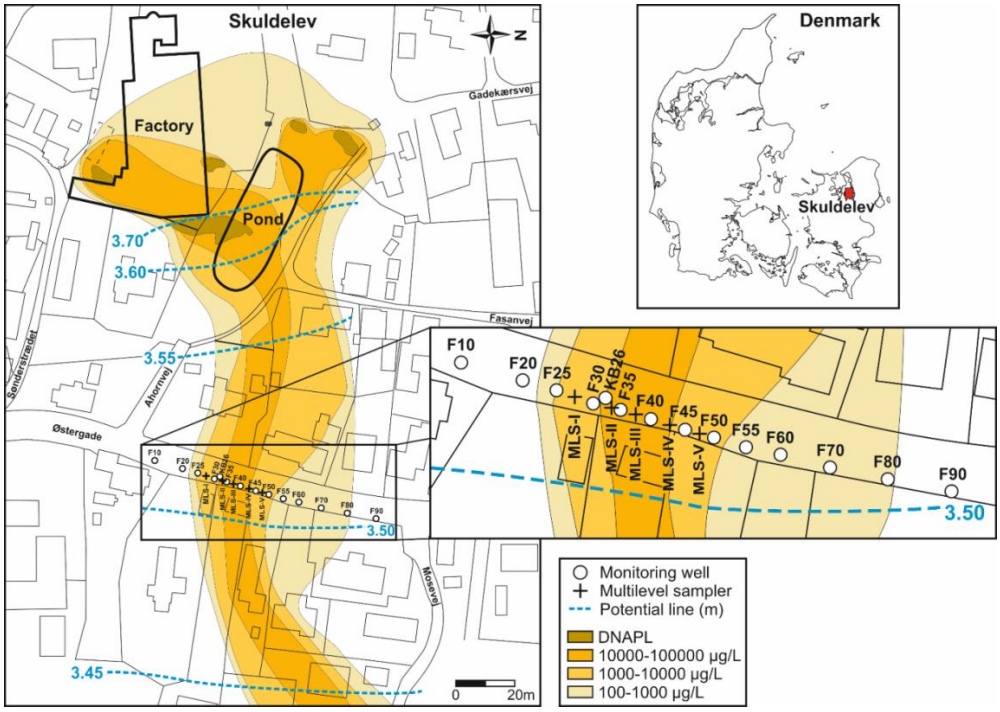

Figure 1. Skuldelev site. Sum of chlorinated compounds contaminant in the upper aquifer and location of Østergade transect
Reproduced from Troldborg et al. (2016)

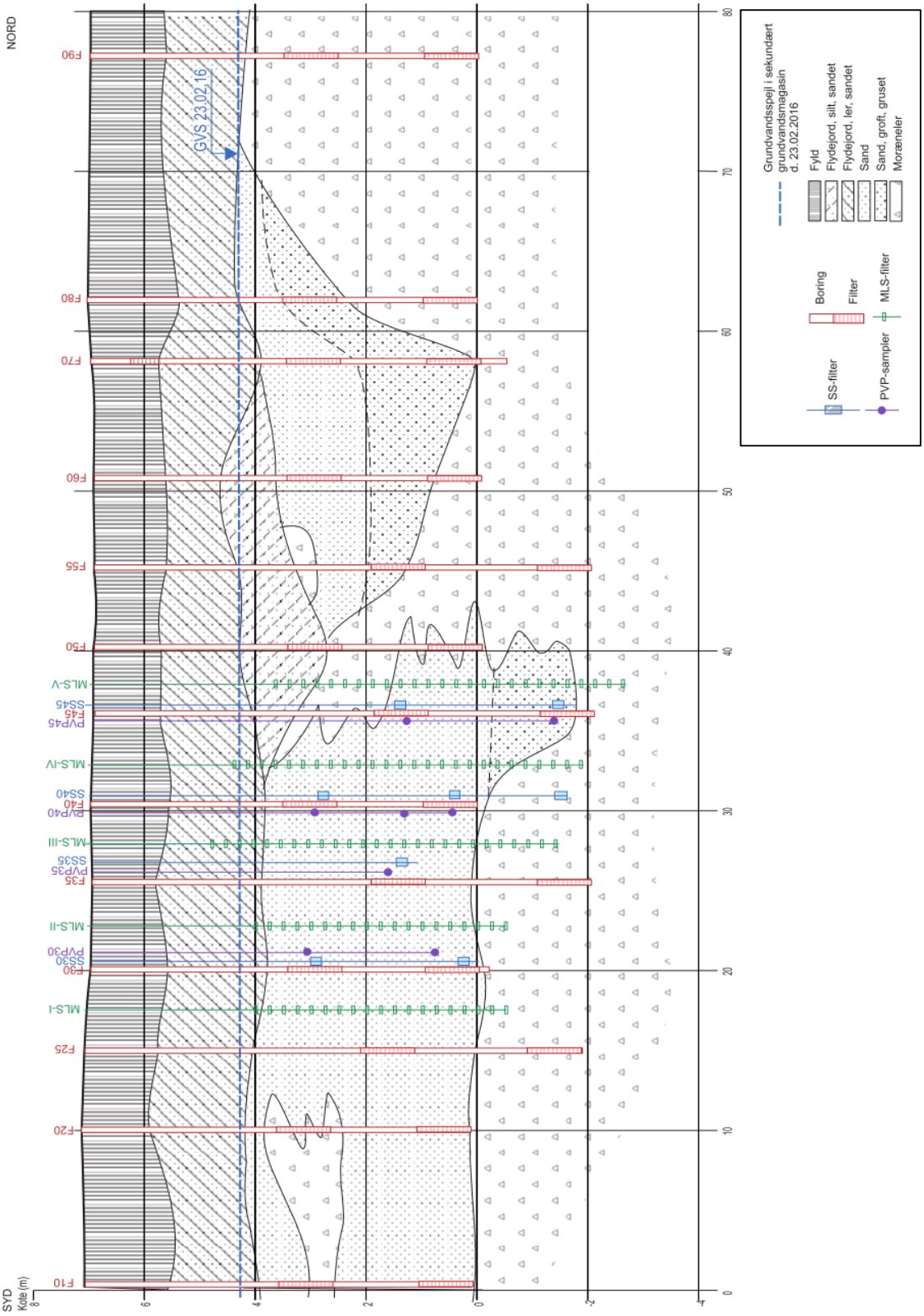

Figure 2: Østergade transect, showing the different screen locations
Reproduced from Dyreborg and Christensen (2016)
(Note: location of well F80 is erroneous)

2. Measurement data overview

This section aims at presenting all the data available and measured since 2008, and is useful for the current objective of estimation of the contaminant mass discharge through the Østergade transect.

2.1 Hydraulic conductivity

A first estimation of the hydraulic conductivity in the Østergade transect was provided by empirical analytical formulations both for the aquifer and underlying clay till based on the soil material properties and grain sizes collected during the drilling of boreholes in 2008 (Lange et al., 2011). These data are used in the later calculations in this report in order to obtain results consistent with the 2008 results for the contaminant mass discharge.

Several measurements were performed later on by slug test and Hydraulic Profiling Tool (HPT) with focus in the transect area where the highest concentrations were observed (i.e. approximately between well F30 and F50). The slug tests were performed twice for different wells, once for a selection of F-wells and another round for the newly installed S-wells. Corresponding data are presented in Appendix A (for the analytical data, only the estimations in the upper aquifer are plotted). In 2016, the measured hydraulic conductivity values ranged from 3.5e-5 m/s to a maximum of 62e-5 m/s, i.e. approximately 3 to 54 m/day (Dyreborg and Christensen, 2016). This data was used for comparison and relevance of the estimated hydraulic conductivity by analytical formulation (the spatial and temporal coverage of this measured dataset being insufficient)

Table 1. Available data on hydraulic conductivity in transect and basic statistical quantities

Available dataset			Summary values		Reference
Year	Month	Remark	Average [m/s]	Standard dev. [m/s]	
2008	/	Analytical formulation(1)	$5.2e^{-5}$	$5.6e^{-5}$	(Lange et al. 2011)
2016	February	Slug test / F-wells	$7.9e^{-5}$	$10e^{-5}$	(NIRAS, 2016a)
2016	February	Slug test / S-wells	$1.9e^{-4}$	$2.3e^{-4}$	(NIRAS, 2016a)

(1) Calculated from grain size distribution based empirical formulas

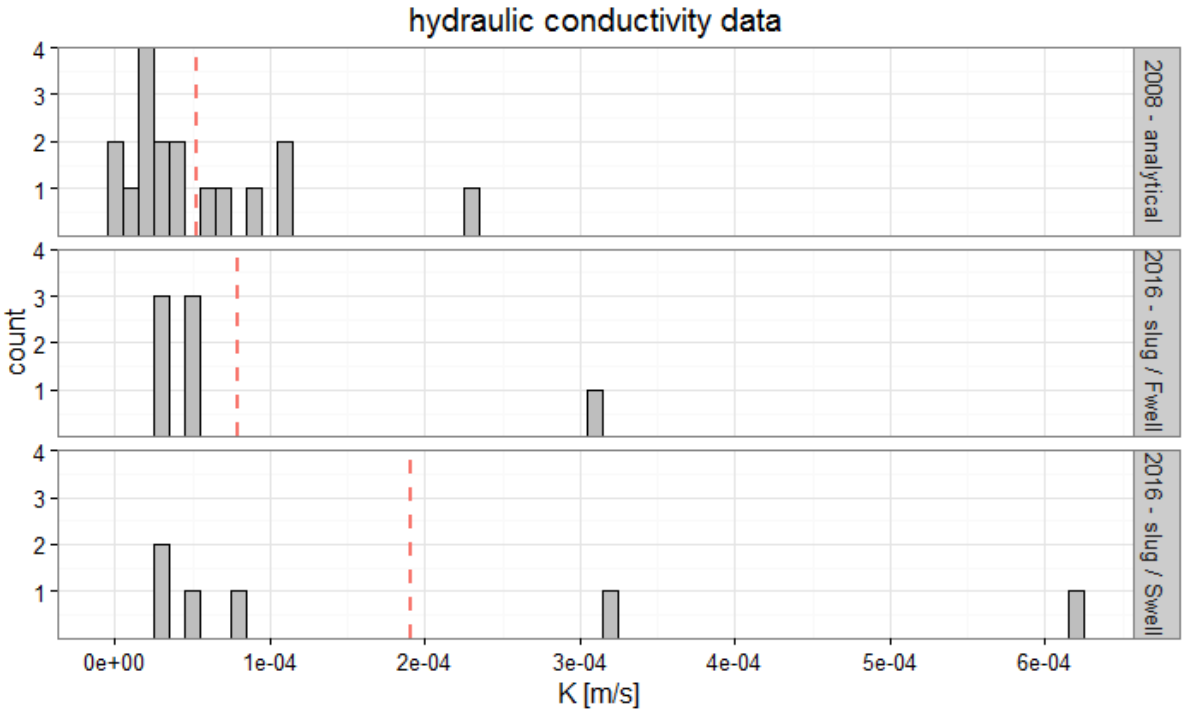

Figure 3. Count histogram of available hydraulic conductivity data
bin width=1e-5 m/s, average marked in dashed red line
Analytical data: upper aquifer data only

2.2 Hydraulic gradient

An evaluation of the hydraulic gradient and a general flow direction in the upper aquifer was conducted by discrete measurements of the water table height at relevant monitoring wells. The data available suggest four campaigns between 2008 to 2009, and one in 2016 (Table 2). Some water table monitoring activities were performed at different time periods, but only cover periods of a few months and not the overall [2008-2016] interval. It was not possible to establish consistent water level measurements in enough boreholes for a calculation of the hydraulic gradient for the entire period.

As mentioned in section 1.3, the groundwater flow direction in the upper aquifer is east, and values for the hydraulic gradient ranged from a minimum of 1.5 ‰ to a maximum value of 3.0 ‰ for the different measurement periods (NIRAS, 2016a).

Table 2. Available data on hydraulic gradient in transect and basic statistical quantities

Available dataset			Summary values			Reference
Year	Month	Remark	Values [‰]	Average [‰]	Standard dev. [‰]	
2008	October		1.6	1.6	/	(NIRAS, 2010)
2009	January		2.1	2.2	0.7	(NIRAS, 2010)
	May		1.5			(NIRAS, 2010)
	July		3.0			(NIRAS, 2010)
2016	February		2.0	2.0	/	(NIRAS, 2016)

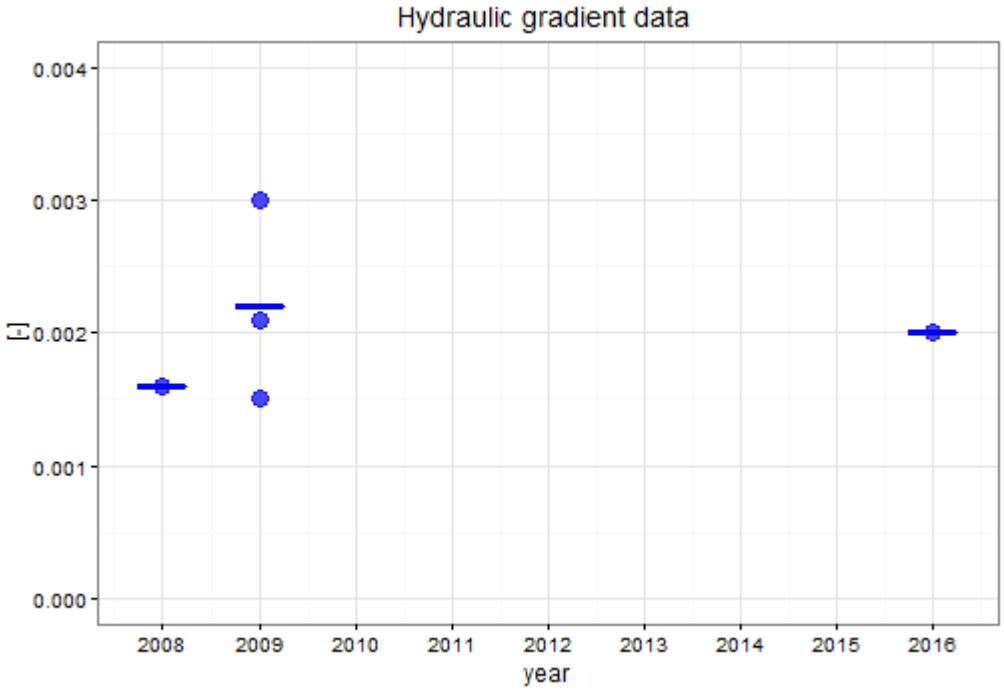

Figure 4. Scatterplot of hydraulic gradient data
bar marker: average data - round marker: dataset value

2.3 Contaminant mass in the source area

The evolution of remaining contaminant mass with time is here inferred by use of the provided estimate of mass removed from the different remediation activities (NIRAS, 2016a; Hansen, 2016). The corresponding data can be found in the risk assessment report by NIRAS (2016a) and Hansen (2016). It is important to keep in mind the mass estimate presented here corresponds to the mass potentially transported within the investigated plume in the upper aquifer towards east. Most of the remediation targeted the mother compound PCE and no precise mass estimate is available for the degradation products already present, nor for the products that may have formed by enhanced degradation due to these activities. Figure 5 presents the evolution of the contaminant mass with time on a yearly basis, in parallel of the different remediation activities.

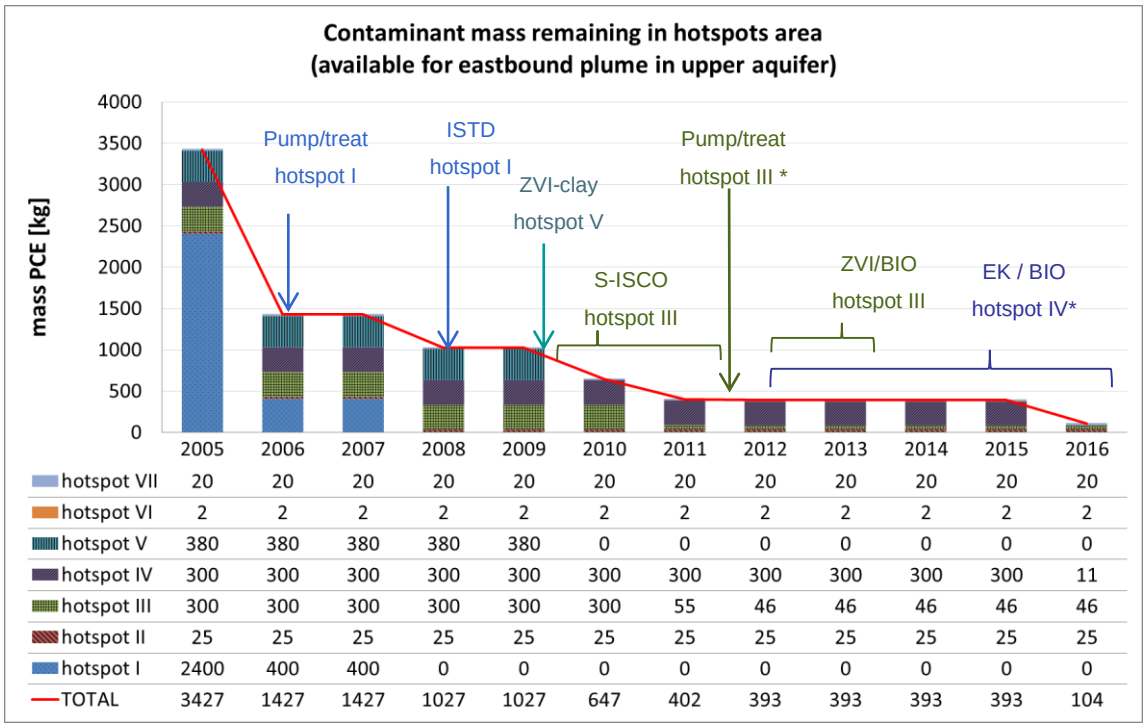

Figure 5. Evolution of the PCE contaminant mass in the source area
Graphic based on the estimation of mass removal by different remediation activities provided by Hansen (2016), reported in Appendix B
(*) : removal reported as PCE and degradation products.

2.4 Contaminant concentration in the transect

Chemical analysis of the groundwater was performed in the transect at different periods from 2008 to 2016. Water was sampled via the F-wells from the very beginning, with additional measurements using the MLS lines from 2009, and S wells from 2015. The chemical analyses were performed by different laboratories and entities during the overall period 2008-2016 (DTU laboratory, ALS, Eurofins). The most recent analyses were carried out by Eurofins. A comparison between the results from the two laboratory ALS and Eurofins was performed in October 2015 (from discussion with NIRAS), and the DTU data was also compared with Eurofins back in 2008.

An overview by boxplot of the concentration data per year is given in Figure 6 below for F-wells and MLS sampling only. The concentration is expressed in PCE eq, i.e. all moles of chlorinated compounds are converted in an equivalent mass of PCE. Summary values are given in Table 3 and Table 4.

Table 3. Available concentration data in transect and associated statistical quantities: F wells Expressed in PCE eq.

Available dataset			Summary values		Reference
Year	Month	Remark	Average [µg/L]	Standard dev. [µg/L]	
2008	July		6070	11689	(Lange et al., 2011)
	August				
	December				
2009	March		5181	10899	(Lange et al., 2011)
	July				
	November				
2012	November		2585	5288	NIRAS data summary xls document
2015	January		2358	5192	NIRAS data summary xls document
	September				
2016	February		2671	5797	(NIRAS, 2016a)

Table 4. Available concentration data in transect and associated statistical quantities: MLS wells Expressed in PCE eq.

Available dataset			Summary values		Reference
Year	Month	Remark	Average [µg/L]	Standard dev. [µg/L]	
2009	March		10088	10067	(Lange et al., 2011)
	July				
	November				
2015	September		4963	5069	NIRAS data summary xls document
2016	February		4596	5912	(NIRAS, 2016a)

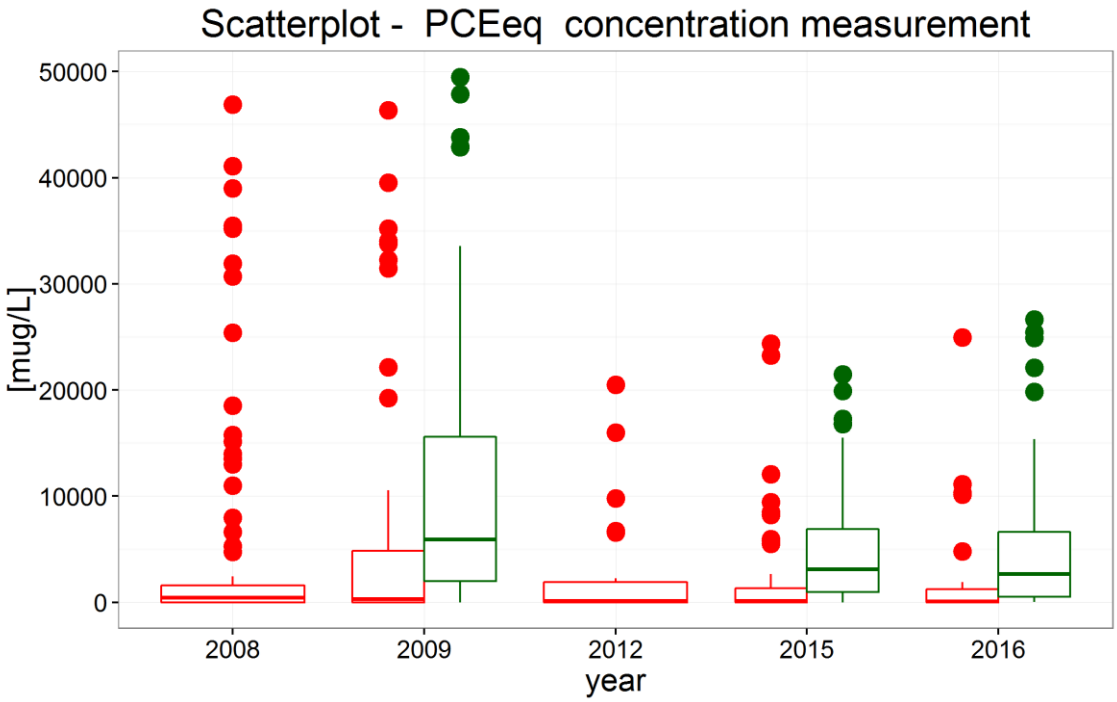

Figure 6. Boxplot of contaminant concentration data
Red: F-wells monitoring / Green: MLS monitoring
Concentration in PCEeq

The spread of data is important with extremely high concentration values estimated around 50 mg/L PCE eq in 2008 and 2009. From 2012, the measured concentrations seem generally lower as it can be seen from the outliers on the boxplot and the significantly different geometric average.

The high concentrations are mostly measured in the area between well F30 and well F45, relatively independently of the considered period, as illustrated below with plots of measurement data from 2008 and 2016 (a similar visualization of all measurement data and compounds is provided in Appendix C).

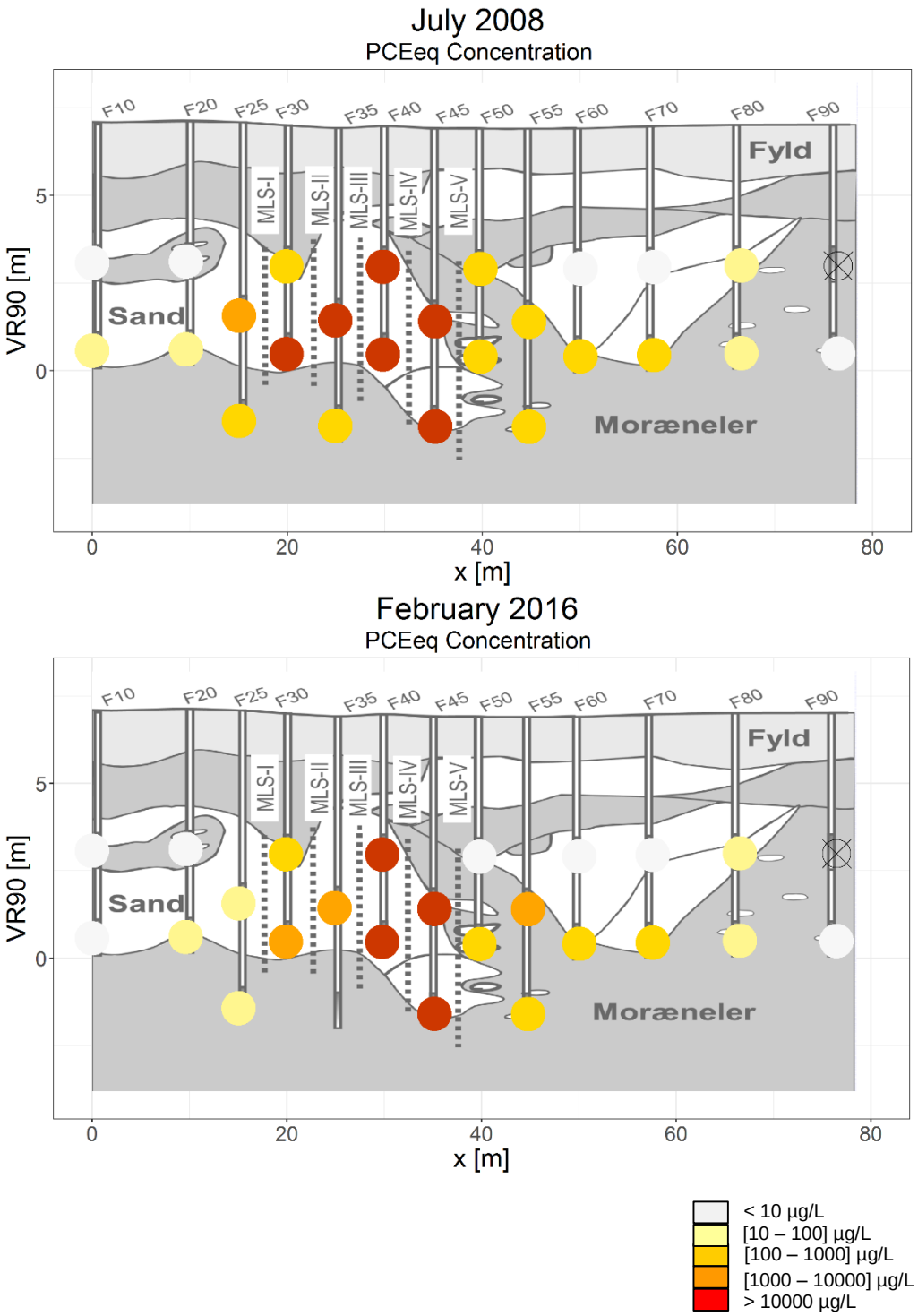

Figure 7. Contaminant concentration comparison for two measurement periods: 2008 and 2016

Highest concentrations found between well F30 and F45

Upper figure : July 2008 / Lower figure : February 2016

2.5 Redox conditions

The redox conditions in the contaminant plume are directly influencing the contaminant mass and products present and detected in the transect.

During the period of interest, most of the activities on site focused on the source area remediation and characterisation of the mass discharge in the Østergade transect. At the present time, the redox conditions in the contaminant plume have only been evaluated in the transect by measurement of redox-sensitive species in 2008 (Lange et al. 2011). At that time, The Østergade transect was characterized by iron to nitrate reduced conditions (Figure 8). Closer to the source (upstream Østergade transect), the conditions were evaluated as more reduced, i.e. nitrate-reducing to methanogenic (not shown, see Lange et al.(2011) for more details).

Some measurements of redox sensitive species also exist for the more recent measurement periods but only in precise locations of the source area in connection with the remediation activities (internal communication with NIRAS). In the recent years, only redox potential were measured in the Østergade transect.

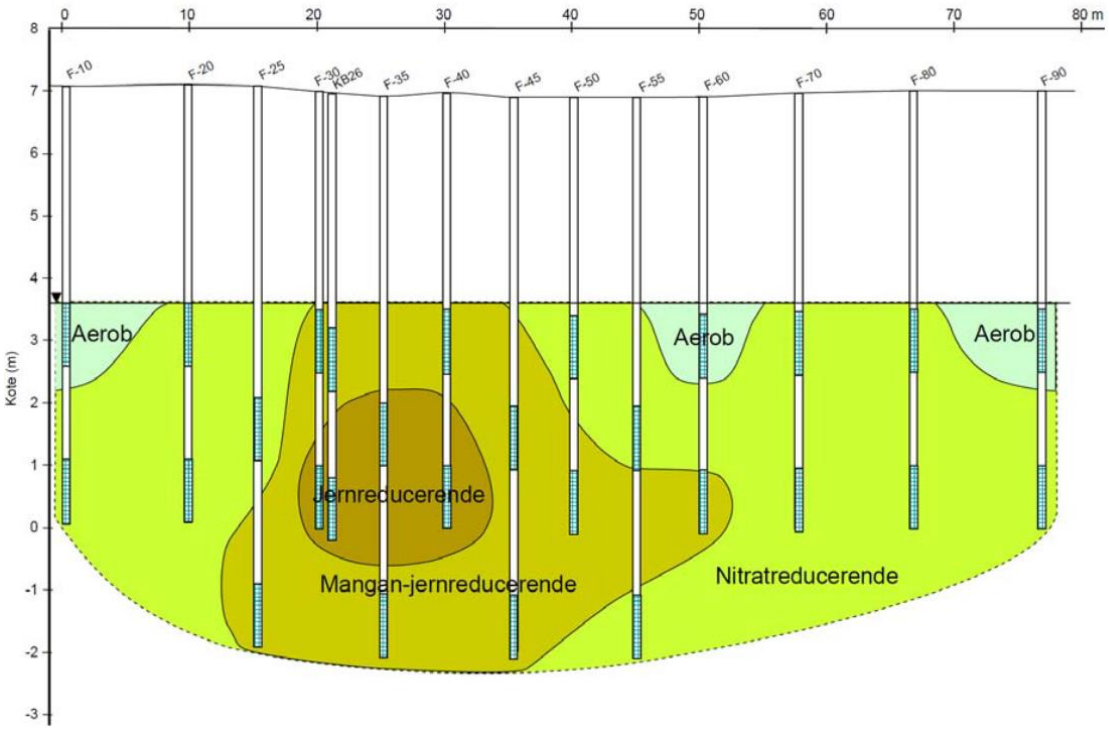

Figure 8. Evaluation of redox condition in the plume – Ny Østerbrogade transect Reproduced from (Lange et al., 2011)

3. Evaluation of contaminant mass discharge

3.1 Methodology

In order to follow the temporal evolution of the contaminant mass discharge (CMD) through the investigated transect, a consistent treatment for each dataset is required. A standard method is chosen after consideration of the available data, i.e. combination of Darcy's velocity measured concentration over a defined surface partitioning as formulated below:

$$J = \sum_{i=1}^{n} A_i * C_i * q \qquad \text{Eq. (1)}$$

With J : contaminant mass discharge [M/T], A_i area of subsurface I [L^2], C_i contaminant concentration [M/L^3], q Darcy's velocity [L/T].

All the work is performed using R software (v 3.1.1) and dedicated packages for statistical and geostatistical analyses.

Two approaches were implemented:

- Method 1 (standard): The contaminant mass discharge calculation is performed using the same calculation parameters used in the initial estimate performed in 2008, i.e. constant hydraulic conductivity throughout the section, constant hydraulic gradient and identical sub surfaces partitioning (Lange et al., 2011). The main parameter values are presented in Table 5. Sub-surface partitioning can be visualized in Appendix D.

Table 5. Main calculation parameters for CMD estimation
Method 1: discrete measurements of concentration and constant hydraulic conductivity

Parameters	Value	Remark
K [m/day]	2.4	Estimate 2008 (Lange et al., 2011)
Hydraulic gradient	0.002	Last estimate, February 16 (NIRAS, 2016)
Overall section [m^2]	380	
Number of subsurfaces [F-wells]	26	See partitioning in Appendix D
Number of subsurfaces [F+MLS combined]	124	See partitioning in Appendix D

- Method 2 (data interpolation): The spatial dependence of the hydraulic gradient and concentration data is accounted for by use of a kriging method and consequent interpolation of the data over a refined grid. Details about the data interpolation and kriging method can be found in Appendix F.

Table 6. Main calculation parameters for CMD estimation

Method 2: concentration and hydraulic conductivity interpolation

Parameters	Value	Remark
K [m/day]	Variable	Kriging method for interpolation
Hydraulic gradient	0.002	Assumed constant
Overall section [m^2]	-	
Number of subsurfaces [Fwells]		Mesh resolution : 10 cm
Number of subsurfaces [F+MLS combined]		Mesh resolution : 10 cm

3.2 Assumptions for contaminant mass discharge calculation

Only the concentration data retrieved from F-wells and MLS wells will be employed, as they were the ones measured during the period from 2008 to 2016.

The concentration for particular points at certain measurement periods were actually not available, e.g. no contamination was detected or no water to sample. For the sake of comparison, the same assumption to handle these cases is required. The guidelines for the assumptions about the calculation are presented below, while a detailed description can be found in Appendix E.

- When the measured concentration for a given compound is under the detection limit, the resulting flux is assumed negligible and forced to zero, especially considering the magnitude of the flux in the sub-surfaces with high concentrations (several orders of magnitude higher).
- When the concentration was not measured, two approaches were used depending on the well type:. For the F-wells, the stable spatial distribution highlighted previously is used. The ratio between the concentration measurement at the closest wells and at the closest measurement period is used to estimate the missing data (Table 13, in Appendix E). For the MLS wells and as the spacing between points is small, the missing data is estimated by averaging the data with the well right above and below or using the same methodology as the F-wells for the deepest wells (Table 14, in Appendix E).
- Depending on the measurement period, some of the upper wells of the MLS could not be sampled due to water table lower than the well locations. Consequently these wells were excluded from all calculation periods for consistency, after making sure the concentrations were not significant if excluded (Table 16, in Appendix E).

The data interpolation by kriging method employed in method 2 assumed a general geological anisotropy of the soil and upper aquifer, based on the deposited nature of the soil. Concentration and hydraulic conductivity data are interpolated over a 10 cm grid. Detail assumptions and validation case of the data interpolation can be found in Appendix F.

3.3 Result quantities and units

Most of the result in the next section will be assessed by use of a PCE equivalent units, which corresponds to a conversion of all moles of chlorinated compounds present into PCE:

$$m_{PCE\ equivalent} = m_{PCE\ equivalent} + M_{PCE} * (n_{TCE} + n_{DCE} + n_{vc}) \quad \text{Eq (2)}$$

m, n, M representing mass, moles and molar mass respectively. The strong advantage of this unit compared to a simple arithmetic sum of all chlorinated compound is to ensure all contamination mass and degradation products are properly accounted for. Indeed a full degradation of PCE to vinyl chloride with time will be constant in terms of PCE equivalent, whereas it will be less in a simple sum, due to the smaller molar weight of the degradation products. This decrease in the arithmetic sum can be misleading, as it can be interpreted as a reduction of contamination while in reality it is a transformation into a degradation product.

Finally the molar ratio is given by the ratio of a specific compound over the sum of all moles of chlorinated compounds. For example when looking at the molar ratio of PCE:

$$\chi = \frac{n_{PCE}}{n_{PCE} + n_{TCE} + n_{DCE} + n_{VC}} \quad \text{Eq. (3)}$$

With *n* being the moles of the given chlorinated compound.

4. Results

4.1 Evolution of the contaminant mass discharge (PCE eq)

In Table 7 and 8 are presented the estimated contaminant mass discharges (CMD), expressed in PCE equivalent for each of the measurement campaigns for method 1 and method 2 respectively. Contaminant mass discharge for each of the individual chlorinated compounds can be found in Appendix G.

Despite the limited number of datasets, the use of the concentration dataset for the F-wells and (MLS+F-well) indicates a general decrease of the contaminant mass discharge between 2008 and 2016. Both methods are in good agreement and exhibit the same trend. The contaminant mass discharge estimated by method 1 decreases from roughly 4 kg to 1.8 kg/yr, i.e. approximately 55% reduction (expressed in PCE eq, F-well dataset). By method 2 using a data interpolation is estimated a decrease from 3.6 kg to 2 kg/yr, i.e. 45% of the contaminant mass discharge in PCEeq (F welldataset). This decrease is in good agreement with the contaminant mass reduction in the source area caused by the remediation activities during the same period.

The two different datasets F and (F+MLS) combined give relatively similar results. It is expected that the results obtained with the F and MLS wells in combination should produce a better estimate due to to a finer discretization of the transect.

4.2 Evolution of the contaminant mass discharge per compound

Considering each chlorinated compound separately, the same trend of mass discharge reduction with time is observed for each compound, exceptVC which slowly increases (Figure 9). These observations are valid for both calculation methods.

A significant drop in mass discharge is observed for the PCE and TCE between 2009 and 2012, and can likely be related to the remediation activities in the source area targetting specifically the PCE mother compound. The PCE mass discharge decreases by 78% while TCE is reduced by 96% between december 2008 and november 2012 (F-well dataset with method 1, Appendix G). Since 2012 the contaminant mass discharge for these two compounds stayed relatively constant.

Generally cisDCE mass discharge also decreased between 2008 and 2015, but the reduction is less significant than for both PCE and TCE with 50% and 45% estimated reduction, using dataset F-well and (F+MLS) combined respectively (method 1, Appendix G). The computation by method 2/data interpolation shows also a reduction but of 33 and 27% only, once again for dataset F and (F+MLS) respectively.

Despite the source remediation activities in the different source areas, a steady and significant increase of VC with time is observed (t-test, α=0.05). All together and with the variation of mass

discharge of the compounds, the composition of the contaminant plume evolves with time, as highlighted by looking at the change in molar ratio (Figure 10 and Figure 12).

Recently between 2015 and 2016 some mass discharge quantities seem to increase again, e.g. cisDCE (F-well calculation, method 2). Nevertheless, the dataset is curently too restrained to conclude if this is a significant increase due to some rebound effect, degradation in the plume and/or increased degradation with the current operation of remediation, or just the temporal variation due to the sampling period combined to calculation assumptions. This point will be addressed further in the next section.

Table 7. Estimation and temporal evolution of CMD throughout Østergade transect
Expressed in PCEeq
F wells dataset – method 1

Period	2008			2009			2012	2015		2016
	Jul	Aug	Dec	Mar	Jul	Nov	Nov	Jan	Sep	Feb
J [kg/y]	3.87	4.85	3.40	4.37	4.11	3.33	1.96	1.65	1.68	1.84
Average $\bar{J}$ [kg/y]	4.37			3.93			1.96	1.67		1.84
Standard deviation σ [kg/y]	0.49			0.54			/	0.02		/

Table 8. Estimation and temporal evolution of CMD throughout Østergade transect
Expressed in PCEeq
(F+MLS) wells dataset – method 1

Period	2008			2009			2012	2015		2016
	Jul	Aug	Dec	Mar	Jul	Nov	Nov	Jan	Sep	Feb
J [kg/y]	/	/	/	3.72	3.72	/	/	/	1.59	1.59
Average $\bar{J}$ [kg/y]				3.72			/	/	1.59	1.59
Standard deviation σ [kg/y]				0.005			/	/		/

Table 9. Estimation and temporal evolution of CMD throughout Østergade transect
Expressed in PCEeq
F wells dataset – method 2 using data interpolation

Period	2008			2009			2012	2015		2016
	Jul	Aug	Dec	Mar	Jul	Nov	Nov	Jan	Sep	Feb
J [kg/y]	3.52	3.83	3.64	3.44	3.60	3.11	1.88	1.60	1.66	2.06
Average $\bar{J}$ [kg/y]	3.66			3.38			1.88	1.63		2.06
Standard deviation σ [kg/y]	0.15			0.25			/	0.02		/

Table 10. Estimation and temporal evolution of CMD throughout Østergade transect
Expressed in PCEeq
(F+MLS) wells dataset – method 2 using data interpolation

Period	2008			2009			2012	2015		2016
	Jul	Aug	Dec	Mar	Jul	Nov	Nov	Jan	Sep	Feb
J [kg/y]	/	/	/	3.31	3.43	/	/	/	1.60	1.40
Average $\bar{J}$ [kg/y]				3.37			/	/	1.60	1.40
Standard deviation σ [kg/y]				0.08			/	/	/	/

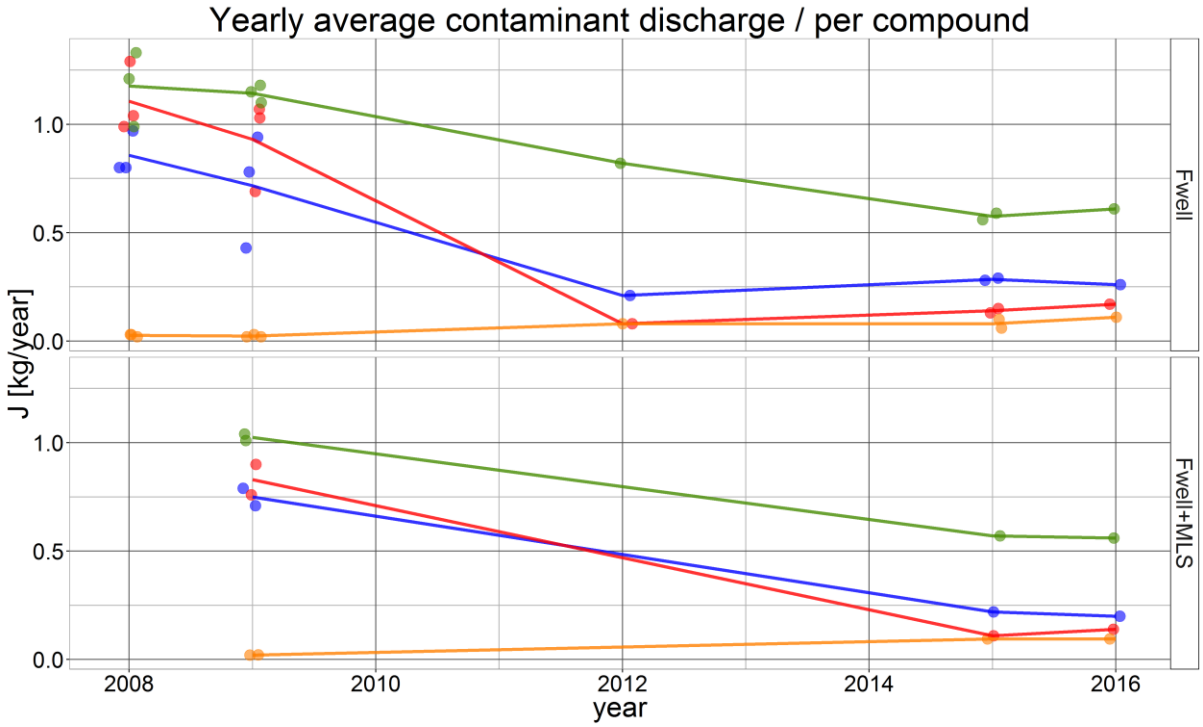

Figure 9. Yearly contaminant mass discharge for the different chlorinated compounds (line)
Method 1 results
Line: average yearly value / round marker: individual dataset
(Values reported in Appendix G.1)

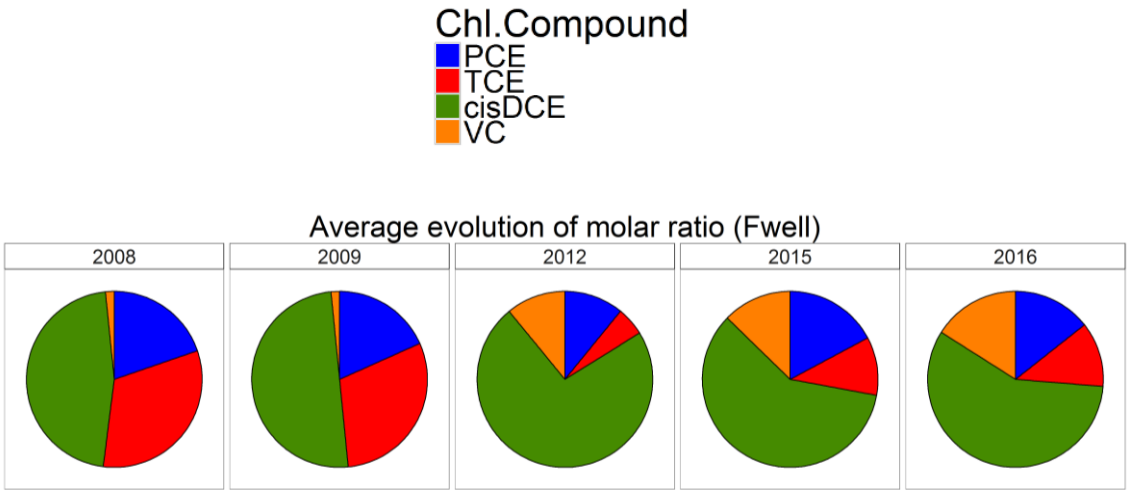

Figure 10. Evolution of the molar ratio for the yearly contaminant mass discharge
Method 1 results
(F wells only)

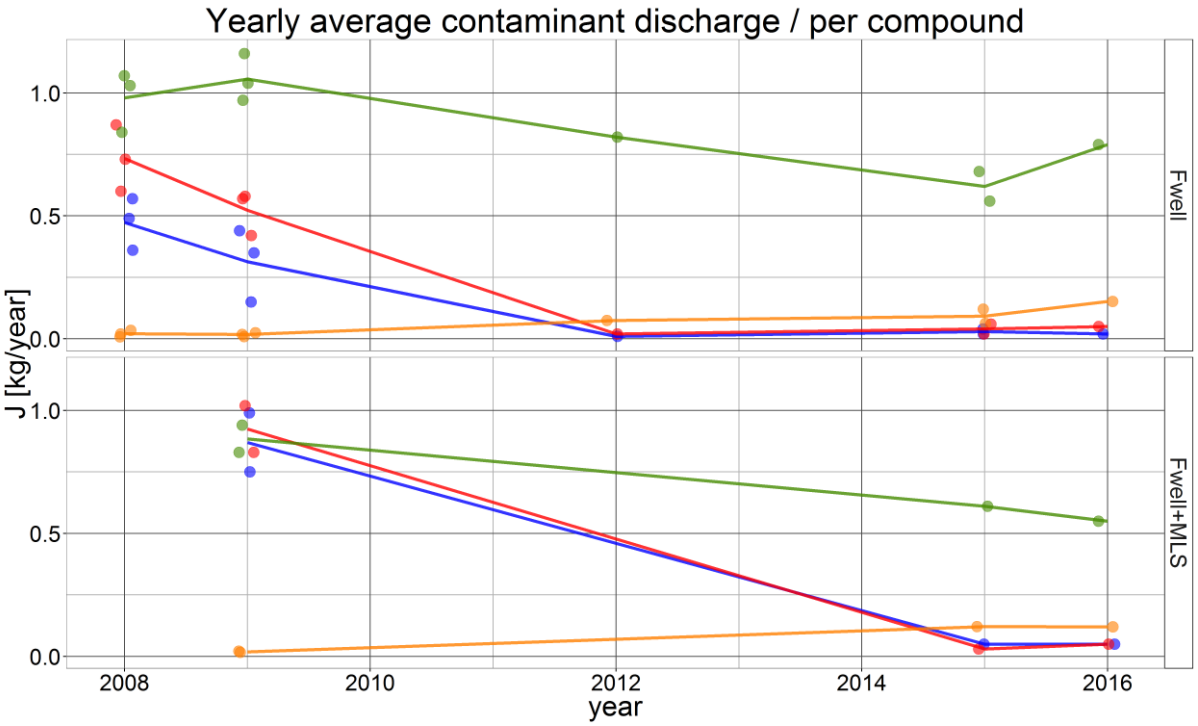

Figure 11. Yearly contaminant mass discharge for the different chlorinated compounds (line)
Method 2 results
Line: average yearly value / round marker: individual dataset
(Values reported in Appendix G.2)

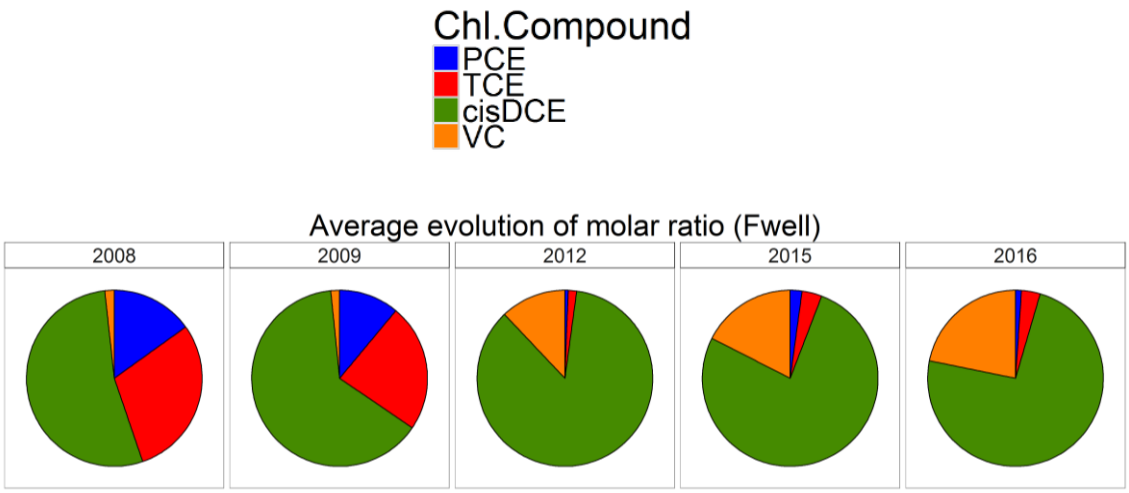

Figure 12. Method 2 calculation by data interpolation.
Evolution of the molar ratio for the yearly contaminant mass discharge
(F-wells only)

5. Spatial and time variation consideration

The computation of the evolution of the contaminant mass discharge requires knowledge about groundwater flow and contamination extent. All these quantities are time dependent and subject to uncertainty in measurements and due to discrete spatial sampling. These aspects and related consequences on the results are discussed in this section.

5.1 Spatial variation of concentration data (transect)

The spatial variation of the contamination in the transect with respect to time can be evaluated by correlation of the data measured at fixed positions, i.e. fixed monitoring wells in this case. Correlation matrices (Pearson's correlation) for the concentration at each of the sampling wells (F-well) is presented in Figure 13 below for the different available measurement campaigns.

Extremely high correlation between the measurement for the period [2008 – 2009] and [2012-2016] are observed for the PCE and TCE compounds. Such a degree of correlation suggests that the spatial distribution of the contamination in the transect is relatively stable over each of these two periods. The low correlation in between the two periods on the other hand suggests that the spatial distribution of PCE and TCE in the transect evolved in between 2009 and 2012, very likely due to the source remediation activities in the source areas and the resulting strong concentration reductions (see Appendix C for visualization).

On the other hand, a generally high and significant correlation is observed for the different measurement periods for cisDCE indicating a relatively stable spatial distribution over the period [2008-2016]. The spatial distribution stayed therefore relatively constant over the period of interest and was weakly affected by the remediation. Finally, a significant degree of correlation is observed between all periods for VC (p-test, α=5%), but it appears clearly that the spatial distribution was modified between the two periods [2008-2009] and [2012-2016]. Visualization of the measurement data in Appendix C reveals this change is mostly caused by higher concentration of VC in the lower part of the aquifer around well F45-1.

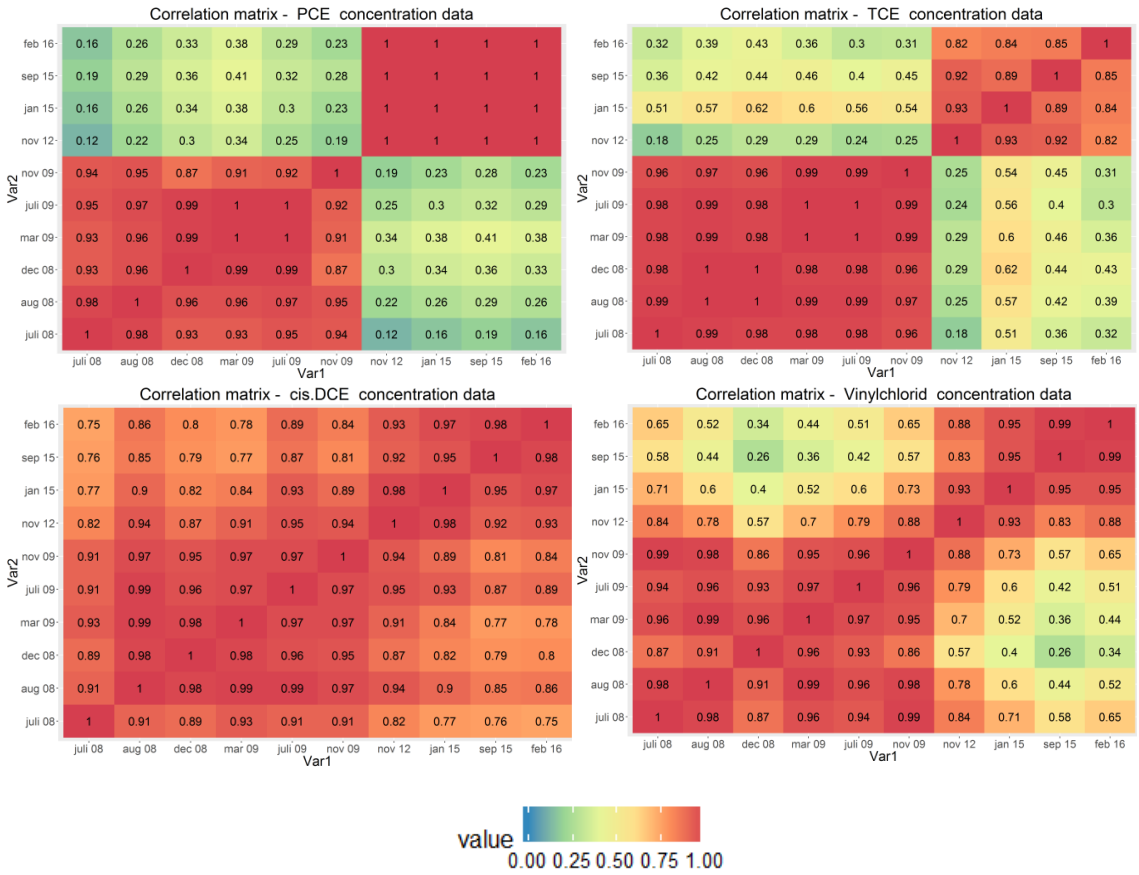

Figure 13. Correlation matrix for the concentration dataset measured at the different Fwells from 2008 to 2016

5.2 Spatial variation in hydraulic conductivity

The hydraulic conductivity in the transect is connected to the permeability of the soil and subject to limited variation with time if the soil is undisturbed and saturated. Consequently, the uncertainty in the determination of K will affect the quantitative value of the contaminant mass discharge, but to a minor degree when the relative evolution of the contaminant mass discharge with respect to time is considered.

Figure 14 shows the interpolated hydraulic conductivity and it appears clearly that an area with high hydraulic conductivity is found in the lower part of the upper aquifer, in agreement with the previous observations and issued reports (Lange et al., 2011; NIRAS, 2016a). High conductivity combined with high concentrations in the area can result in a significant increase of contaminant mass discharge, not captured by the calculation method 1. The results obtained show that these variations have indeed an effect on the evolution of the estimated CMD with smaller reduction of

cisDCE discharge and more important discharge of VC compared to method 1. However, these variations are still limited and the results are within the same order of magnitude. Consequently the trends of reduction/augmentation observed by method 1 are still valid even considering these spatial variations.

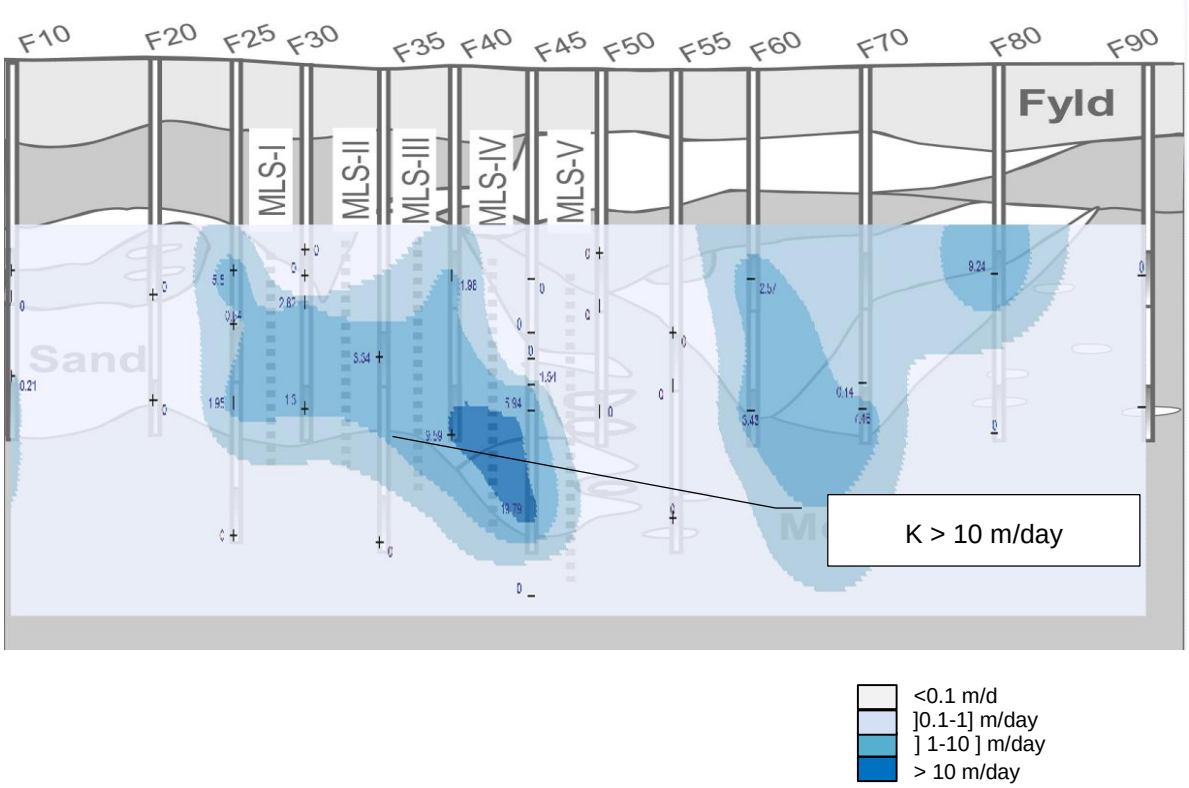

Figure 14. Visualization of the hydraulic conductivity distribution in Østergade transect
Estimation by data interpolation from kriging method (see Appendix F for details)
Input dataset from Lange et al. (2011)

5.3 Temporal hydraulic head variation

The calculations in Section 4 are performed with the assumption of a steady hydraulic gradient through the investigated transect. However the scatterplot of hydraulic gradient data in Figure 4 shows hydraulic gradient variations by a factor 2, ranging from approximately 0.0015 to 0.003 in 2009. It is reasonable as a first approximation that such a variation occurs yearly and will affect the yearly contaminant mass discharge.

The general water balance and consequently the hydraulic head in the aquifers are partly influenced by the amount of precipitation infiltrating. The precipitation distribution at the closest measuring station over the considered period exhibits high coefficient of variation of almost 80% for the year 2008 to 2010, compared to the most recent years where the coefficient of variation ranges from 39 to 56% for the last 3 years (Figure 15 and Table 11). Consequently the overall variation of hydraulic head may be reduced during the last measurement periods compared to

2008-2010, but is still dependent on the time of performing the measurements, and on the history of precipitation and water table variations.

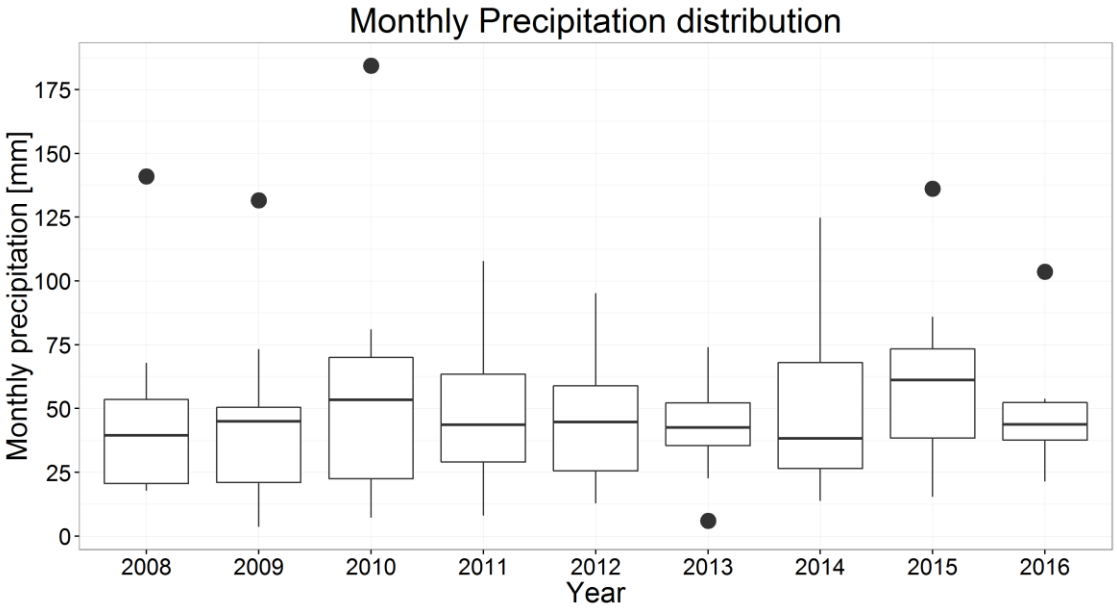

Figure 15. Boxplot of monthly precipitation for the year 2008 to 2015 representing 25, 50 and 75 quartile, extreme or 1.5xIQR value for whiskers, outlier as dots. DMI Measuring station 5825 at Jyllinge renseanlæg

Table 11. Mean, standard deviation and Coefficient of Variation monthly precipitation – station 5825 at Jyllinge renseanlæg

Year	Mean [mm]	Standard dev. σ [mm]	CV = σ/ Mean. [%]
2008	45.1	35.5	78.7
2009	45.6	34.7	76.0
2010	57.9	57.9	79.0
2011	52.0	45.7	63.3
2012	48.6	32.9	52.4
2013	39.3	25.5	42.4
2014	53.1	17.8	56.7
2015	60.8	32.0	52.7
2016	48.8	19.4	39.7

Figure 17 illustrates the variation of water head at four monitored wells, depicted in Figure 16, in the upper aquifer for the period [2008 to 2011], in parallel of the precipitation received (measuring station 5825 , moving average – 30 days periods). Fast responses of the upper aquifer are clearly visible when rain episodes are experienced. Some variations observed before 2010 and at well KB10-1 look suspicious with sudden and abrupt changes of water table and cannot easily be interpreted. The restrained number of monitoring points in the plume does

not allow further post-treatment of the data and the estimation of a variation of hydraulic gradient, especially for the most recent years.

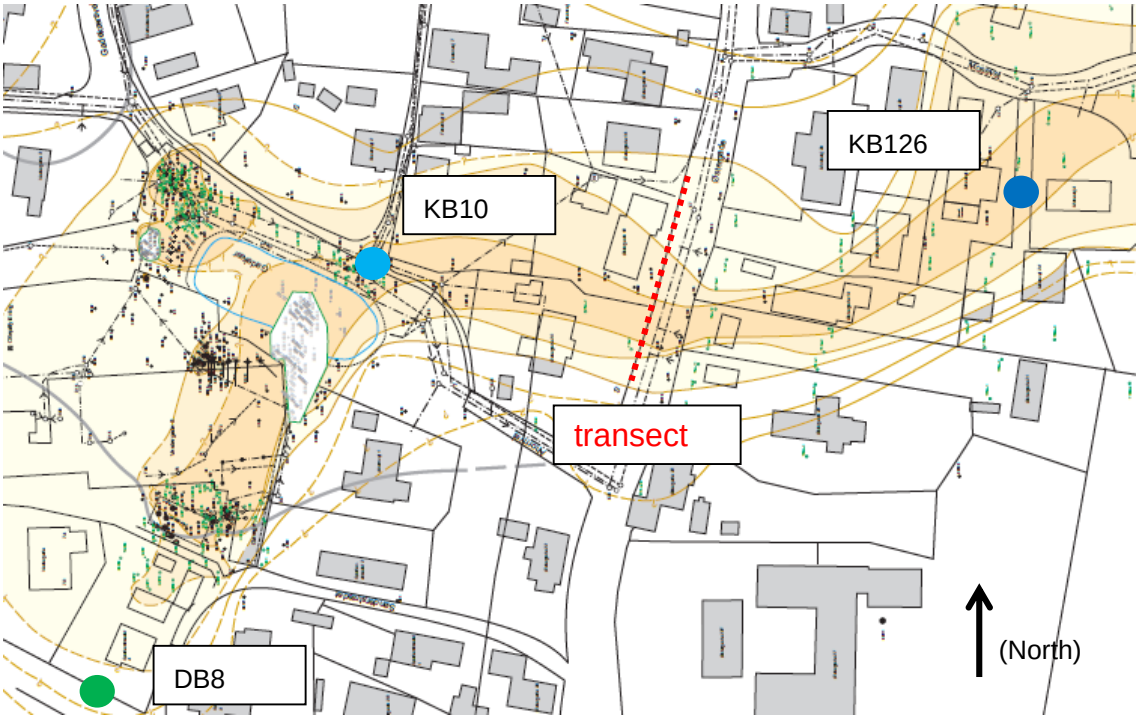

Figure 16. Water table monitoring location for the selected wells in the upper aquifer

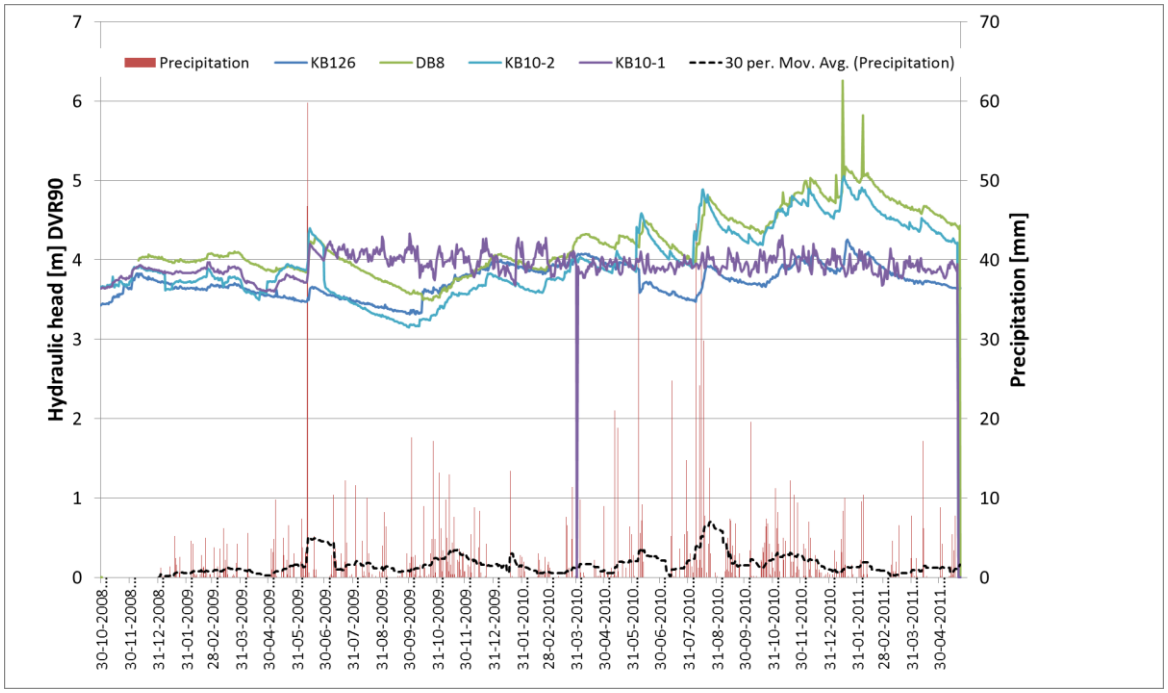

Figure 17. Hydraulic head monitoring in the upper aquifer for selected wells comparison to daily precipitation and moving average (year 2009, part of 2010, 2011)

5.4 Temporal variation in source area and vicinity

In the following figures are presented the temporal evolutions of concentration at a few selected wells (Figure 18), in parallel with the estimation of contaminant mass remaining in the source area (Figure 19). The investigated wells are at the edge of the source area and upstream transect (Figure 19 a, b respectively)

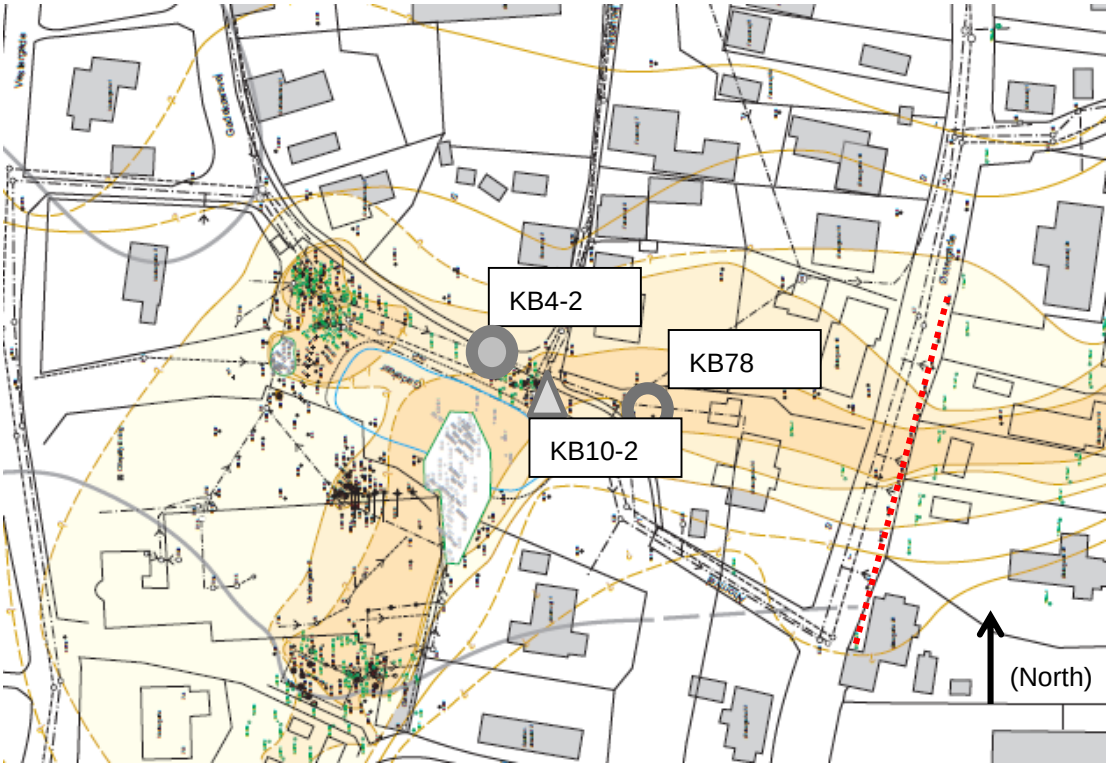

Figure 18. Temporal variation of concentration for selected wells in the upper aquifer close to the source area

At the edge of the source area (well KB4 to 10), the concentration drops with the mass of PCE. Due to the lack of concentration data between 2005 and 2008, it is challenging to evaluate if the concentration reduction observed in the period 2008 to 2010 is connected to the simultaneous ISTD remediation and ISCO (occurring from September to December 2008 in hotspot I and in December 2009 and 2010 in hotspot III respectively), or even to the strong pump/treat action in 2006 combined with a relatively long residence time. The data in KB78 (upstream transect) also show a simultaneous decrease, but the sampling period of 7 years is too long to lead to any relevant conclusion.

An assessment of the residence time was carried out by use of a Monte Carlo simulation using available data (see Appendix H for estimation). The outcome of the simulation suggests that the change in concentration in the hotspot I will be detected at the edge of the source area from 0.7 up to at least 2.2 years, depending on the location of the contaminant in the hotspot, retardation factor and groundwater seepage velocity. In other terms, the concentration drops observed at the edge of the source area from 2008 (and later on) are likely responses to concentration drops in the hotspot I occurring from 2008 and a maximum of 2 years previously. Consequently

the concentration drop observed at the edge of the source area from 2008 to 2010 is likely connected to the remediation starting in 2008, and not the pumping operation in 2006.

It is important to keep in mind that these calculations are based on data available and no dedicated measurements for this purpose. Results are therefore subject to high uncertainty and should therefore be considered accordingly.

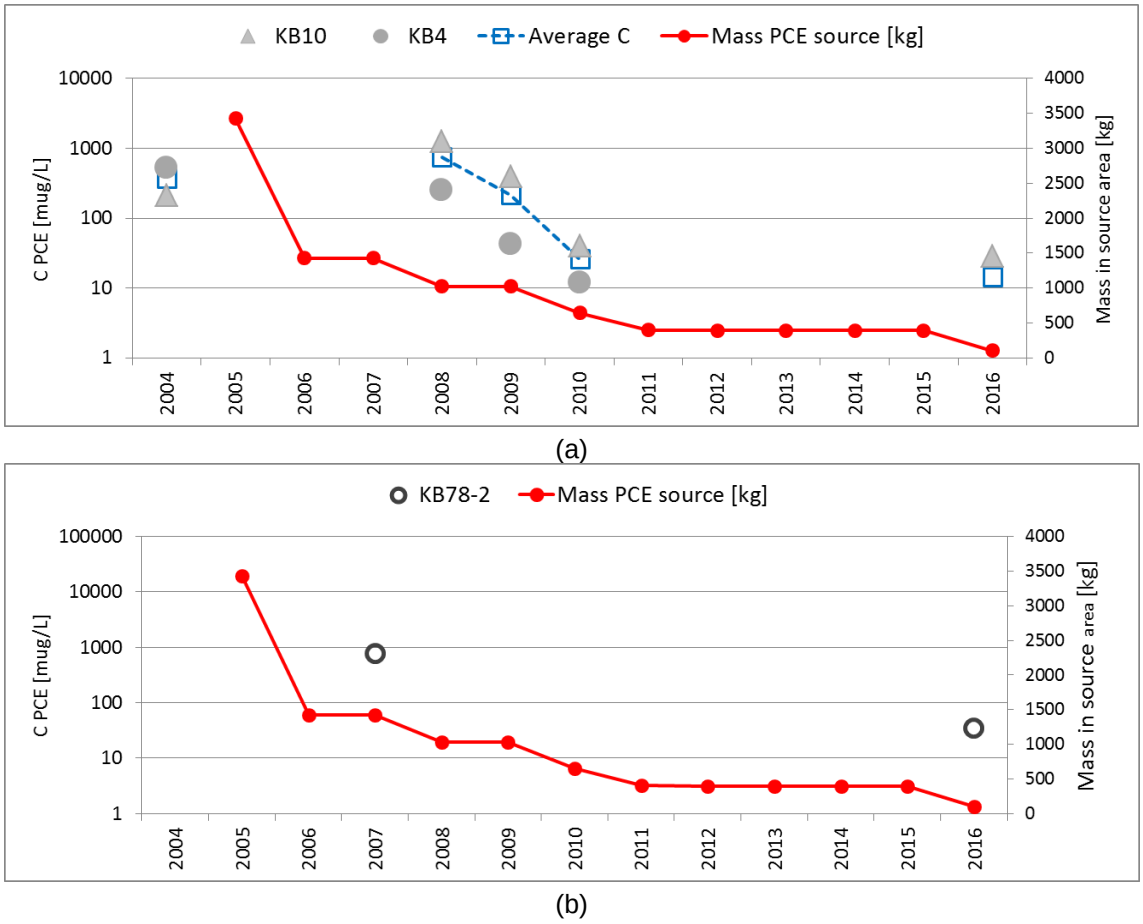

Figure 19. Evolution of average PCE concentration at selected wells compared to mass PCE in source area

(a): at the edge of source area (b) upstream transect,

5.5 Temporal variation downstream of source area

Figure 20 presents a time evolution of the contaminant mass in the source area, in parallel with the mean concentration in the transect and the corresponding contaminant discharge. The general decrease of all quantities almost simultaneously suggests that the remediation activities and contaminant mass reduction in the source area may have led to a simultaneous reduction of contaminant loading into the plume and consequently a decrease in contaminant mass discharge through the plume seen from the transect.

However, the relatively long distance and possible retardation between the source and the transect location requires to take a closer look at the residence time to ensure these quantities are all linked.

The residence time between hotspot I where the first remediation takes place and the transect is carried out using a similar methodology as the one presented in section 5.4. For the PCE, the residence time is estimated to lie between from 2 to up to 17 years, while for the most mobile VC, this estimated residence time ranges from 1.3 to 10 years (Appendix I). Consequently, the concentration/CMD decrease observed from 2008 to 2012 in the transect could be related to both remediation activities in 2008 and 2010, but also the initial pump and treat activity carried out in 2006.

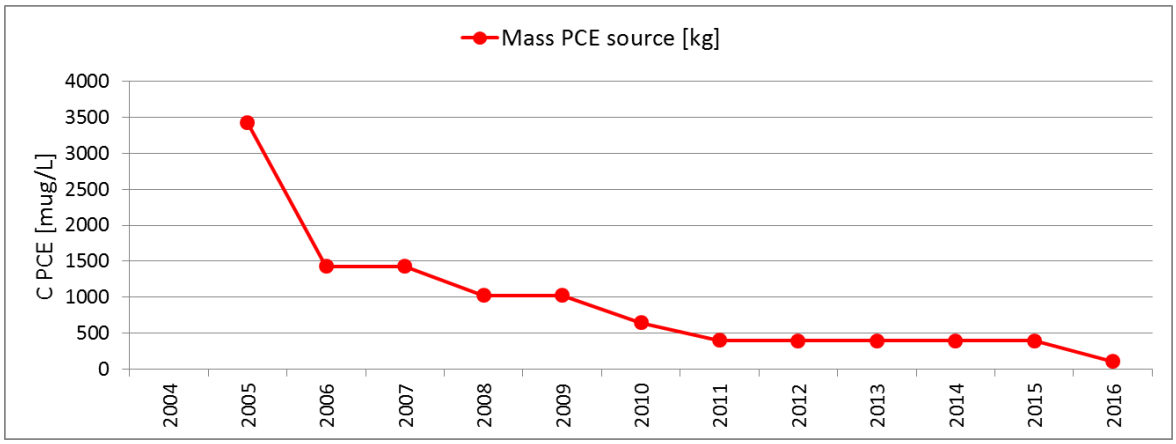

(a)

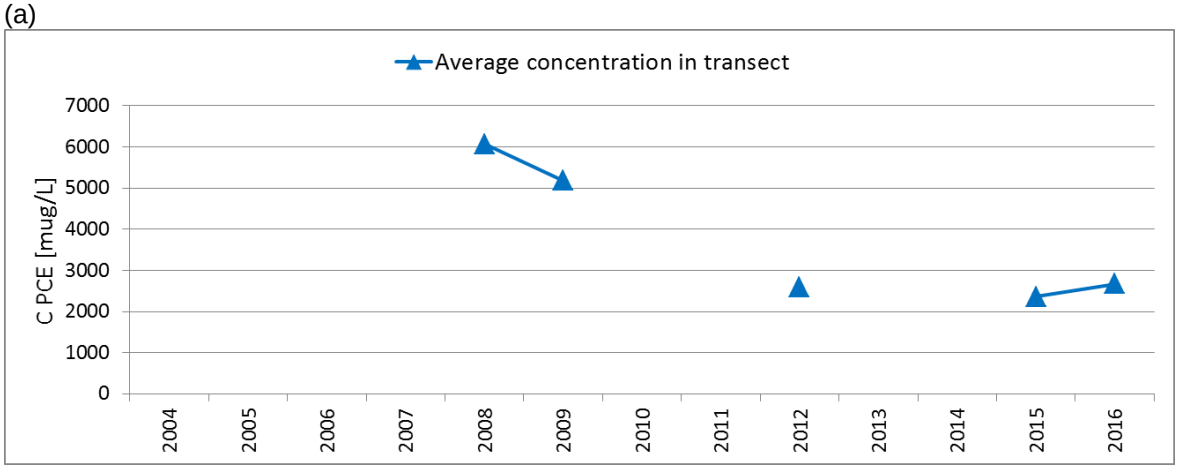

(b)

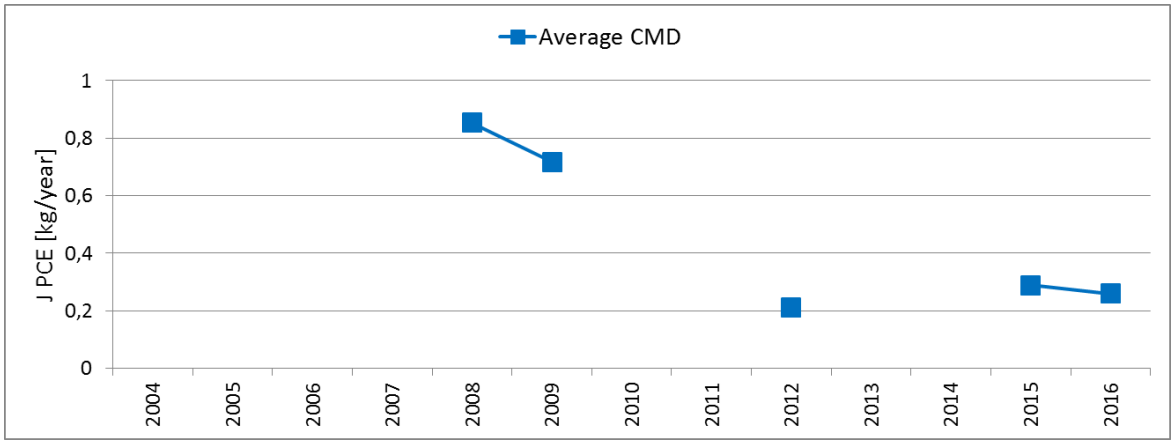

(c)

Figure 20. Evolution of average PCE concentration and CMD in the transect Compared to mass PCE in the source area
(a): Mass PCE in source area (b) Average PCE eq. concentration – see Table 3 (c) PCE mass discharge (Appendix G)

5.6 Source strength consideration

The relationship between the remaining DNAPL mass in the source area, the resulting concentration and related discharge to the downstream plume are complex phenomena. Research suggests that the DNAPL contaminant mass and averaged dissolved concentration (and consequently mass discharge) are dependent on DNAPL distribution and hydrogeologic properties and can be related by a power function of the form (Falta et al. 2005a, 2005b; Basu et al. 2008):

$$\left(\frac{C(t)}{C_o}\right) = \left(\frac{M(t)}{M_o}\right)^{\Gamma} \qquad \text{Eq. (4)}$$

With *C(t)* average concentration of dissolved contaminant leaving the source zone, *M(t)* contaminant mass, and *Γ* an empirical parameter. This approach provides a good insight into the long term behavior of the source (illustration in Figure 21)*:* the source will be depleted at a finite time by dissolution for values of *Γ <1*, while for *Γ <1* the source has a theoretical infinite life time and long tailing with low dissolved concentrations.

Although appealing, this approach encompasses several constraints that limit its range of application when applied in-situ. Equation (4) implies that both concentration and mass are evaluated simultaneously and from a given reference time. In the current project, data regarding mass are given as estimate once a year while the concentration data are measured at different time steps further downstream the hotspot areas and therefore shifted in time due to the groundwater transport. Furthermore, the creation of sequential degradation to by-products with different transportation time due to different sorption properties challenges even more the approach. Some of these limitations were highlighted through extensive field work or simulations, e.g. Fjordboege et al. (2012b) with the remediation in the hotspot V, or the work by

Chambon et al. (2010). It is ultimately believed that such an approach cannot reasonably be applied to a complex site such as Skuldelev with multi hotspot areas and without proper dedicated measurements.

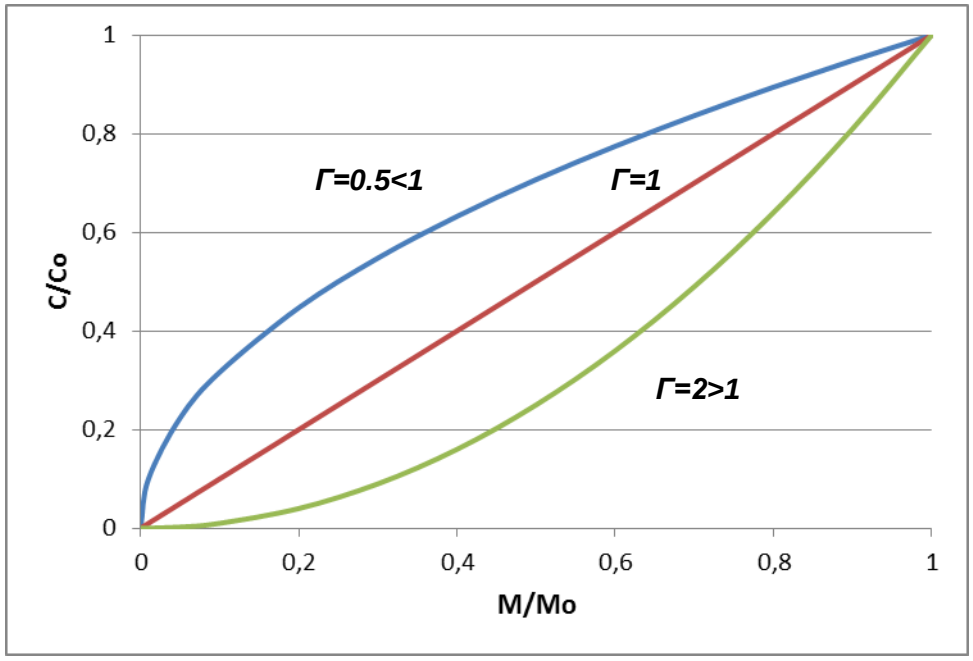

Figure 21. Theoretical power law representation:
Relationship between dissolved concentration and remaining mass of contaminant in the source area

6. Discussion

The previous examinations of the temporal and spatial variations support the results presented in section 5, i.e. a general decrease of the contaminant mass discharge in the Østergade transect. This result is independent of the method and considered dataset. This decrease occurs in parallel with the mass reduction of the PCE mother compound in the source area, leading to a decrease of dissolved concentration and reduced contaminant loading to the plume. This decrease does not occur simultaneously to the decrease in mass and concentration at the edge of the source area (and further downstream for that matter) due to the residence time and sorption phenomena between the source area and the control transect.

This overall decrease was characterized in PCE equivalent, i.e. all chlorinated compounds combined and accounted together. The results differ slightly when all compounds were considered separately: While PCE and TCE discharges were reduced substantially; the reduction of the cisDCE compound was more moderate and it was shown that VC has steadily increased since 2008. The increase of degradation products quantities raises the question of the origin of these compounds.

From a global study perspective, the numerous data on site mostly focus at a local source scale and were targeting the different hotspots individually. Data focusing on the plume are relatively limited and hinder a proper estimation of the contaminant mass discharge and its variation. Particularly, the absence of monitoring data prevents the evaluation of the hydraulic gradient variation, especially in the recent years which has certainly an effect on the estimated mass reduction. Furthermore no characterization of the redox conditions in the plume was recently performed. It is therefore nearly impossible to conclude if the degradation products detected in the transect are forming within the plume due to reduced conditions or are simply transported from the source area, e.g. due to the evolution of redox conditions with the remediation. Finally, the absence of concentration data between 2004 and 2008 when the first remediation activity occurs makes difficult the characterization of plume and source interaction

7. Conclusion

On behalf of Region Hovedstaden, DTU performed an evaluation and CMD calculation at Østergade in Skuldelev. The calculation is based on a coherent and systematic use of the chemical and hydrogeological data collected since 2008 by different companies and institutions.

For consistency, a standard calculation based on the estimation of Darcy's velocity in combination with contaminant concentrations and area discretization of the transect was proposed for all dataset available for the designated F-wells and F+MLS combined. A second method using a data interpolation by kriging method was also performed to ensure that the spatial variations of the concentration data in the transect were accounted for.

Both methods are in good agreement and the following conclusions are made:

- A reduction of the contaminant mass discharge is observed at the Østergade transect, especially during the period 2008-2011 for the PCE equivalent. The methods used for this study estimate a 45% to 55% reduction of chlorinated solvents mass discharge between 2009 and 2012.
- This general reduction is observed in parallel with the mass reduction in the source area originating from different remediation activities starting in 2006.
- The spatial distribution of the compounds in the transect certainly evolved after 2008 and especially for PCE and TCE. These variations are very likely caused by the remediation in the source area.
- The mass discharge and ratio of chlorinated compounds in the plume evolved between 2008 and 2016. While PCE and TCE were significantly reduced (and their spatial distribution altered), DCE exhibits a more subtle reduction in mass, while vinyl chloride actually increased steadily.

Compound	Mass discharge range * February 2016
PCE	[0.02-0.26] kg/year
TCE	[0.05-0.17] kg/year
cisDCE	[0.54-0.79] kg/year
VC	[0.09-0.15] kg/year

** : dependent on the method and dataset used*

Despite extensive datasets, some of the observations and statements made cannot be fully explained as most of the data collected focused on the source area. Particularly, the evaluation and evolution of redox conditions in the plume and a more thorough water table monitoring would facilitate the interpretation and the assessment of the variation of contaminant discharge at Østergade.

References

Basu, N. B., Rao, S. C., Falta, R. W., Annable, M. D., Jawitz, J. W., and Hatfield, K. (2008): Temporal evolution of DNAPL source and contaminant flux distribution: Impacts of source mass depletion. Journal of Contaminant Hydrology, 95(3-4), 93–109.

Chambon, J. C. C., Broholm, M. M., Binning, P. J., and Bjerg, P. L. (2010). Modeling multi-component transport and enhanced anaerobic dechlorination processes in a single fracture-clay matrix system. Journal of Contaminant Hydrology, 112(1-4), 77–90.

Devlin, J.F. (2003): A spreadsheet method of estimating best fit hydraulic gradients using head data from multiple wells. Ground Water, v. 41, no. 3, 316-320

Dyreborg S. and Christensen A.C. (2016): Fluxmåling I grundvand: Sammenligning af methoder til bestemmelse af flux ved grundvandsfuregninger. Report to Danish Ministry of environment and food by NIRAS. ISBN: unknwon

Falta, R. W., Rao, P. S., and Basu, N. (2005a): Assessing the impacts of partial mass depletion in DNAPL source zones - I. Analytical modeling of source strength functions and plume response. Journal of Contaminant Hydrology, 78(4), 259–280.

Falta, R. W., Basu, N., and Rao, P. S. (2005b). Assessing impacts of partial mass depletion in DNAPL source zones: II. Coupling source strength functions to plume evolution. Journal of Contaminant Hydrology, 79(1-2), 45–66.

Fjordboege, A.S., Riis, C., Christensen, A.G., and Kjeldsen P. (2012a) ZVI-Clay remediation of a chlorinated solvent source zone, Skuldelev, Denmark: 1. Site description and contaminant source mass reduction. Journal of Contaminant Hydrology, v. 140-141, 56-66

Fjordboege, A. S., Lange, I. V., Bjerg, P. L., Binning, P. J., Riis, C., and Kjeldsen, P. (2012b). ZVI-Clay remediation of a chlorinated solvent source zone, Skuldelev, Denmark: 2. Groundwater contaminant mass discharge reduction. Journal of Contaminant Hydrology, 140-141, 67–79.

Hansen, M.H. (2016): Skuldelev, masser i hotspot områder. Note 1222096638 to Region Hovedstaten.

Lange I.V., Troldborg, M., Santos M.C., Binning, P.J. and Bjerg, P.L. (2011): Kvantificering af foruregningsflux i transekt ved Skuldelev. Datarapport. DTU miljø.

NIRAS (2010): Vestergade 5, skuldelev. Regelmæssig pejling af grundvandsstand. Note to Region Hovedstadenm Koncern Miljø.

NIRAS (2016a): Skuldelev: samlet risikovurdering. Note to Region Hovedstaten. Dokument nr. 1219994489

NIRAS (2016b):EK Bio, statusrapport efter cyklus 2. Note to Region Hovedstaten

Oliver, A. M. and Webster, R. (2015): Basic Steps in Geostatistics: the Variogram and Kriging. Springer. ISBN 9783319158648.

Troldborg, M., NOWAK, W., Lange, I.V., Santos, M.C., Binning, P.J. and Bjerg, P.L. (2012): Application of Bayesian geostatistics for evaluation of mass discharge uncertainty at contaminated sites. Water Resources Research, v. 48.

A Hydraulic conductivity data

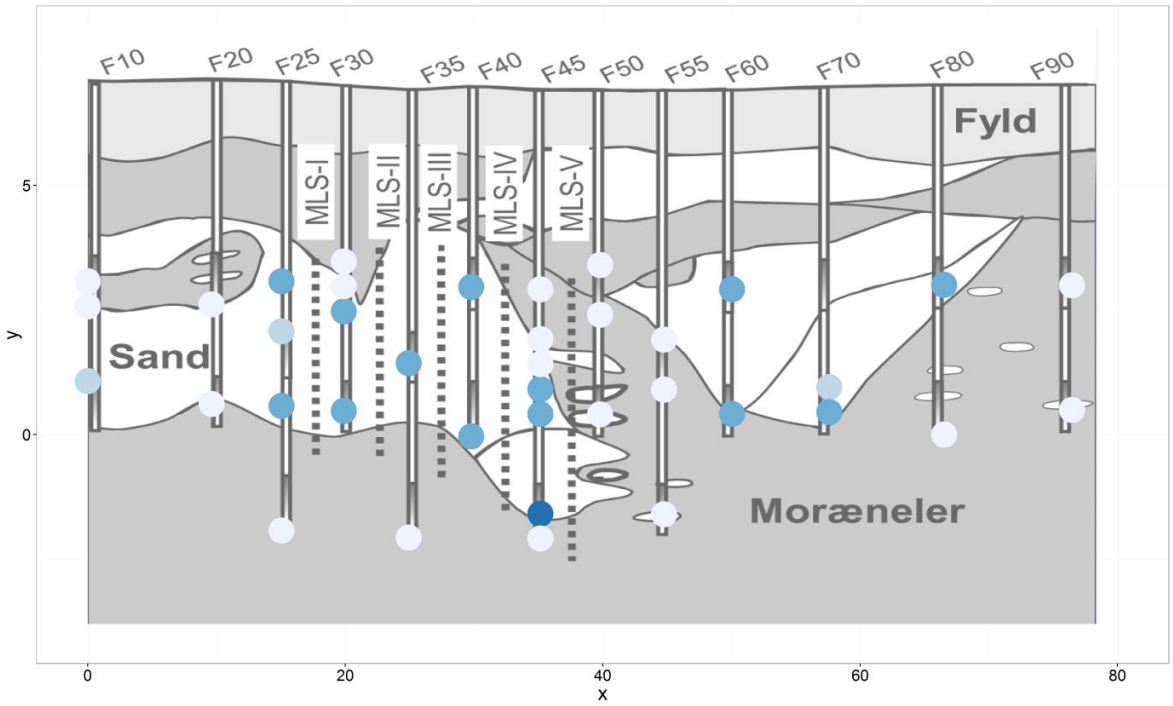

Figure 22. Hydraulic conductivity data
data reported by Lange et al. (2011)

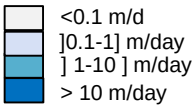

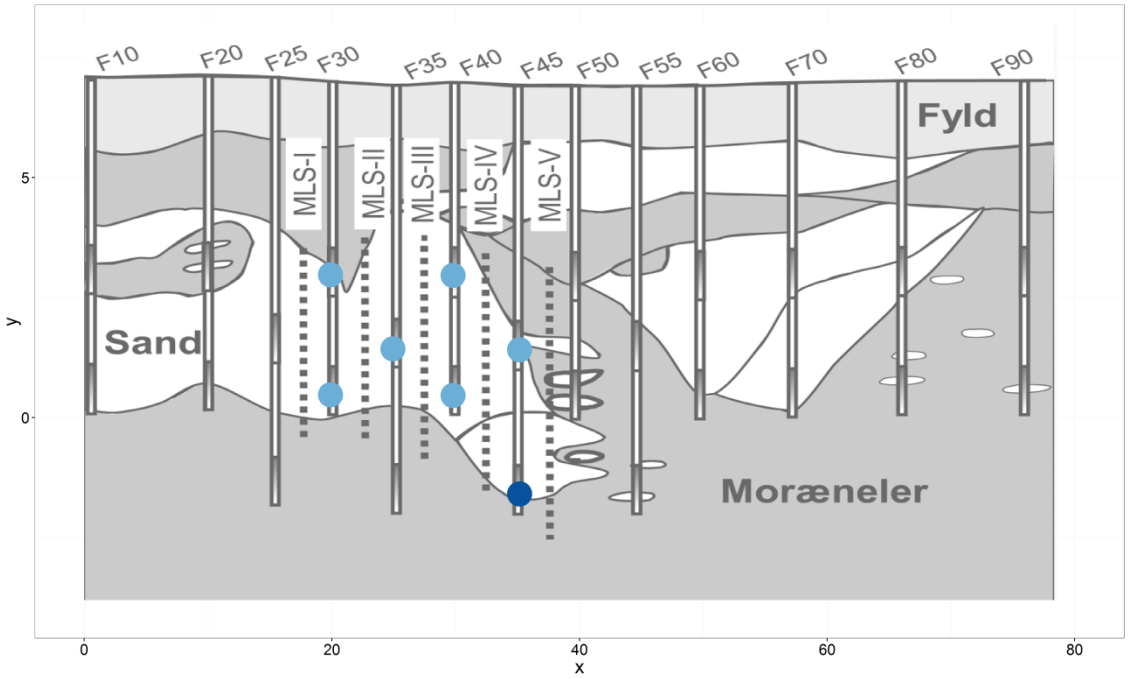

Figure 23. Hydraulic conductivity data, reported by NIRAS (2016)
F-well (not shown on transect)

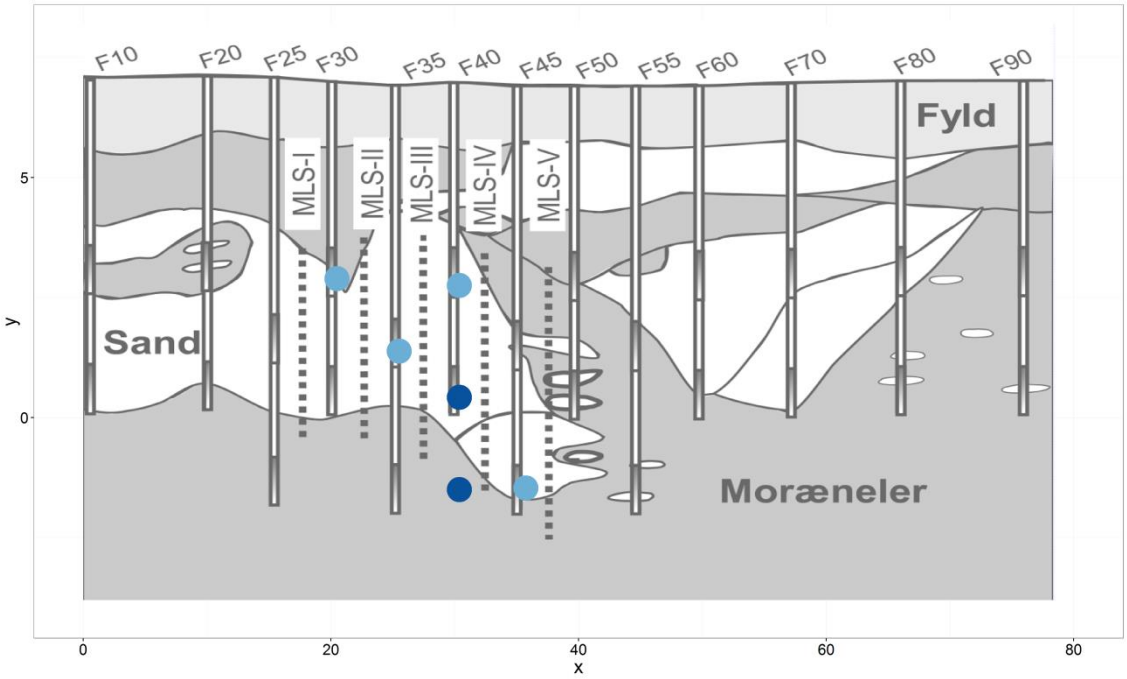

Figure 24. Hydraulic conductivity data, reported by NIRAS (2016)

Swell (not shown on transect)

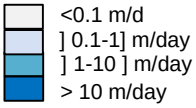

B Contaminant mass in source area

Table 12. Evolution of contaminant mass in the different hotspots

Table reproduced from Hansen (2016)

Hot spot omr.	Samlet masse før oprensning							
Hot spot I	2.400 kg PCE	2006 1.255 L fri fase (ca. 2.000 kg) oppumpet	Sept.-Dec. 2008 Ca. 400 kg PCE fjernet ved ISTD					
Hot spot II	540 kg PCE							
Hot spot III	300 kg PCE	Nov.-Dec 2009 S-ISCO oprensning	November 2010 S-ISCO oprensning	Masse tilbage inden ZVI: 55 kg PCE November 2011 ZVI injektion	Dec. 2011-Jan. 2012 Pump & Treat. Estimat: Fjernet 9 kg PCE og nedbrydnings-produkter	Aug. 2012 ZVI/BIO Injektion	Nov. 2013 ZVI/BIO Injektion	
Hot spot IV	Ca. 300 kg PCE (1)	Masse efter cyklus 2 af EK BIO oprensning 6,5 kg chlorerede ethener = 11 kg PCE ekvivalenter (marts 2016)						
Hot spot V	Ca. 380 kg PCE	Dec. 2009 Ca. 0 kg tilbage (>99 % fjernet)						
Hot spot VI	Ca. 1,5 kg PCE							

(1): Erroneous value. Total value is approximately 780 kg, with only 25 kg flowing towards east (NIRAS, 2016).

C Contaminant concentration data

C.1. Fwells data – PCE eq

Data collected from (Lange et al. 2011) and summary sheet of measurement data provided by NIRAS.

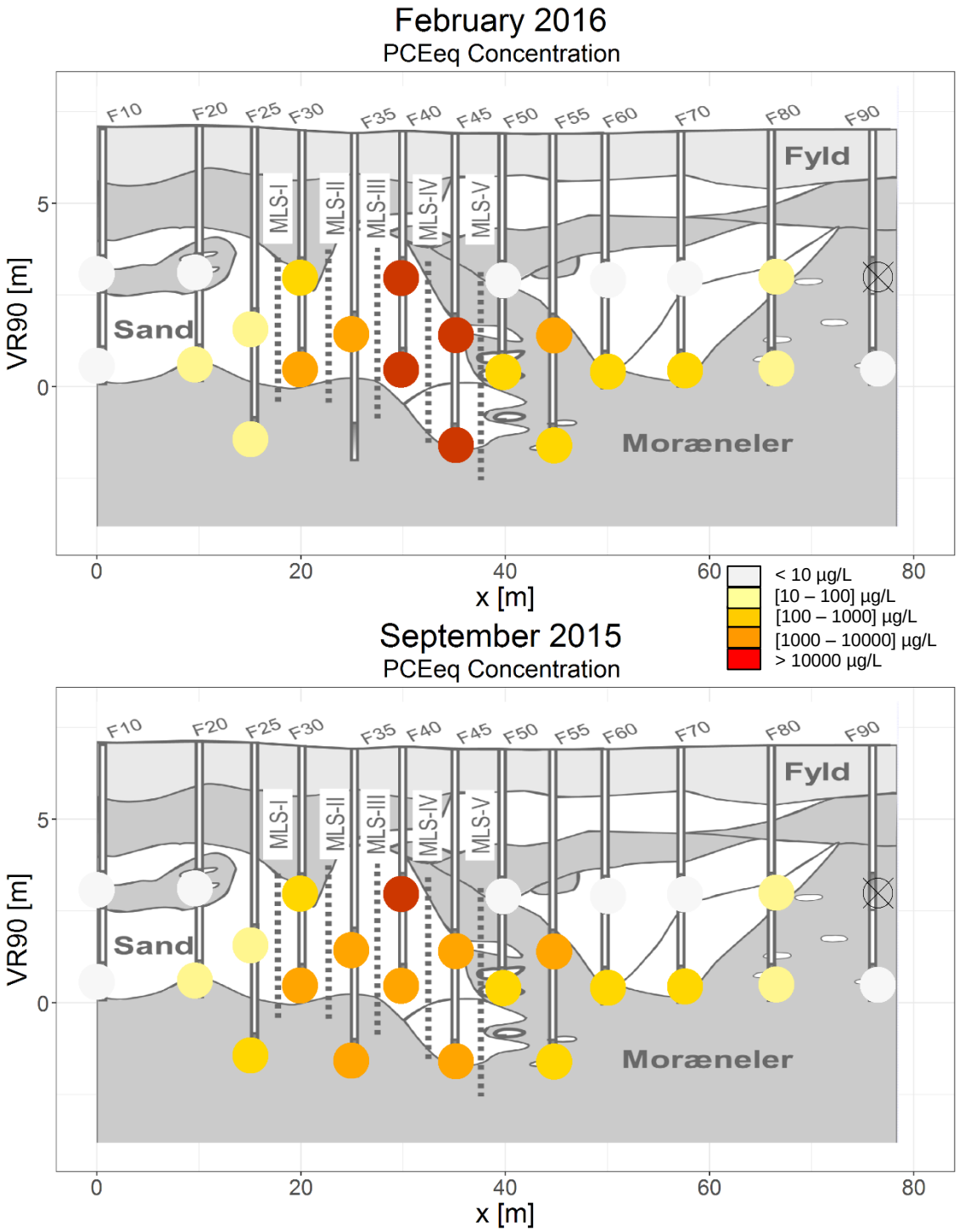

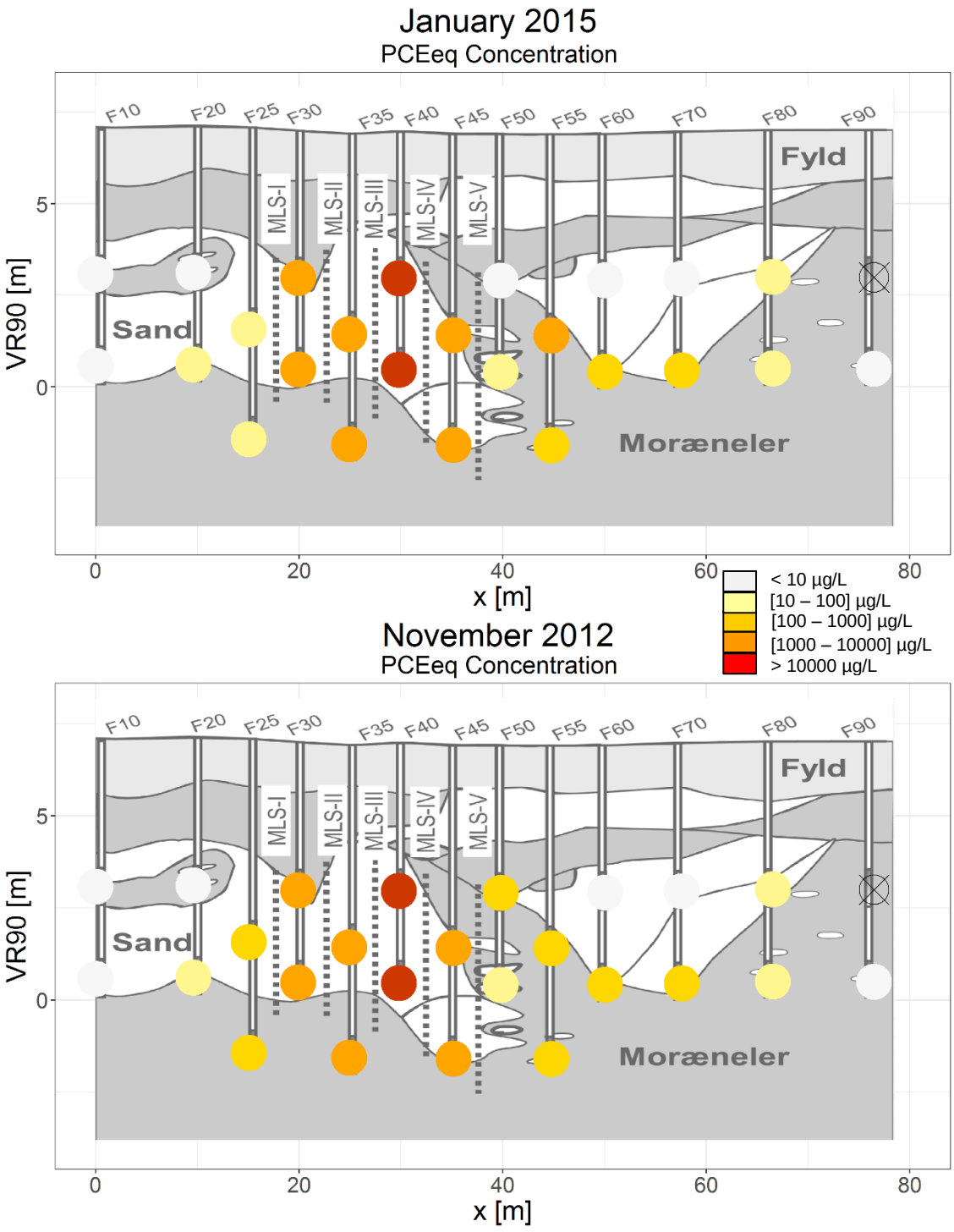
January 2015
PCEeq Concentration
F10
F20
F25
F30
F35
F40
F45
F50
F55
F60
F70
F80
F90
MLS-I
MLS-II
MLS-III
MLS-IV
MLS-V
Fyld
Sand
Moræneler
VR90 [m]
5
0
0
20
40
60
80
x [m]
< 10 µg/L
[10 – 100] µg/L
[100 – 1000] µg/L
[1000 – 10000] µg/L
> 10000 µg/L
November 2012
PCEeq Concentration
F10
F20
F25
F30
F35
F40
F45
F50
F55
F60
F70
F80
F90
MLS-I
MLS-II
MLS-III
MLS-IV
MLS-V
Fyld
Sand
Moræneler
VR90 [m]
5
0
0
20
40
60
80
x [m]

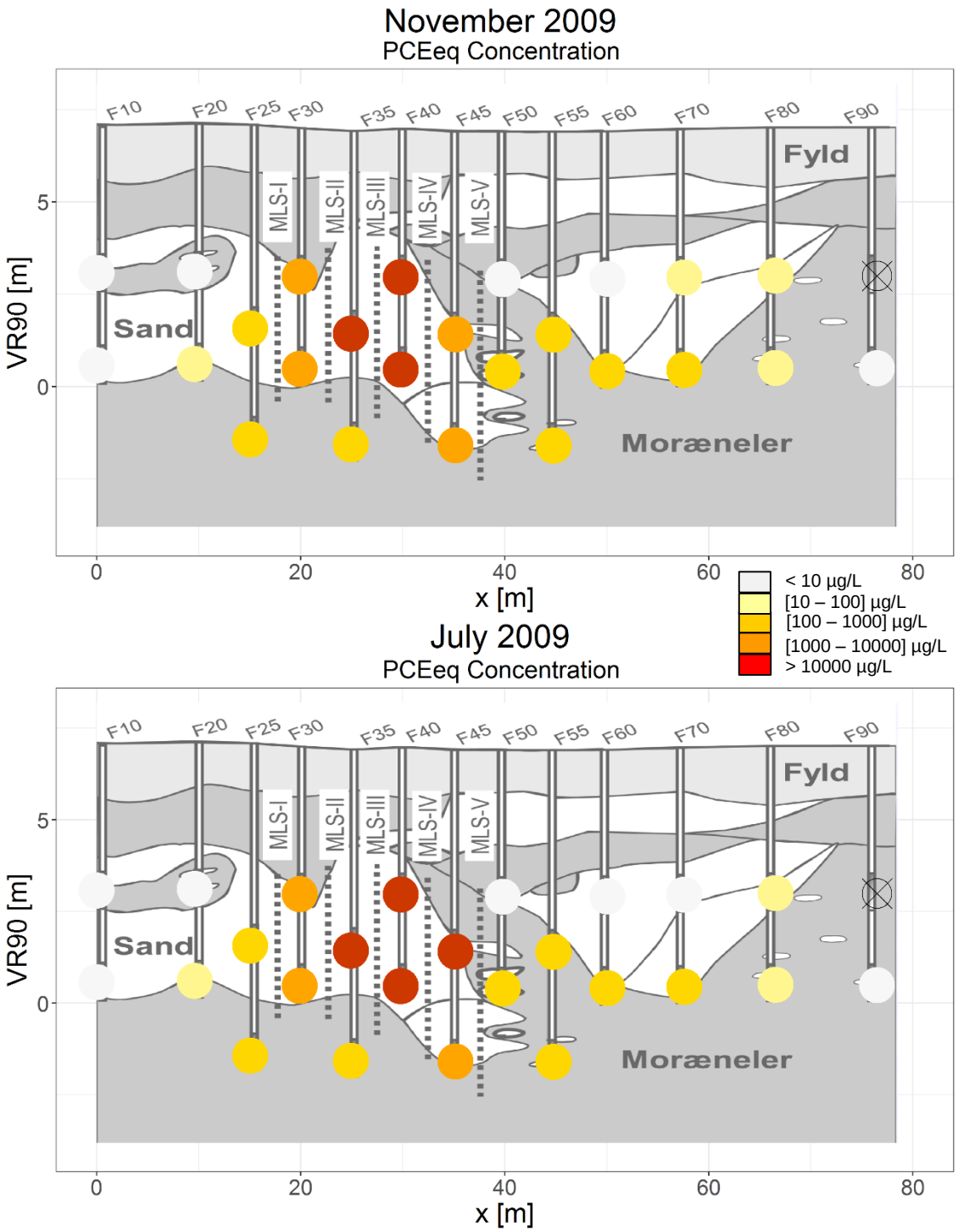
November 2009
PCEeq Concentration
F10
F20
F25
F30
F35
F40
F45
F50
F55
F60
F70
F80
F90
MLS-I
MLS-II
MLS-III
MLS-IV
MLS-V
Fyld
Sand
Moræneler
VR90 [m]
5
0
0
20
40
60
80
x [m]
< 10 µg/L
[10 – 100] µg/L
[100 – 1000] µg/L
[1000 – 10000] µg/L
> 10000 µg/L
July 2009
PCEeq Concentration
F10
F20
F25
F30
F35
F40
F45
F50
F55
F60
F70
F80
F90
MLS-I
MLS-II
MLS-III
MLS-IV
MLS-V
Fyld
Sand
Moræneler
VR90 [m]
5
0
0
20
40
60
80
x [m]

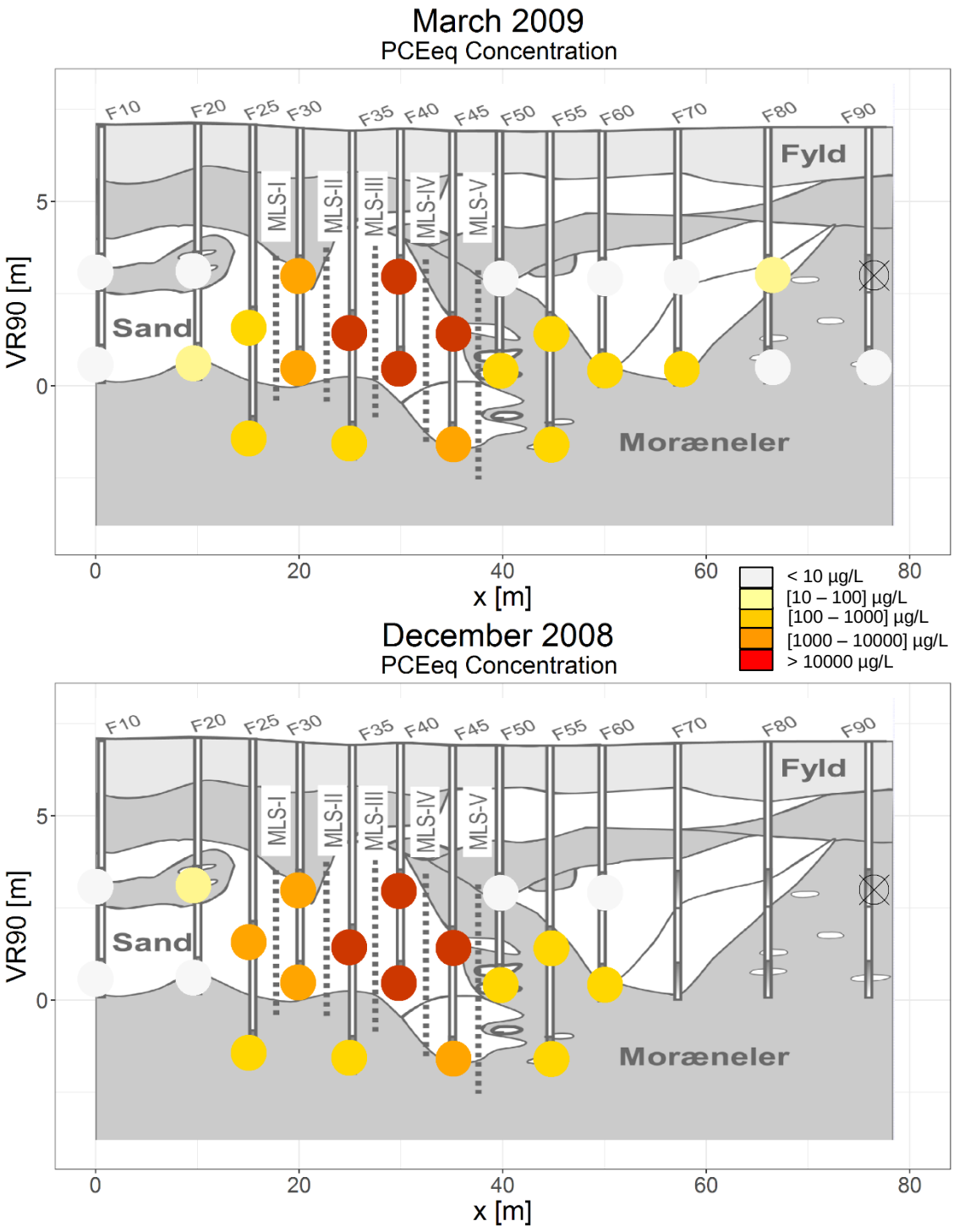
March 2009
PCEeq Concentration
F10
F20
F25
F30
F35
F40
F45
F50
F55
F60
F70
F80
F90
MLS-I
MLS-II
MLS-III
MLS-IV
MLS-V
Fyld
Sand
Moræneler
VR90 [m]
5
0
0
20
40
60
80
x [m]
< 10 µg/L
[10 – 100] µg/L
[100 – 1000] µg/L
[1000 – 10000] µg/L
> 10000 µg/L
December 2008
PCEeq Concentration
F10
F20
F25
F30
F35
F40
F45
F50
F55
F60
F70
F80
F90
MLS-I
MLS-II
MLS-III
MLS-IV
MLS-V
Fyld
Sand
Moræneler
VR90 [m]
5
0
0
20
40
60
80
x [m]

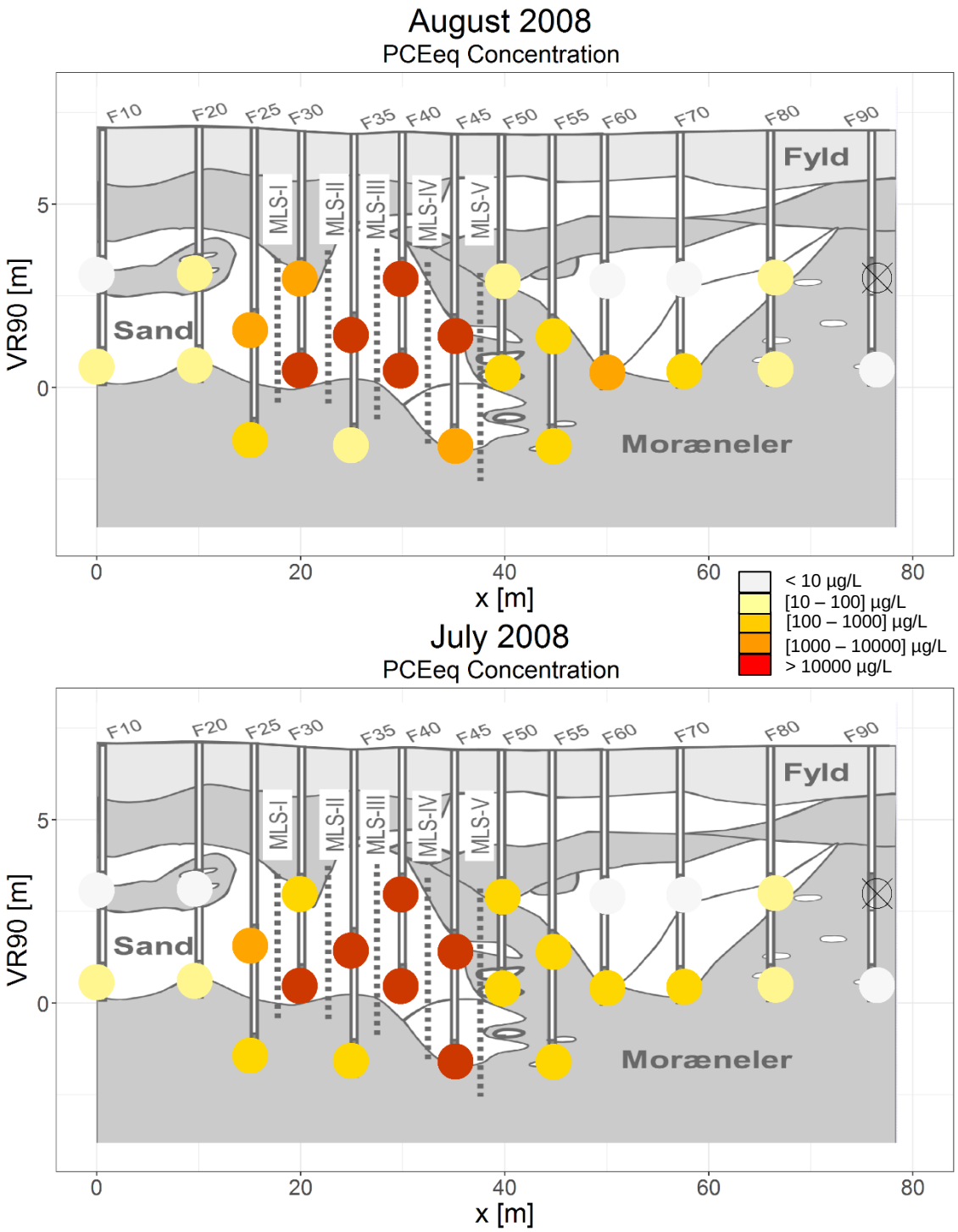
August 2008
PCEeq Concentration
F10
F20
F25
F30
F35
F40
F45
F50
F55
F60
F70
F80
F90
MLS-I
MLS-II
MLS-III
MLS-IV
MLS-V
Fyld
Sand
Moræneler
VR90 [m]
5
0
0
20
40
60
80
x [m]
< 10 µg/L
[10 – 100] µg/L
[100 – 1000] µg/L
[1000 – 10000] µg/L
> 10000 µg/L
July 2008
PCEeq Concentration
F10
F20
F25
F30
F35
F40
F45
F50
F55
F60
F70
F80
F90
MLS-I
MLS-II
MLS-III
MLS-IV
MLS-V
Fyld
Sand
Moræneler
VR90 [m]
5
0
0
20
40
60
80
x [m]

C.2. Fwells data – PCE

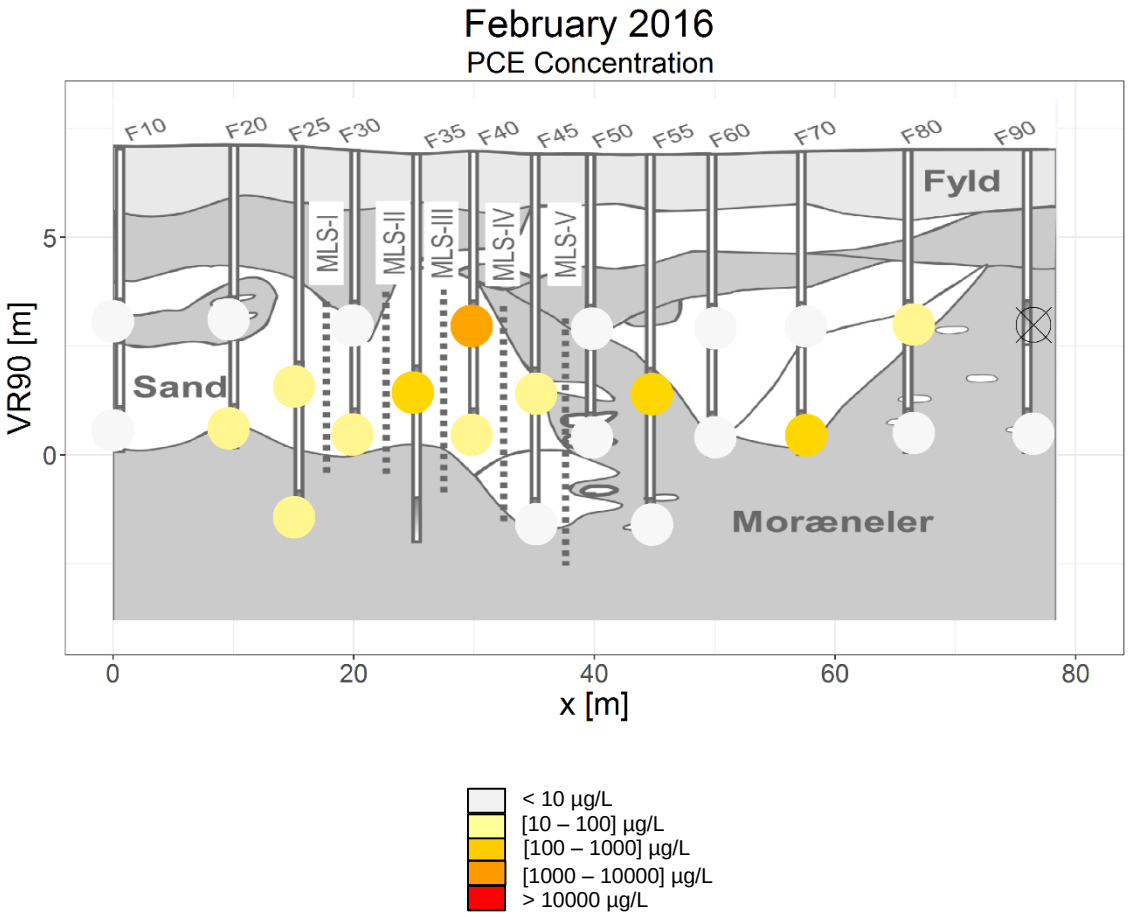

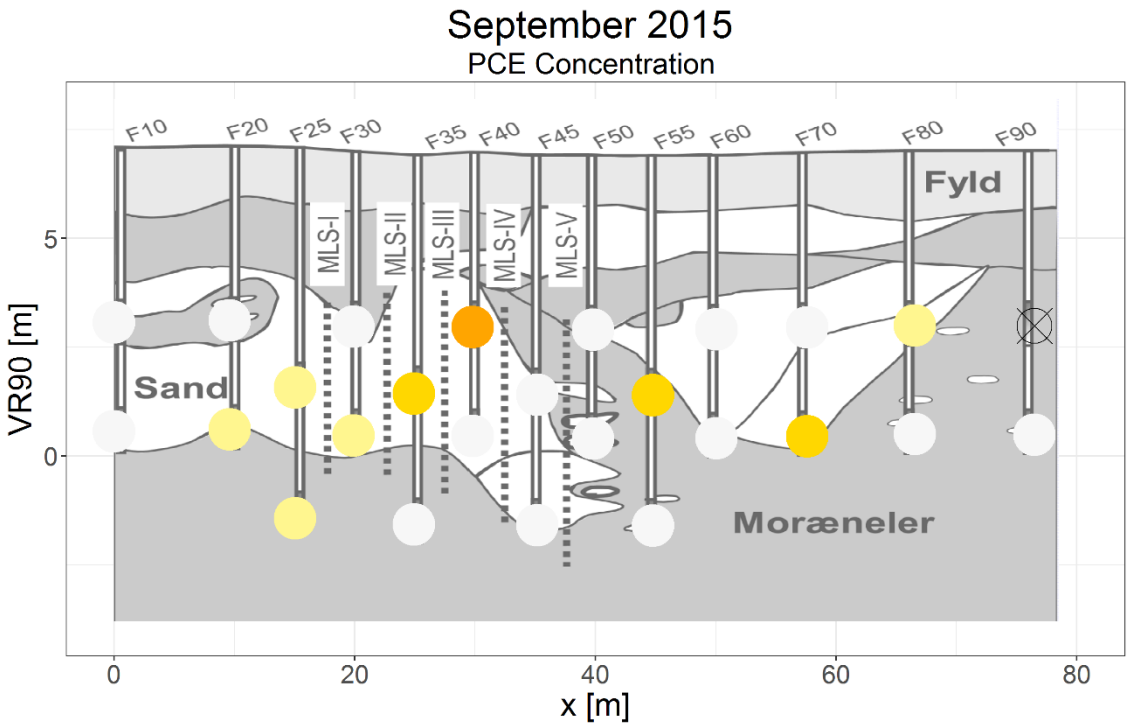
September 2015
PCE Concentration
F10
F20
F25
F30
F35
F40
F45
F50
F55
F60
F70
F80
F90
MLS-I
MLS-II
MLS-III
MLS-IV
MLS-V
Fyld
Sand
Moræneler
VR90 [m]
5
0
0
20
40
60
80
x [m]

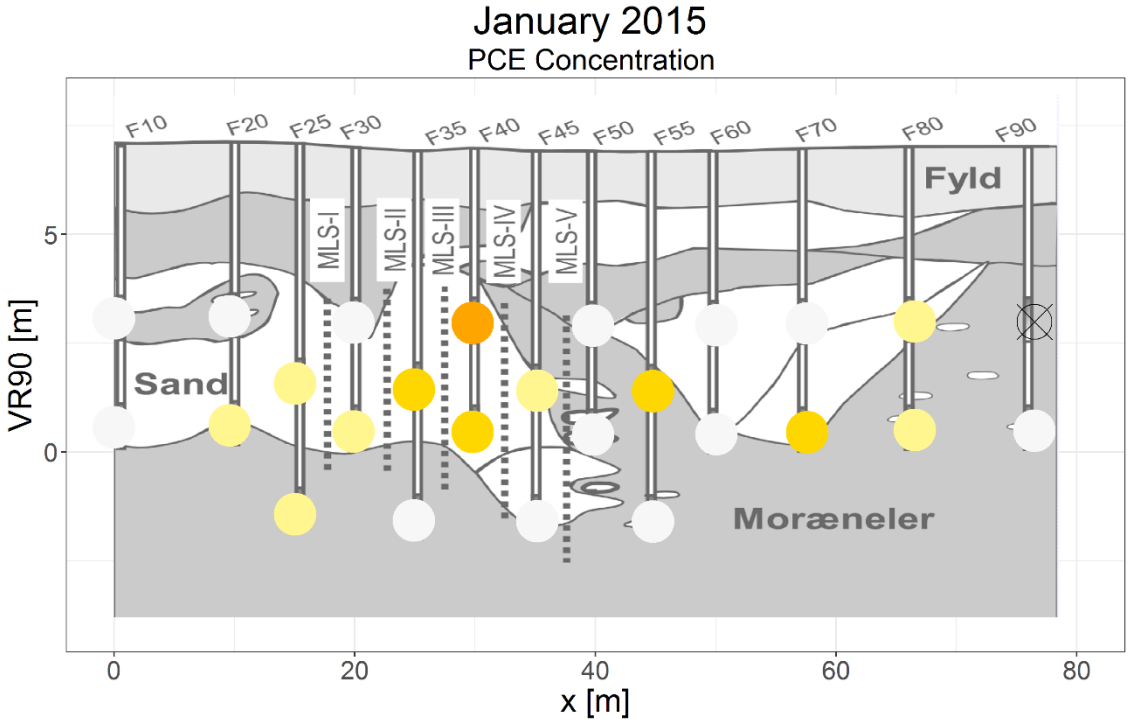
January 2015
PCE Concentration
F10
F20
F25
F30
F35
F40
F45
F50
F55
F60
F70
F80
F90
MLS-I
MLS-II
MLS-III
MLS-IV
MLS-V
Fyld
Sand
Moræneler
VR90 [m]
5
0
0
20
40
60
80
x [m]

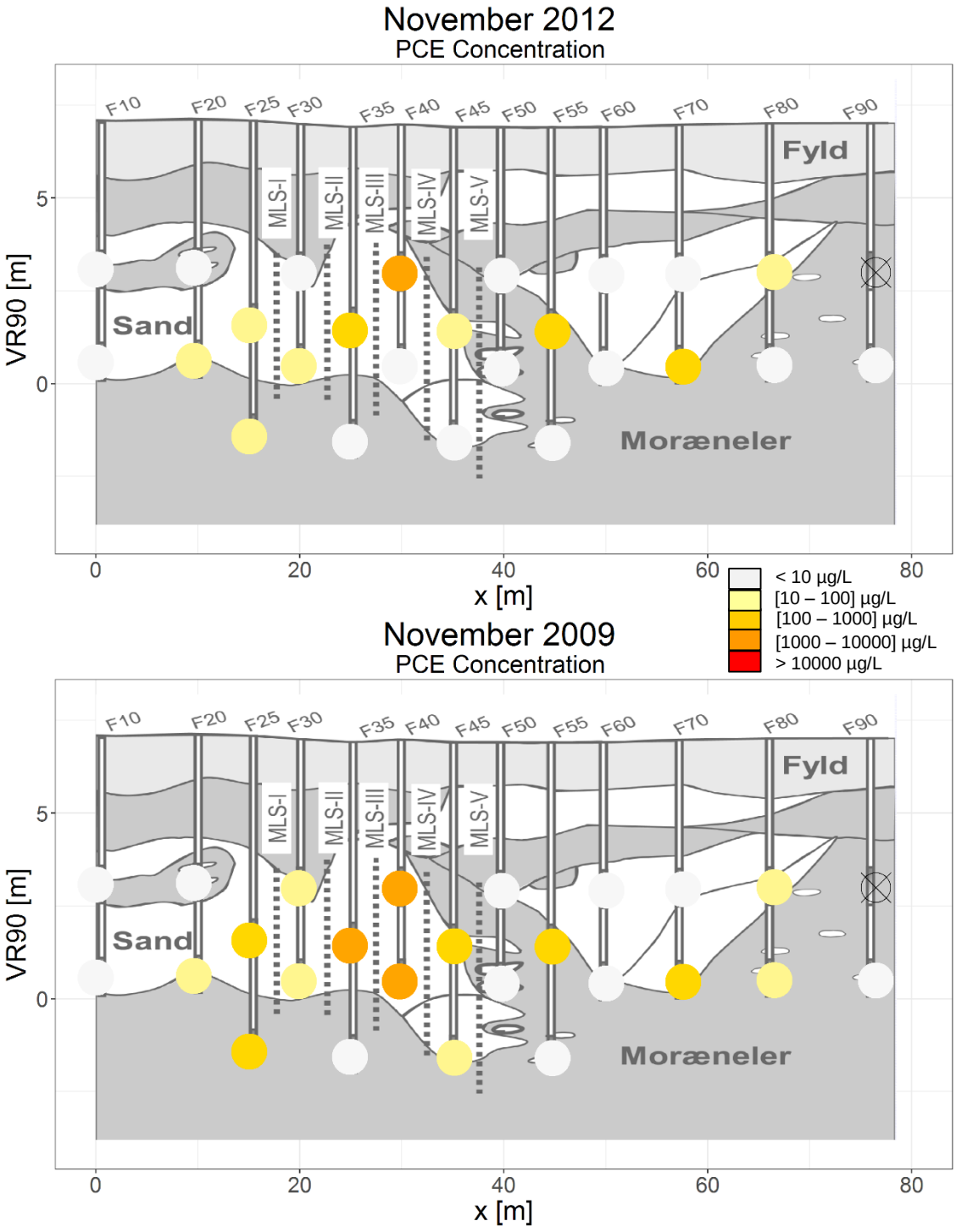
November 2012
PCE Concentration
F10
F20
F25
F30
F35
F40
F45
F50
F55
F60
F70
F80
F90
MLS-I
MLS-II
MLS-III
MLS-IV
MLS-V
Fyld
Sand
Moræneler
VR90 [m]
5
0
0
20
40
60
80
x [m]
< 10 µg/L
[10 – 100] µg/L
[100 – 1000] µg/L
[1000 – 10000] µg/L
> 10000 µg/L
November 2009
PCE Concentration
F10
F20
F25
F30
F35
F40
F45
F50
F55
F60
F70
F80
F90
MLS-I
MLS-II
MLS-III
MLS-IV
MLS-V
Fyld
Sand
Moræneler
VR90 [m]
5
0
0
20
40
60
80
x [m]

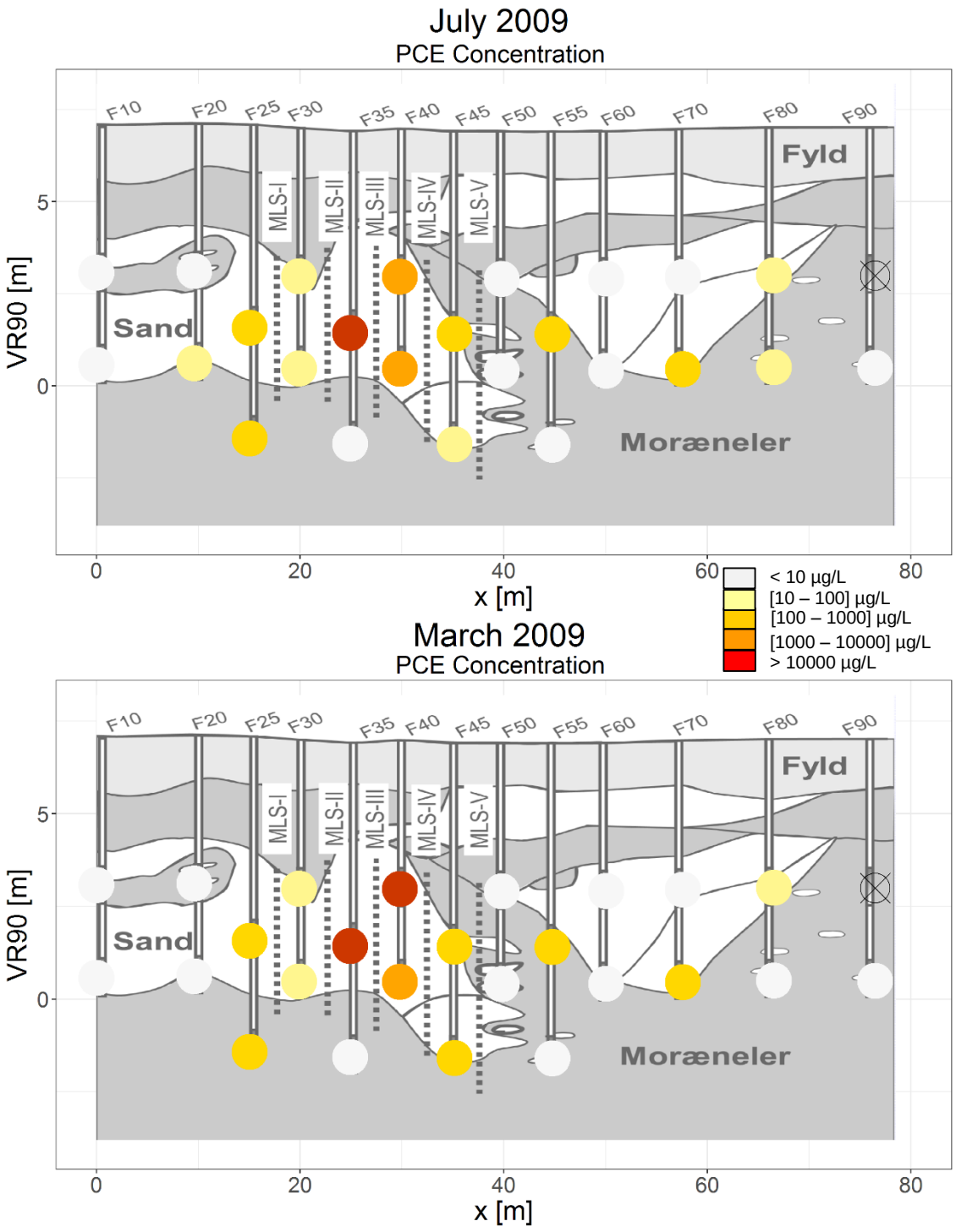
July 2009
PCE Concentration
F10
F20
F25
F30
F35
F40
F45
F50
F55
F60
F70
F80
F90
MLS-I
MLS-II
MLS-III
MLS-IV
MLS-V
Fyld
Sand
Moræneler
VR90 [m]
x [m]
< 10 µg/L
[10 – 100] µg/L
[100 – 1000] µg/L
[1000 – 10000] µg/L
> 10000 µg/L
March 2009
PCE Concentration

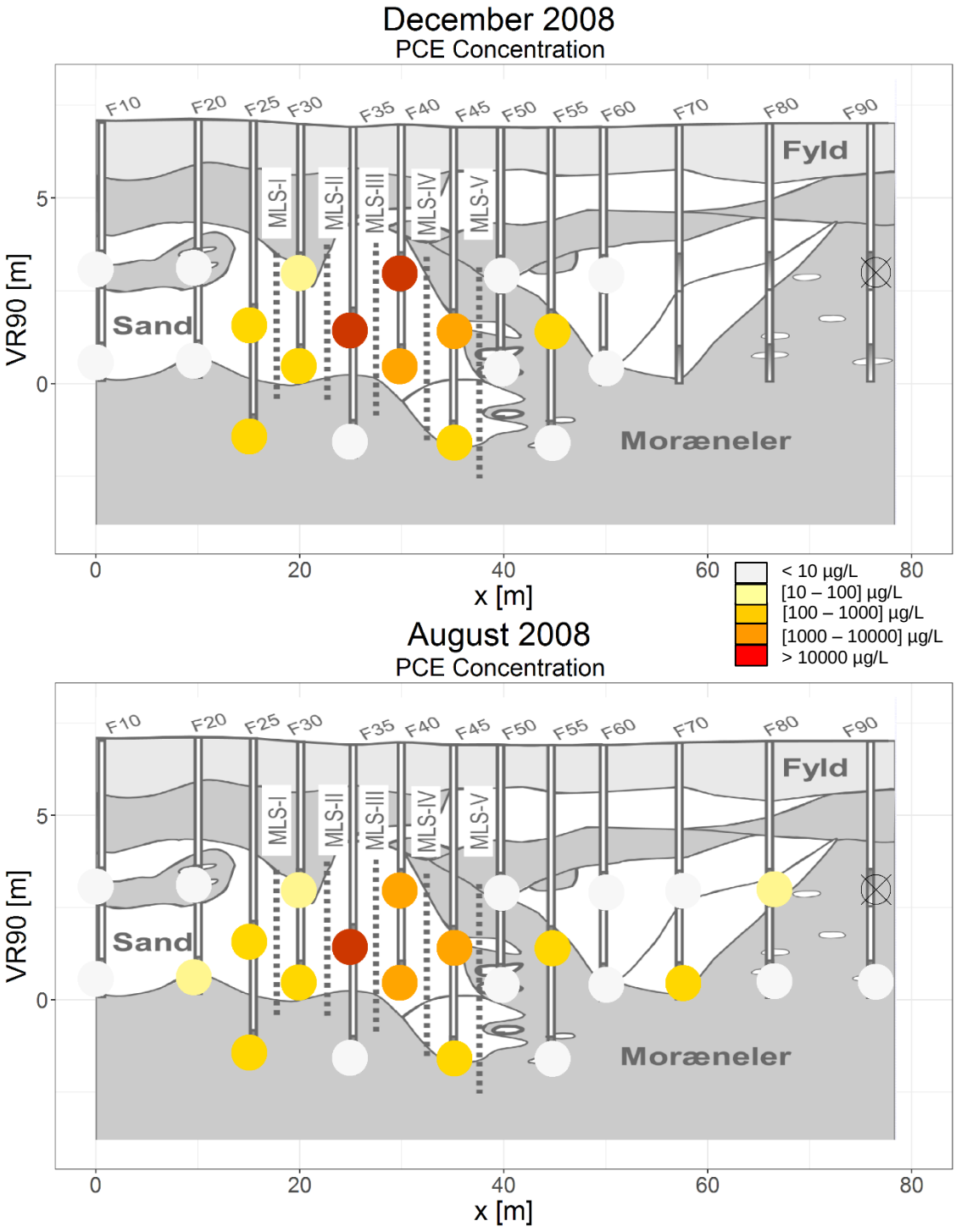
December 2008
PCE Concentration
F10
F20
F25
F30
F35
F40
F45
F50
F55
F60
F70
F80
F90
MLS-I
MLS-II
MLS-III
MLS-IV
MLS-V
Fyld
Sand
Moræneler
VR90 [m]
5
0
0
20
40
60
80
x [m]
< 10 µg/L
[10 – 100] µg/L
[100 – 1000] µg/L
[1000 – 10000] µg/L
> 10000 µg/L
August 2008
PCE Concentration
F10
F20
F25
F30
F35
F40
F45
F50
F55
F60
F70
F80
F90
MLS-I
MLS-II
MLS-III
MLS-IV
MLS-V
Fyld
Sand
Moræneler
VR90 [m]
5
0
0
20
40
60
80
x [m]

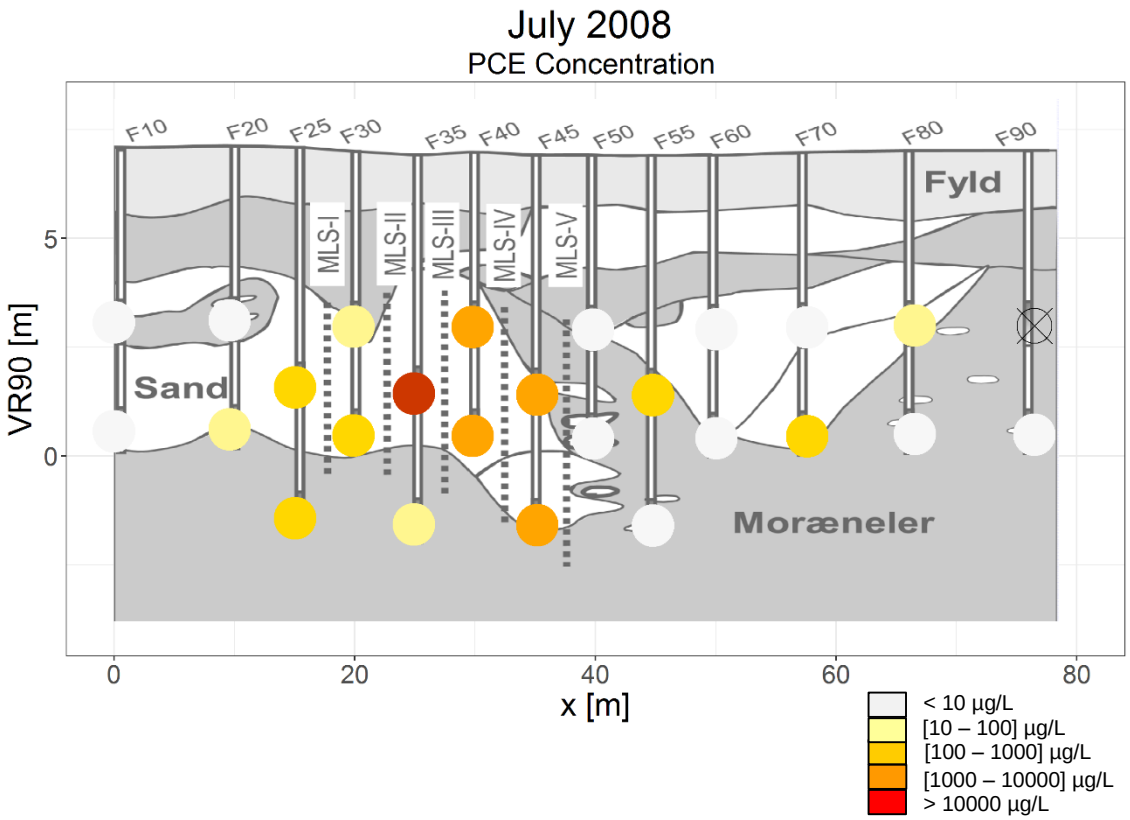
July 2008
PCE Concentration
F10
F20
F25
F30
F35
F40
F45
F50
F55
F60
F70
F80
F90
MLS-I
MLS-II
MLS-III
MLS-IV
MLS-V
Fyld
Sand
Moræneler
VR90 [m]
5
0
0
20
40
60
80
x [m]
< 10 µg/L
[10 – 100] µg/L
[100 – 1000] µg/L
[1000 – 10000] µg/L
> 10000 µg/L

C.3. Fwells data – TCE

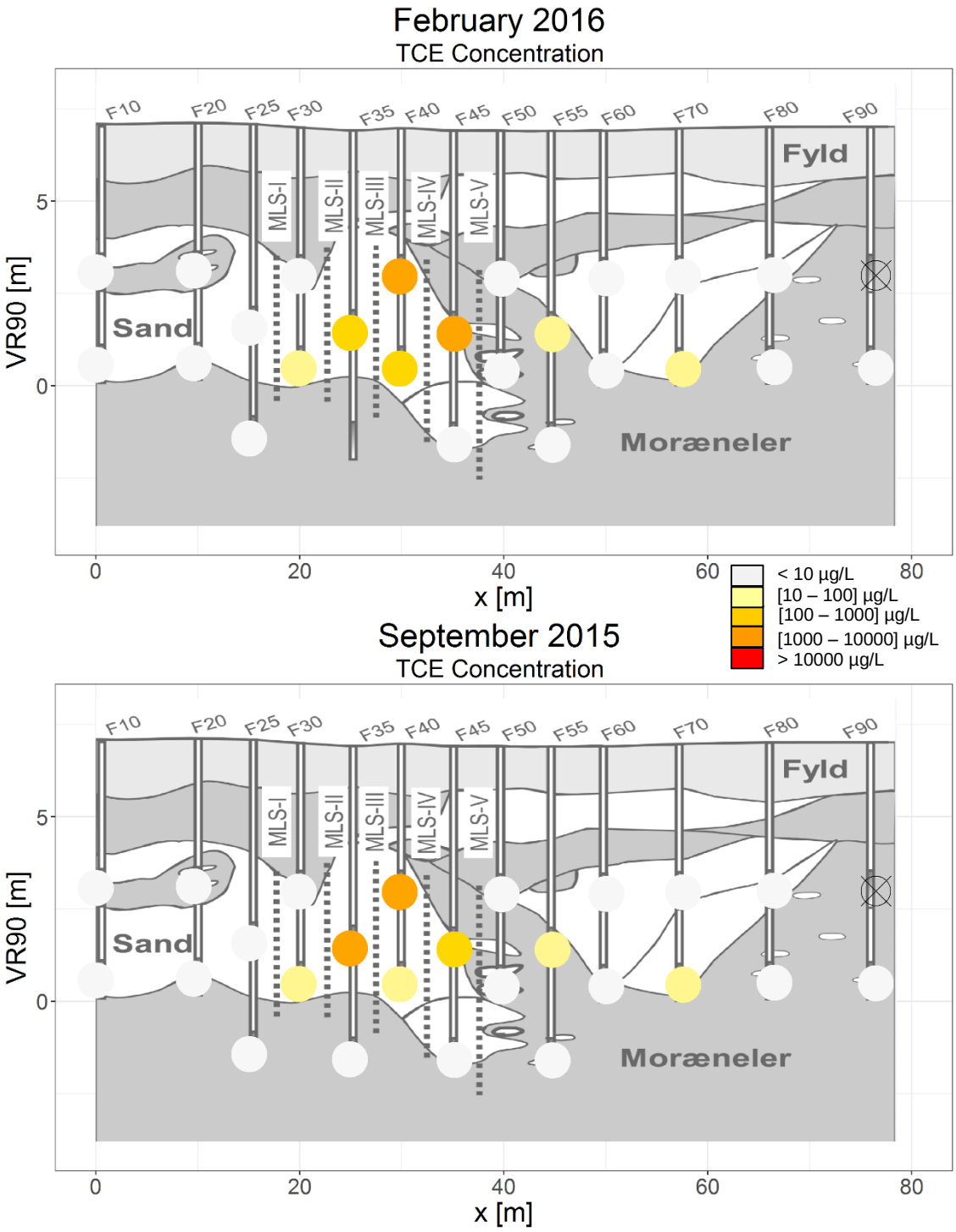

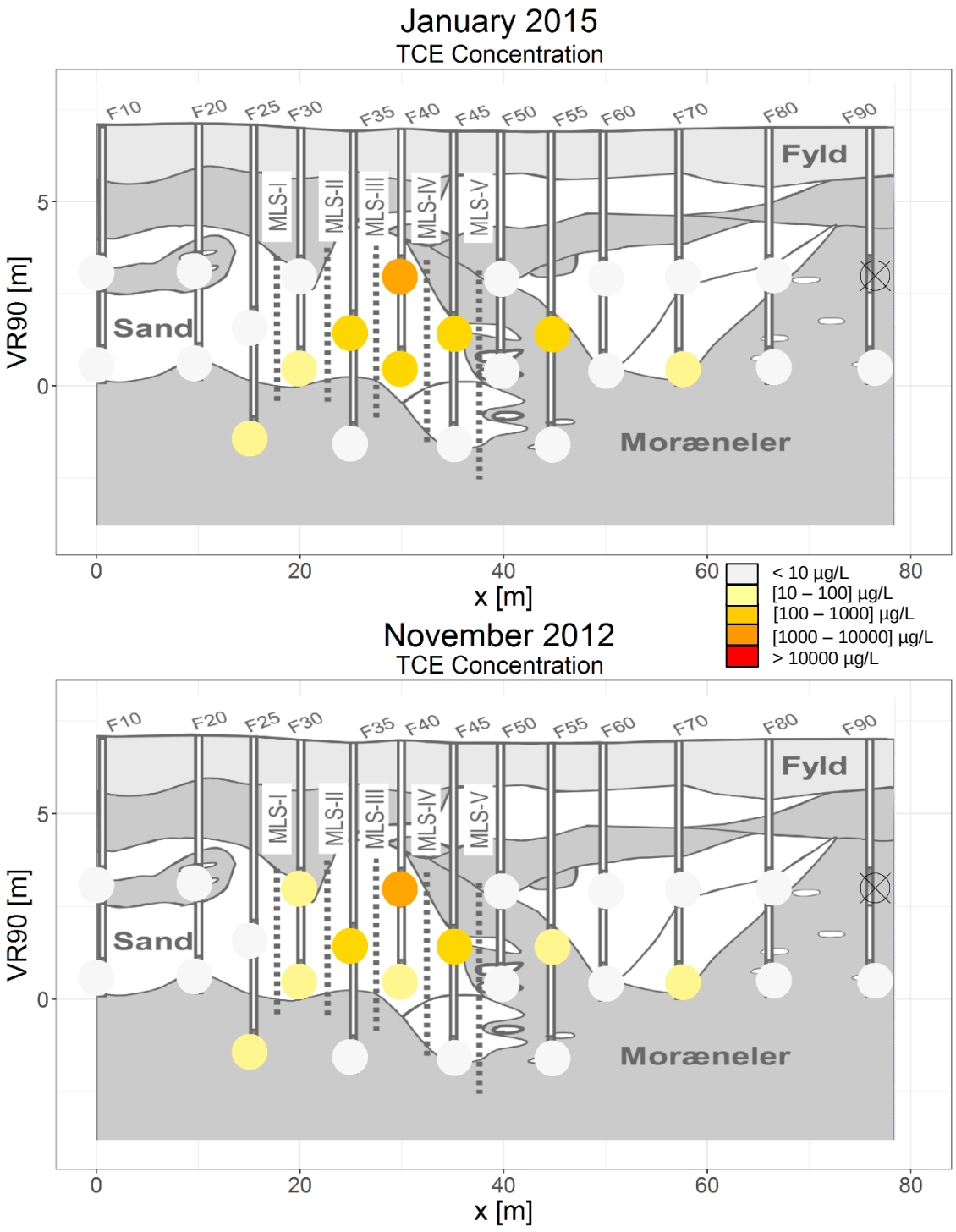
January 2015
TCE Concentration
F10
F20
F25
F30
F35
F40
F45
F50
F55
F60
F70
F80
F90
MLS-I
MLS-II
MLS-III
MLS-IV
MLS-V
Fyld
Sand
Moræneler
VR90 [m]
5
0
0
20
40
60
80
x [m]
< 10 µg/L
[10 – 100] µg/L
[100 – 1000] µg/L
[1000 – 10000] µg/L
> 10000 µg/L
November 2012
TCE Concentration
F10
F20
F25
F30
F35
F40
F45
F50
F55
F60
F70
F80
F90
MLS-I
MLS-II
MLS-III
MLS-IV
MLS-V
Fyld
Sand
Moræneler
VR90 [m]
5
0
0
20
40
60
80
x [m]

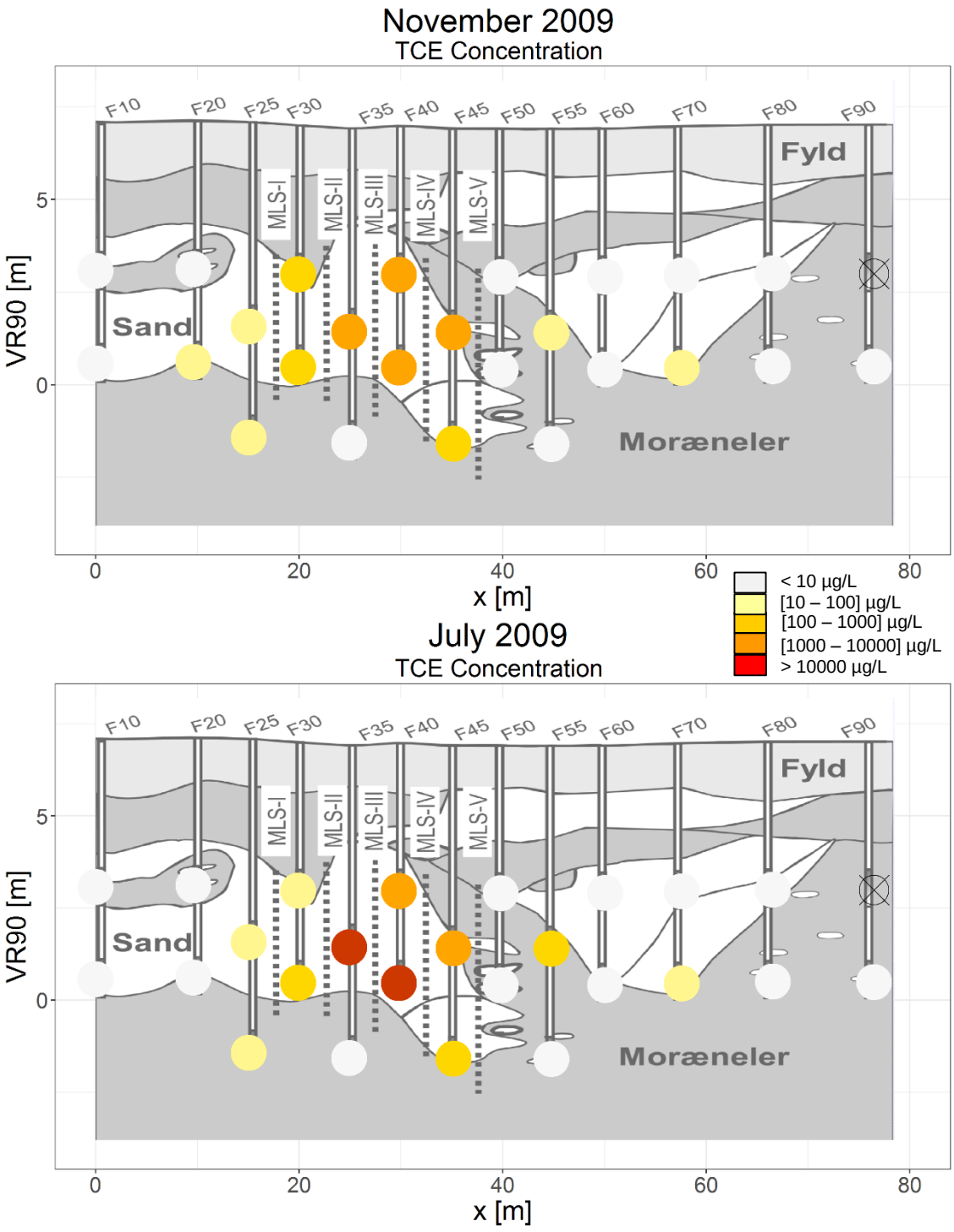
November 2009
TCE Concentration
F10
F20
F25
F30
F35
F40
F45
F50
F55
F60
F70
F80
F90
MLS-I
MLS-II
MLS-III
MLS-IV
MLS-V
Fyld
Sand
Moræneler
VR90 [m]
5
0
0
20
40
60
80
x [m]
< 10 µg/L
[10 – 100] µg/L
[100 – 1000] µg/L
[1000 – 10000] µg/L
> 10000 µg/L
July 2009
TCE Concentration
F10
F20
F25
F30
F35
F40
F45
F50
F55
F60
F70
F80
F90
MLS-I
MLS-II
MLS-III
MLS-IV
MLS-V
Fyld
Sand
Moræneler
VR90 [m]
5
0
0
20
40
60
80
x [m]

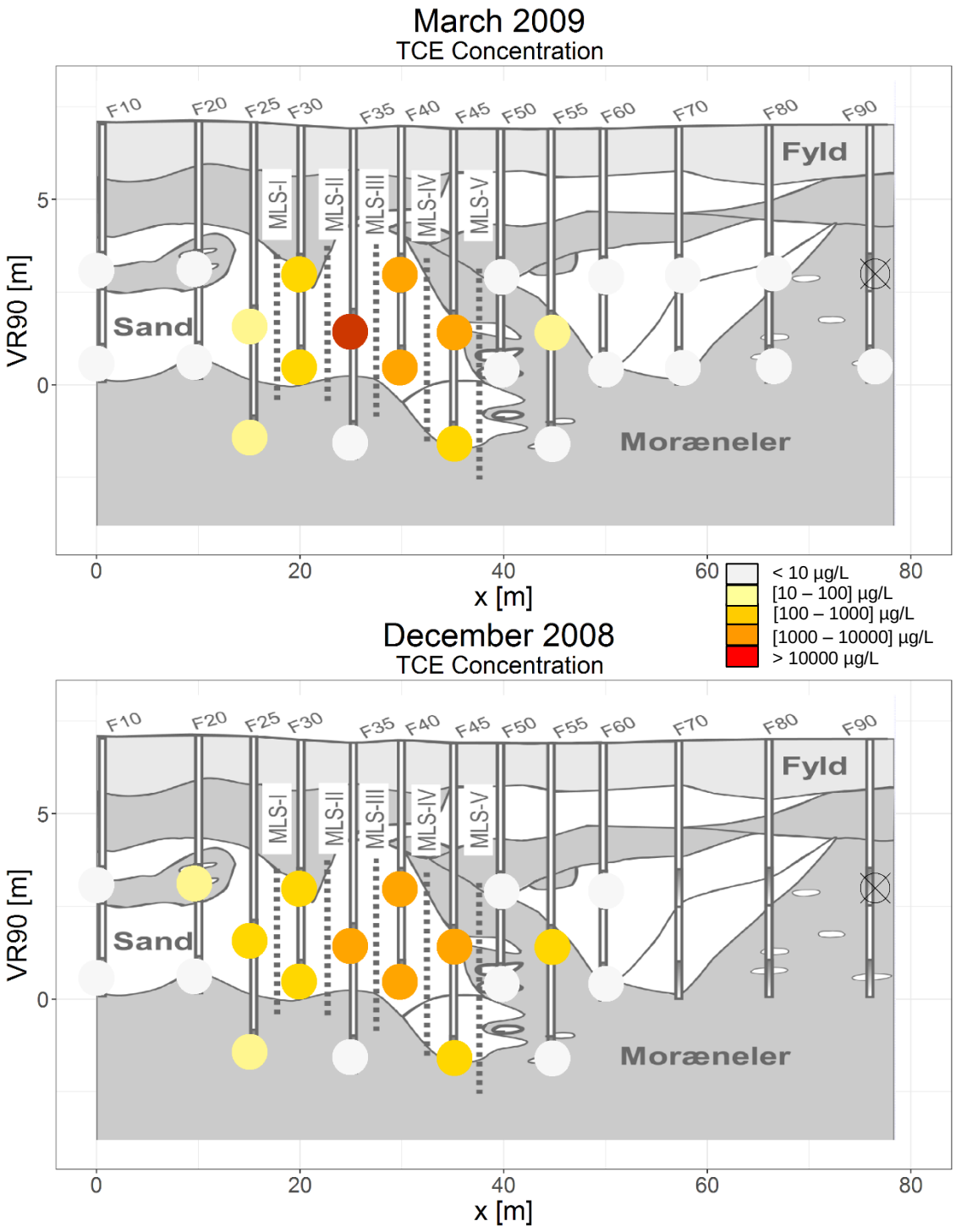
March 2009
TCE Concentration
F10
F20
F25
F30
F35
F40
F45
F50
F55
F60
F70
F80
F90
MLS-I
MLS-II
MLS-III
MLS-IV
MLS-V
Fyld
Sand
Moræneler
VR90 [m]
5
0
0
20
40
60
80
x [m]
< 10 µg/L
[10 – 100] µg/L
[100 – 1000] µg/L
[1000 – 10000] µg/L
> 10000 µg/L
December 2008
TCE Concentration
F10
F20
F25
F30
F35
F40
F45
F50
F55
F60
F70
F80
F90
MLS-I
MLS-II
MLS-III
MLS-IV
MLS-V
Fyld
Sand
Moræneler
VR90 [m]
5
0
0
20
40
60
80
x [m]

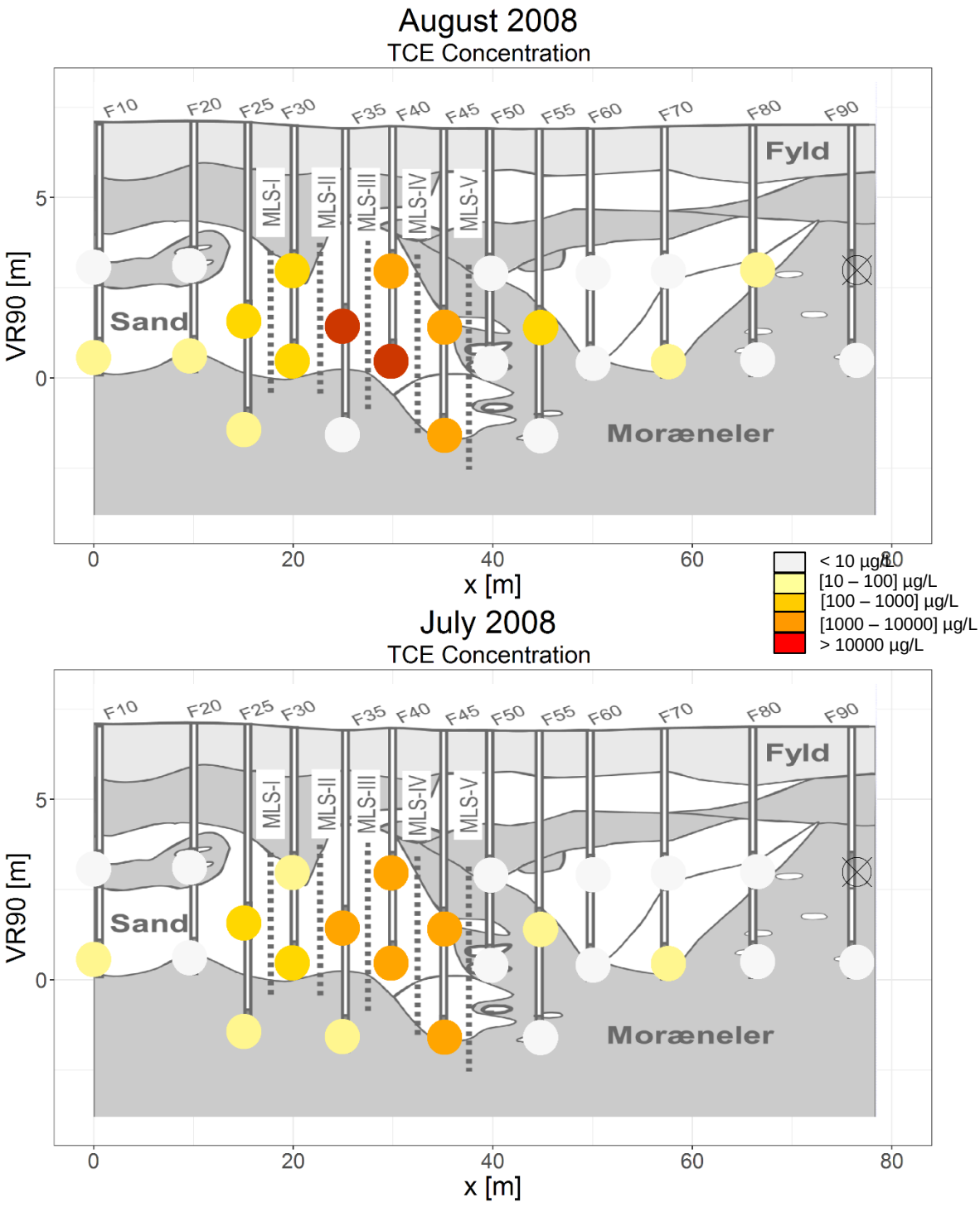
August 2008
TCE Concentration
F10
F20
F25
F30
F35
F40
F45
F50
F55
F60
F70
F80
F90
MLS-I
MLS-II
MLS-III
MLS-IV
MLS-V
Fyld
Sand
Moræneler
VR90 [m]
5
0
0
20
40
60
80
x [m]
< 10 µg/L
[10 – 100] µg/L
[100 – 1000] µg/L
[1000 – 10000] µg/L
> 10000 µg/L
July 2008
TCE Concentration
F10
F20
F25
F30
F35
F40
F45
F50
F55
F60
F70
F80
F90
MLS-I
MLS-II
MLS-III
MLS-IV
MLS-V
Fyld
Sand
Moræneler
VR90 [m]
5
0
0
20
40
60
80
x [m]

C.4. Fwells data – cisDCE

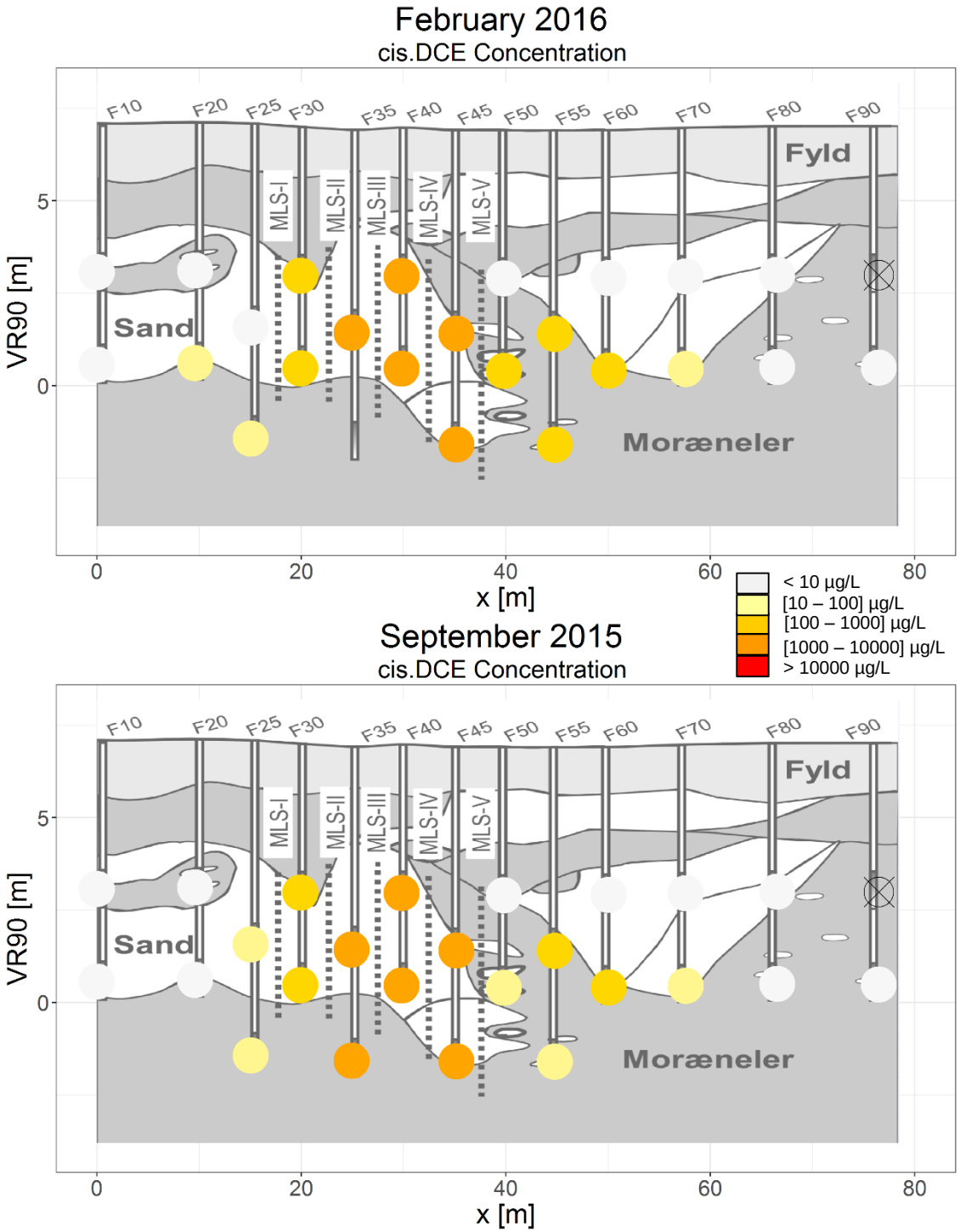

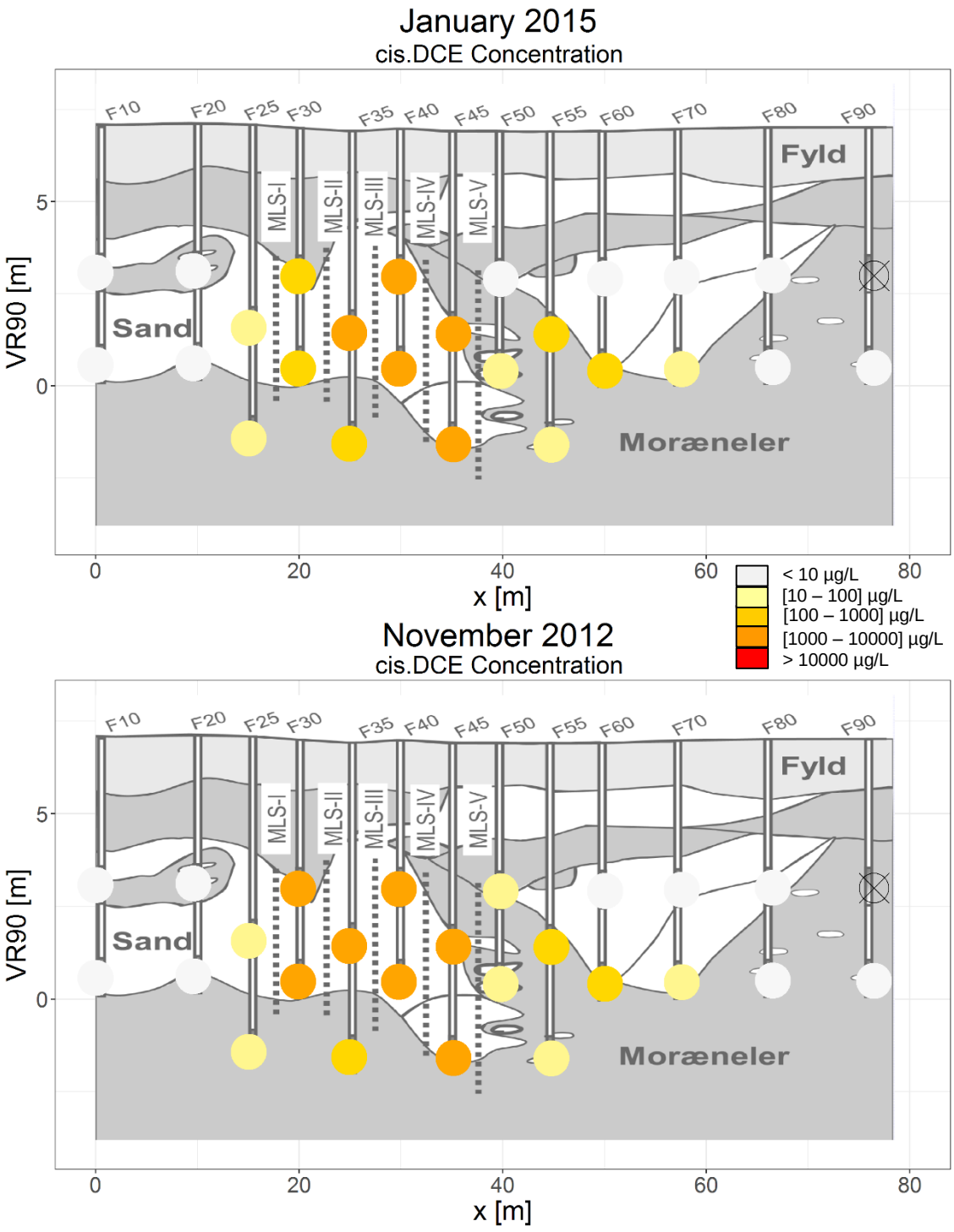
January 2015
cis.DCE Concentration
F10
F20
F25
F30
F35
F40
F45
F50
F55
F60
F70
F80
F90
MLS-I
MLS-II
MLS-III
MLS-IV
MLS-V
Fyld
Sand
Moræneler
VR90 [m]
5
0
0
20
40
60
80
x [m]
< 10 µg/L
[10 – 100] µg/L
[100 – 1000] µg/L
[1000 – 10000] µg/L
> 10000 µg/L
November 2012
cis.DCE Concentration
F10
F20
F25
F30
F35
F40
F45
F50
F55
F60
F70
F80
F90
MLS-I
MLS-II
MLS-III
MLS-IV
MLS-V
Fyld
Sand
Moræneler
VR90 [m]
5
0
0
20
40
60
80
x [m]

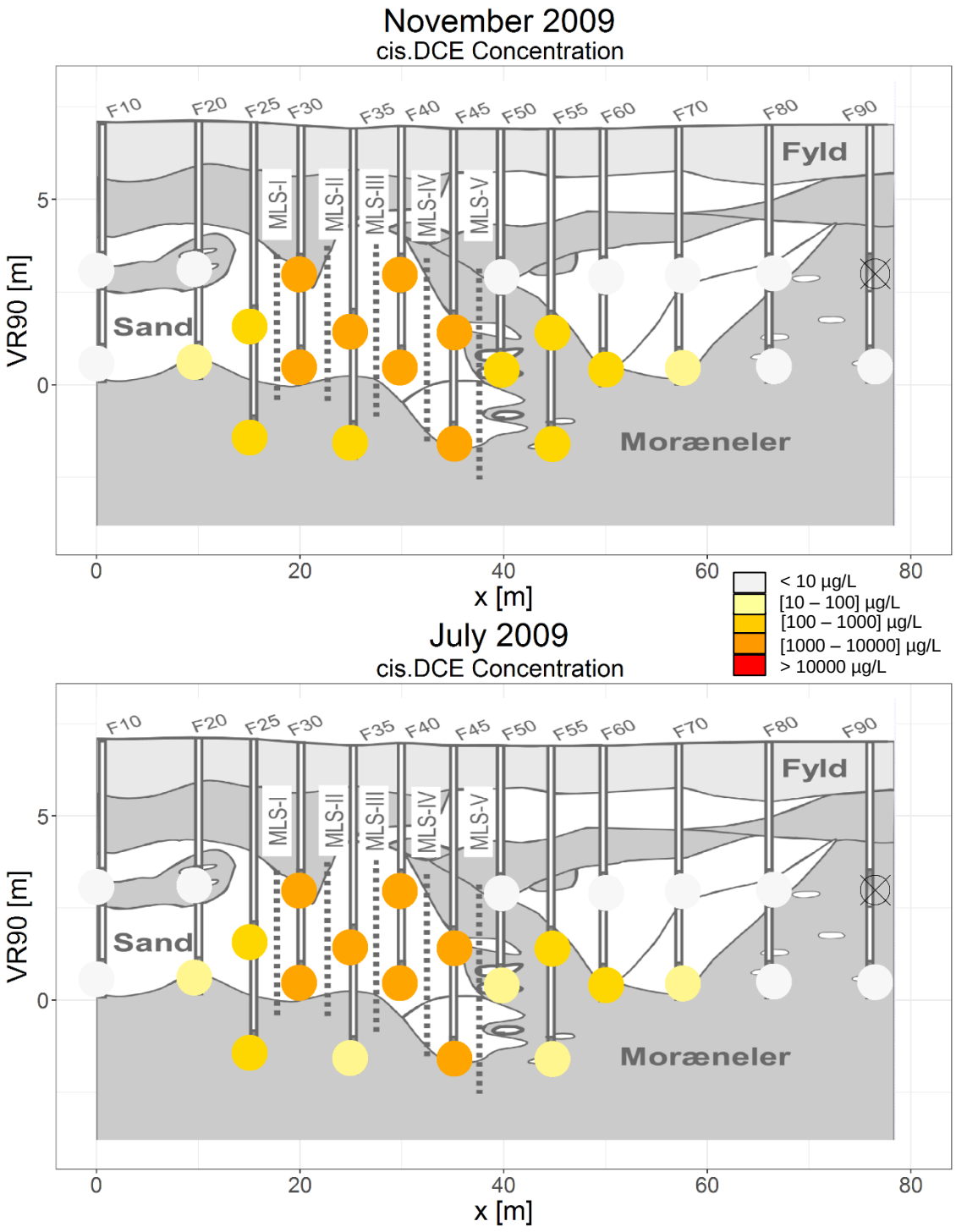
November 2009
cis.DCE Concentration
F10
F20
F25
F30
F35
F40
F45
F50
F55
F60
F70
F80
F90
MLS-I
MLS-II
MLS-III
MLS-IV
MLS-V
Fyld
Sand
Moræneler
VR90 [m]
5
0
0
20
40
60
80
x [m]
< 10 µg/L
[10 – 100] µg/L
[100 – 1000] µg/L
[1000 – 10000] µg/L
> 10000 µg/L
July 2009
cis.DCE Concentration
F10
F20
F25
F30
F35
F40
F45
F50
F55
F60
F70
F80
F90
MLS-I
MLS-II
MLS-III
MLS-IV
MLS-V
Fyld
Sand
Moræneler
VR90 [m]
5
0
0
20
40
60
80
x [m]

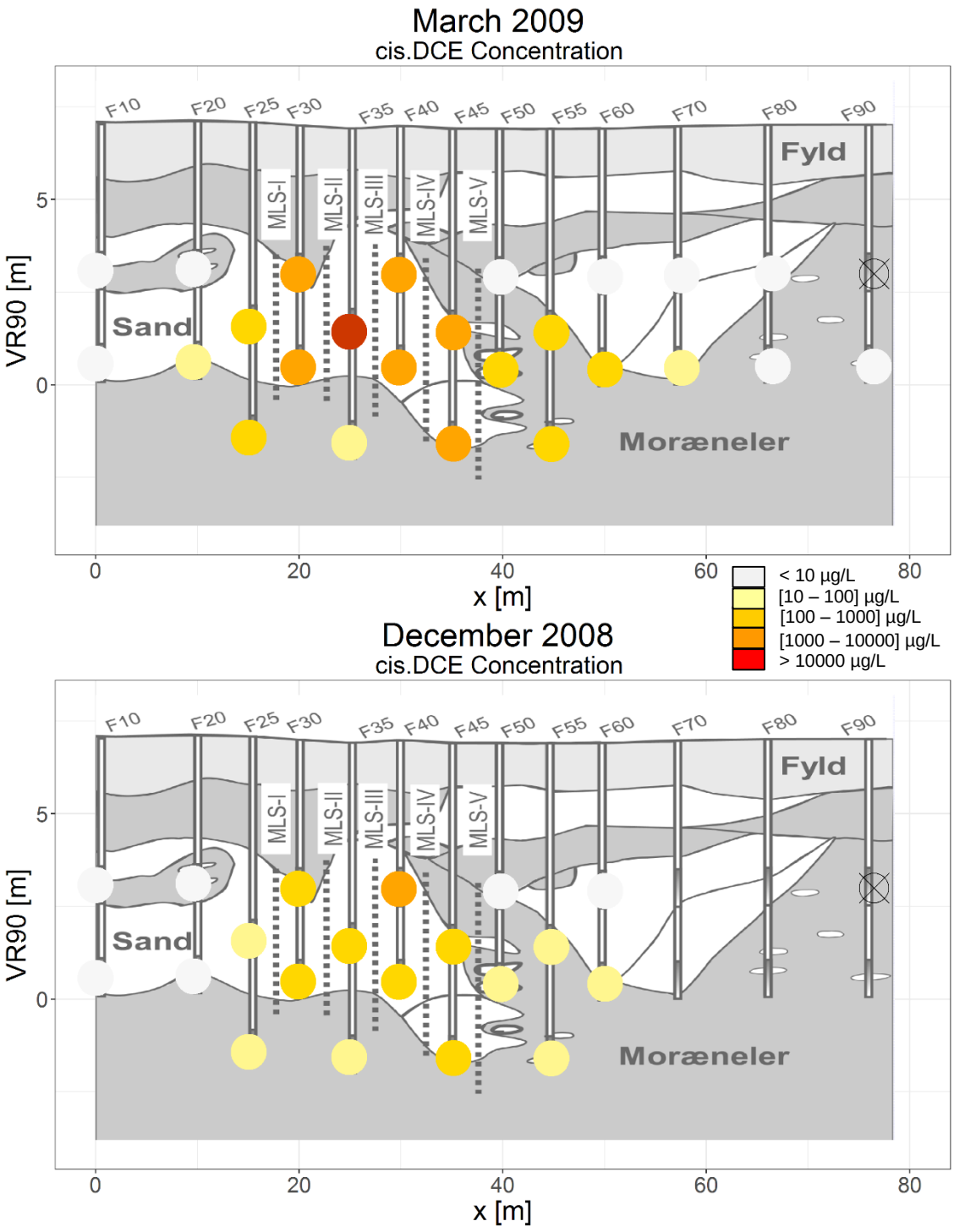
March 2009
cis.DCE Concentration
F10
F20
F25
F30
F35
F40
F45
F50
F55
F60
F70
F80
F90
MLS-I
MLS-II
MLS-III
MLS-IV
MLS-V
Fyld
Sand
Moræneler
VR90 [m]
5
0
0
20
40
60
80
x [m]
< 10 µg/L
[10 – 100] µg/L
[100 – 1000] µg/L
[1000 – 10000] µg/L
> 10000 µg/L
December 2008
cis.DCE Concentration
F10
F20
F25
F30
F35
F40
F45
F50
F55
F60
F70
F80
F90
MLS-I
MLS-II
MLS-III
MLS-IV
MLS-V
Fyld
Sand
Moræneler
VR90 [m]
5
0
0
20
40
60
80
x [m]

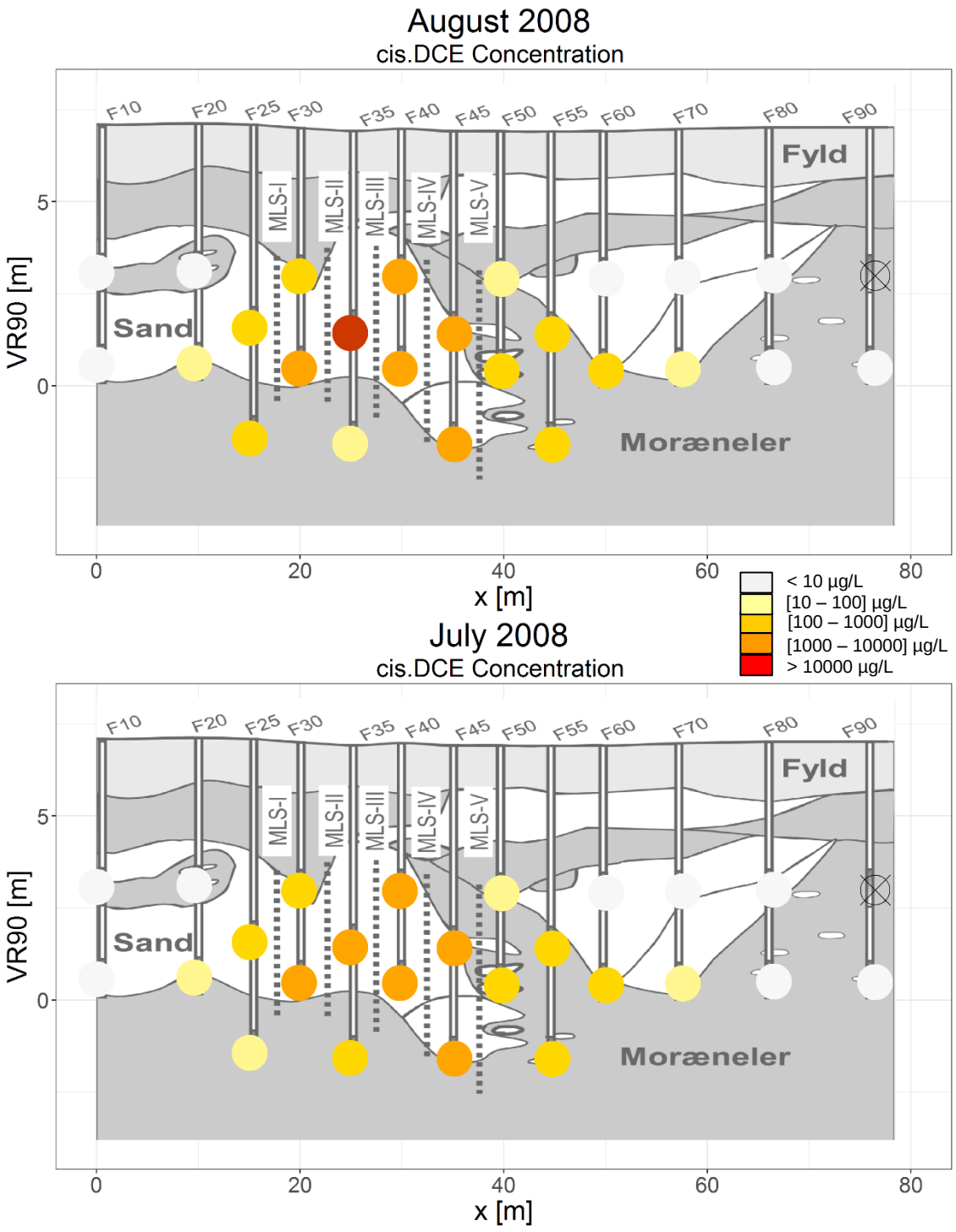
August 2008
cis.DCE Concentration
F10
F20
F25
F30
F35
F40
F45
F50
F55
F60
F70
F80
F90
MLS-I
MLS-II
MLS-III
MLS-IV
MLS-V
Fyld
Sand
Moræneler
VR90 [m]
5
0
0
20
40
60
80
x [m]
< 10 µg/L
[10 – 100] µg/L
[100 – 1000] µg/L
[1000 – 10000] µg/L
> 10000 µg/L
July 2008
cis.DCE Concentration
F10
F20
F25
F30
F35
F40
F45
F50
F55
F60
F70
F80
F90
MLS-I
MLS-II
MLS-III
MLS-IV
MLS-V
Fyld
Sand
Moræneler
VR90 [m]
5
0
0
20
40
60
80
x [m]

C.5. Fwells data – VC

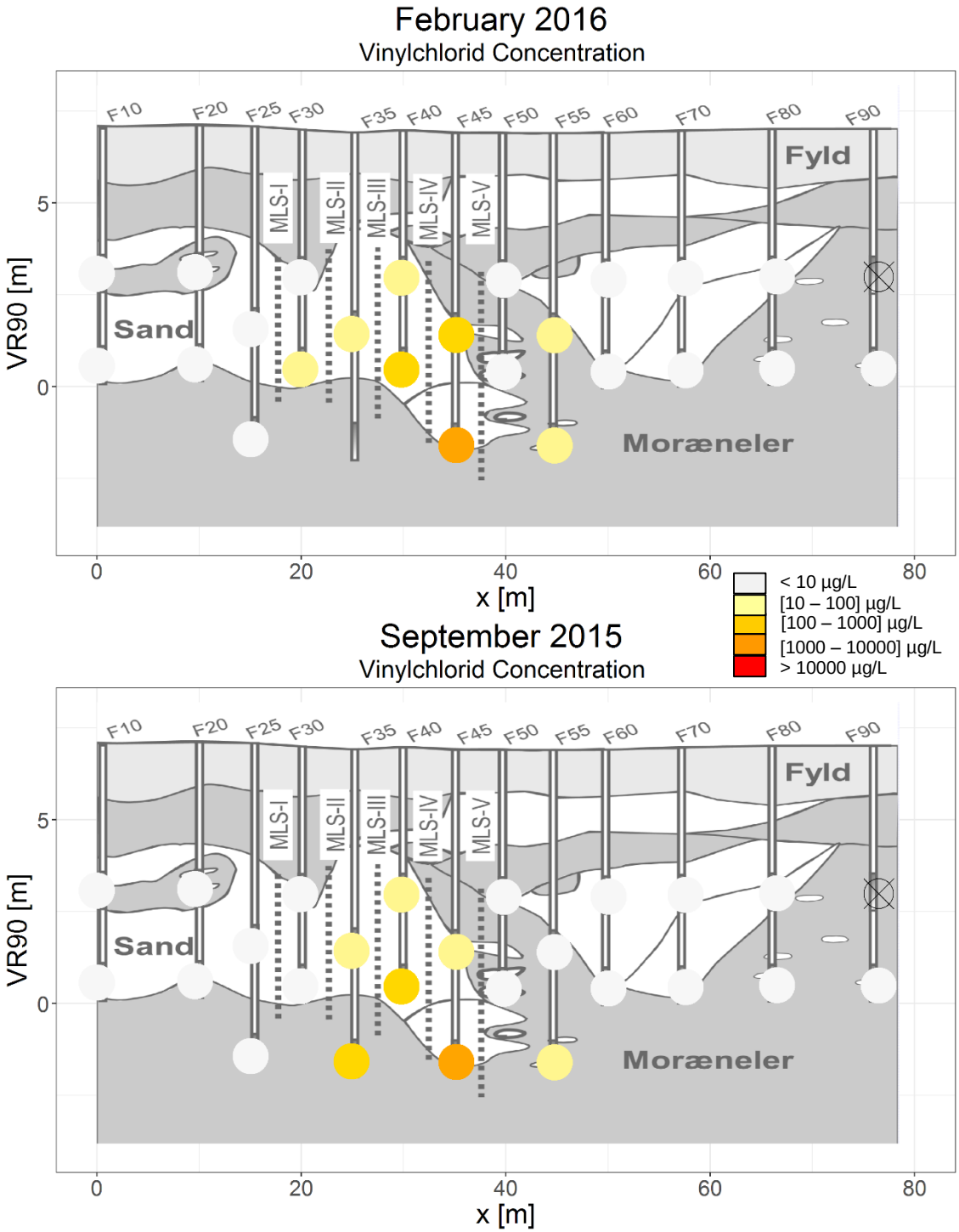

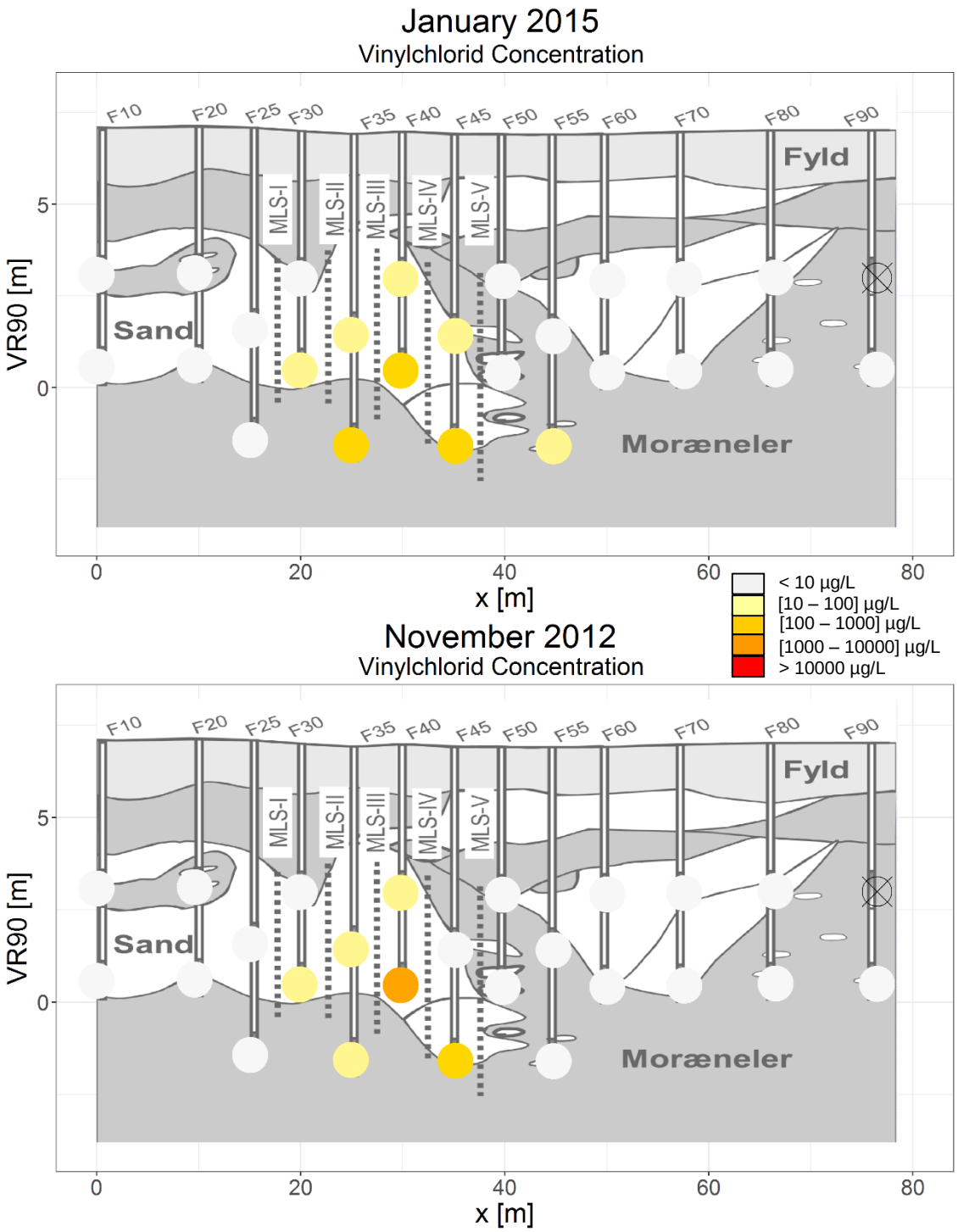
January 2015
Vinylchlorid Concentration
F10
F20
F25
F30
F35
F40
F45
F50
F55
F60
F70
F80
F90
MLS-I
MLS-II
MLS-III
MLS-IV
MLS-V
Fyld
Sand
Moræneler
VR90 [m]
5
0
0
20
40
60
80
x [m]
< 10 µg/L
[10 – 100] µg/L
[100 – 1000] µg/L
[1000 – 10000] µg/L
> 10000 µg/L
November 2012
Vinylchlorid Concentration
F10
F20
F25
F30
F35
F40
F45
F50
F55
F60
F70
F80
F90
MLS-I
MLS-II
MLS-III
MLS-IV
MLS-V
Fyld
Sand
Moræneler
VR90 [m]
5
0
0
20
40
60
80
x [m]

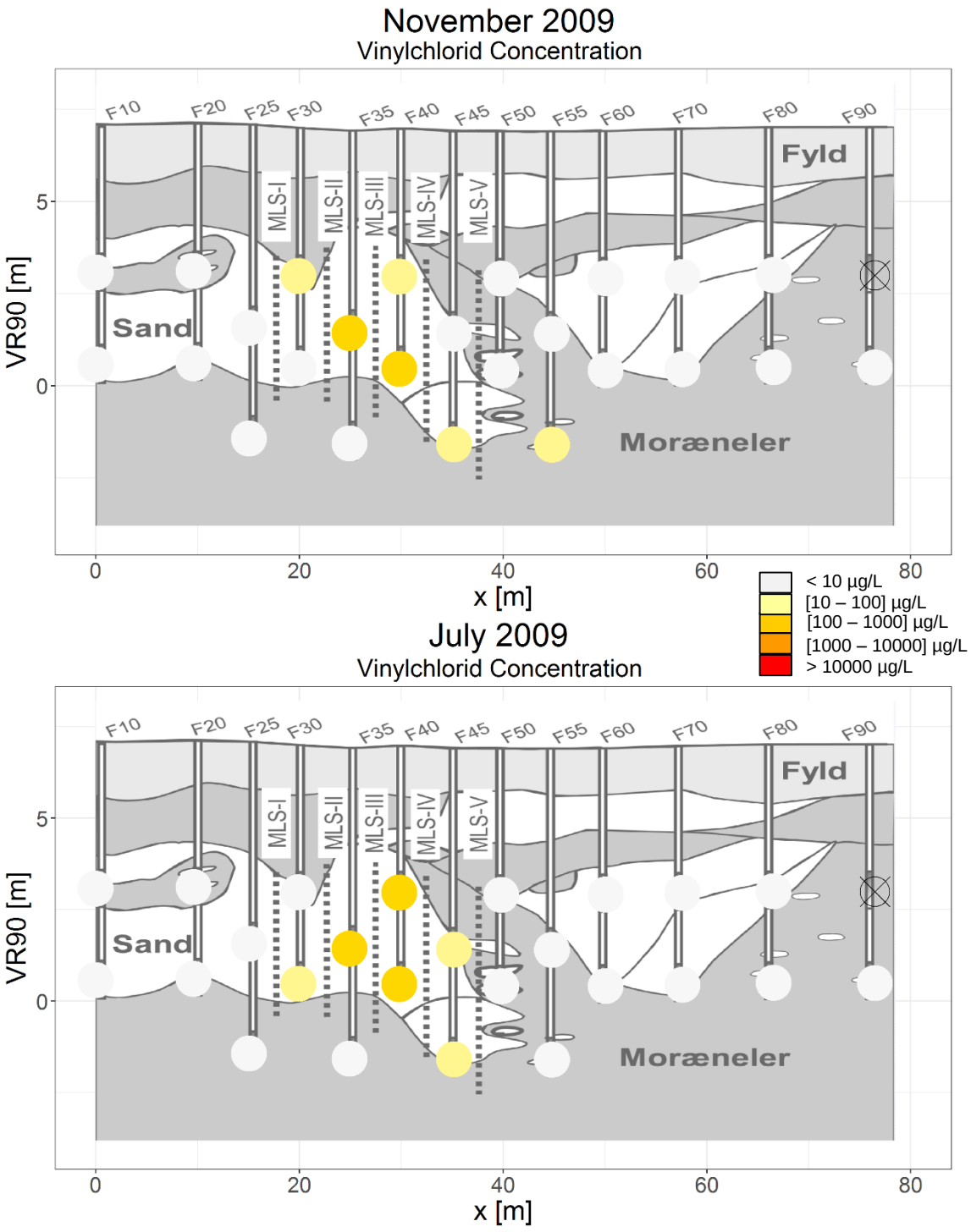
November 2009
Vinylchlorid Concentration
F10
F20
F25
F30
F35
F40
F45
F50
F55
F60
F70
F80
F90
MLS-I
MLS-II
MLS-III
MLS-IV
MLS-V
Fyld
Sand
Moræneler
VR90 [m]
5
0
0
20
40
60
80
x [m]
< 10 µg/L
[10 – 100] µg/L
[100 – 1000] µg/L
[1000 – 10000] µg/L
> 10000 µg/L
July 2009
Vinylchlorid Concentration
F10
F20
F25
F30
F35
F40
F45
F50
F55
F60
F70
F80
F90
MLS-I
MLS-II
MLS-III
MLS-IV
MLS-V
Fyld
Sand
Moræneler
VR90 [m]
5
0
0
20
40
60
80
x [m]

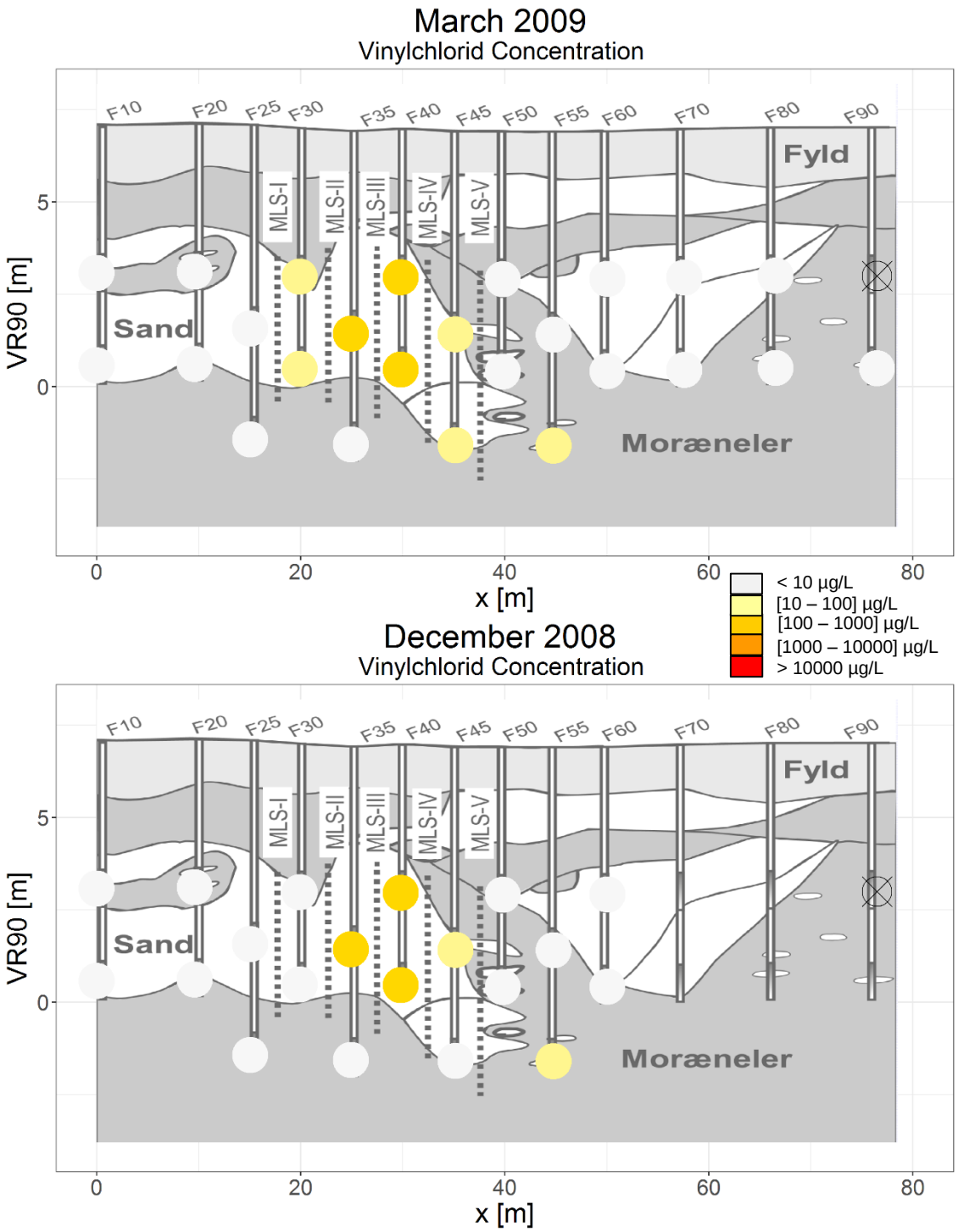
March 2009
Vinylchlorid Concentration
F10
F20
F25
F30
F35
F40
F45
F50
F55
F60
F70
F80
F90
MLS-I
MLS-II
MLS-III
MLS-IV
MLS-V
Fyld
Sand
Moræneler
VR90 [m]
5
0
0
20
40
60
80
x [m]
< 10 µg/L
[10 – 100] µg/L
[100 – 1000] µg/L
[1000 – 10000] µg/L
> 10000 µg/L
December 2008
Vinylchlorid Concentration
F10
F20
F25
F30
F35
F40
F45
F50
F55
F60
F70
F80
F90
MLS-I
MLS-II
MLS-III
MLS-IV
MLS-V
Fyld
Sand
Moræneler
VR90 [m]
5
0
0
20
40
60
80
x [m]

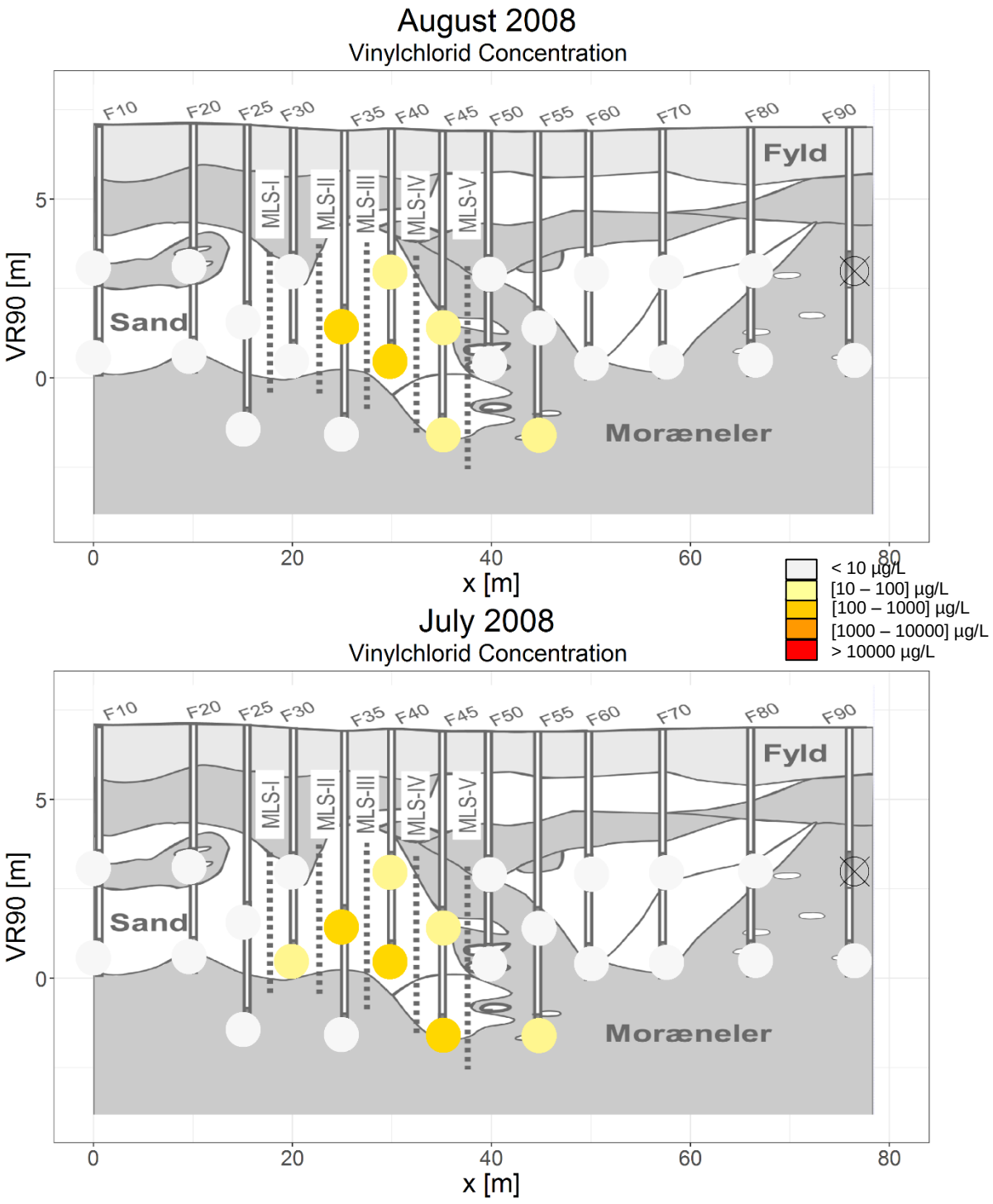
August 2008
Vinylchlorid Concentration
F10
F20
F25
F30
F35
F40
F45
F50
F55
F60
F70
F80
F90
MLS-I
MLS-II
MLS-III
MLS-IV
MLS-V
Fyld
Sand
Moræneler
VR90 [m]
5
0
0
20
40
60
80
x [m]
< 10 µg/L
[10 – 100] µg/L
[100 – 1000] µg/L
[1000 – 10000] µg/L
> 10000 µg/L
July 2008
Vinylchlorid Concentration
F10
F20
F25
F30
F35
F40
F45
F50
F55
F60
F70
F80
F90
MLS-I
MLS-II
MLS-III
MLS-IV
MLS-V
Fyld
Sand
Moræneler
VR90 [m]
5
0
0
20
40
60
80
x [m]

D Visualization of transect and sub surface partitioning: Method 1

D.1. F wells

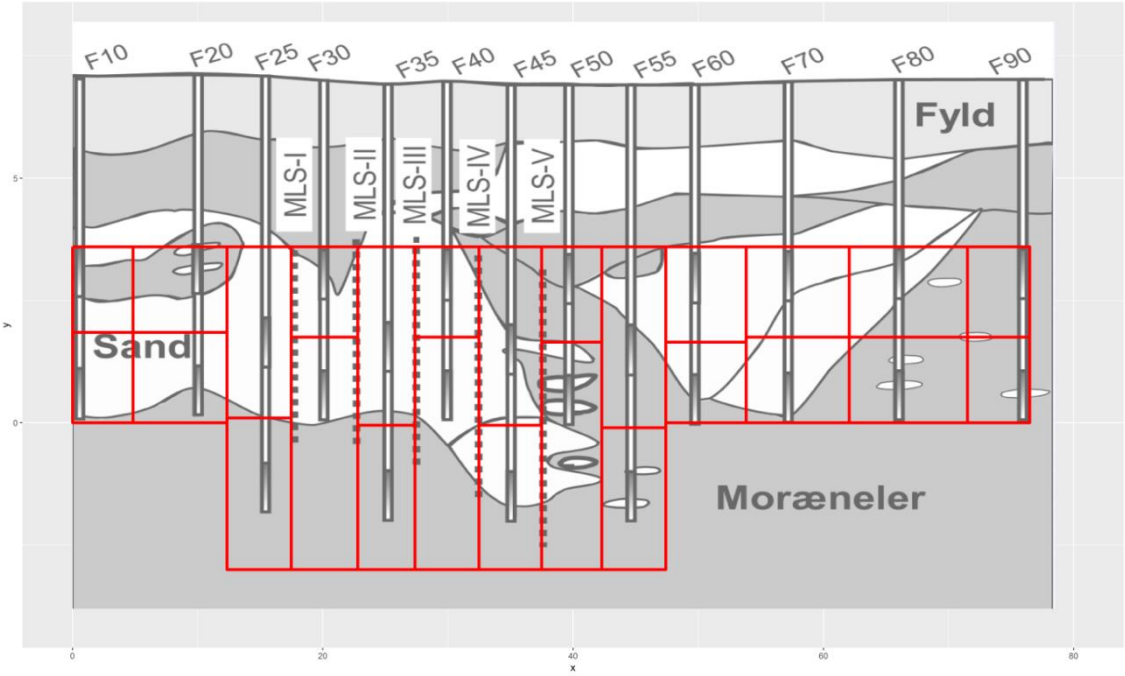

D.2. F+MLS wells

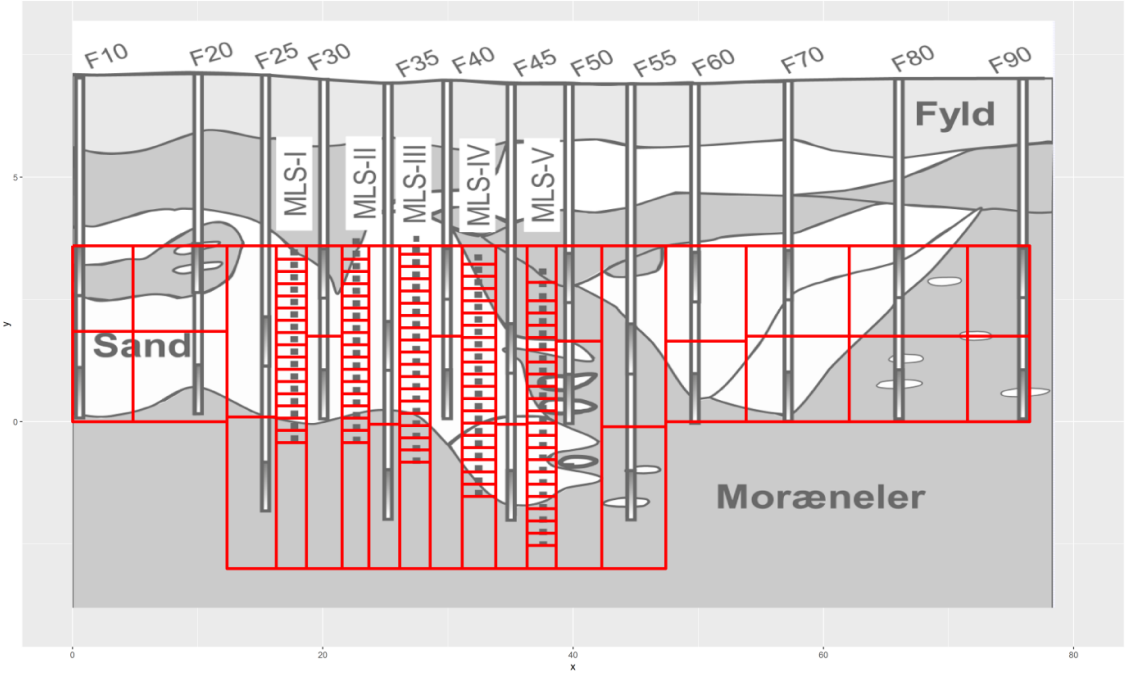

E Calculation assumptions details

The detailed assumptions for the handling of non available data are presented in the Table 13 for the F wells and Table 14 for the MLS lines.

Table 13. Assumption for missing data: F dataset

Date	Well	Assumption
July 2008	F35-2	Based on ratio F35-2/F40-1 in August 2008
	F80-1	Based on ratio F80-2/F80-1 in August 2008
Dec 2008	F55-2	Based on ratio F55-1/F55-2 in March 2009

Table 14. Assumption for missing data: MLS dataset

Date	Well	Assumption
Mar 2009	MLS3-4	Average MLS3-2/ MLS3-5
	MLS4-1	Based on ratio F4-2-1/F4-1 in nov 2009
	MLS5-13	Average MLS5-12/MLS5-14
	MLS5-2	Average MLS5-12/MLS5-14
*Jul 09	MLS1-17	Average MLS1-16/MLS1-18
	MLS2-11	Average MLS2-10/MLS2-12
	MLS2-2	Average MLS2-1/MLS2-3
	MLS3-20	Average MLS3-19/MLS3-21
	MLS4-1	Based on ratio F4-2-1/F4-1 in nov 2009
	MLS5-1	Based on ratio F5-2-1/F5-1 in feb 2016
Sep 2015	MLS2-11	Average MLS2-10/MLS2-12
All periods	MLS1-18 and above	Excluded, mostly above water table
	MLS2-18 and above	Excluded, mostly above water table
	MLS3-22 and above	Excluded, mostly above water table
	MLS4-22 and above	Excluded, mostly above water table
	MLS5-22 and above	Excluded, mostly above water table

F Data interpolation by kriging method: Method 2

The effect of spatial variation of contaminant with respect to the resulting contaminant discharge requires an interpolation of the data measured at discrete locations. Furthermore, it is important that all datasets are treated in a systematic and coherent manner. This task is carried out by use of a kriging method for the dataset of interest. Kriging methods are commonly used in the field geostatistics and environment pollution. The method typically accounts for the spatial correlation between degree and distance weighted average of the discrete data. Review of such methods are not part of the scope here and more details can be found in Oliver and Webster (2015) for example.

The work was carried out by use of R software and the dedicated package *gstats*. For all treated dataset, an ordinary Kriging method is applied. A log transform was carried out prior to variogram estimation to deal with outliers and skewness. A certain degree of anisotropy is expected in the different datasets due to the deposit nature of the different material layers in the soil. Correlation length are expected to be longer in the horizontal direction.

Interpolation of hydraulic conductivity data

Only the dataset found in Lange et al. (2011) was used for the hydraulic conductivity as this latter was providing more data spread over the overall transect. The variogram is presented in Figure 25 with the chosen fitting model: a spherical model was used to fit the dataset, an anisotropy ratio of 0.35 was chosen (principal direction being horizontal), range of 20 m. and silk of 20.

The relevance of the model was assessed by comparison to the measurement and judged as satisfying for the application (Figure 26).

Figure 25. Experimental variogram (dots) and fitting model (line)
Direction 90°: Horizontal direction / 0°:vertical

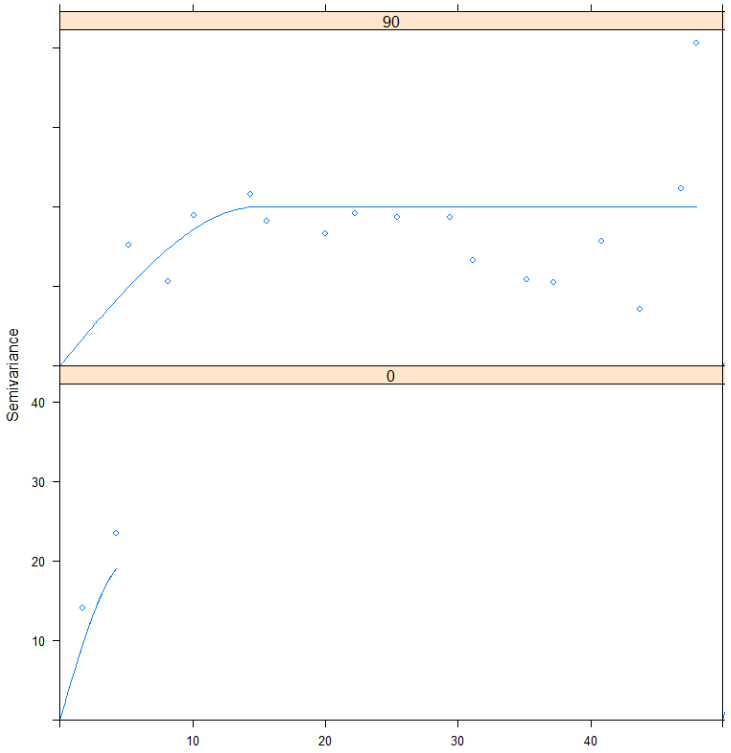

Figure 26. Comparison between interpolated hydraulic conductivity and measurement
Dataset available in Lange. et al. (2011)

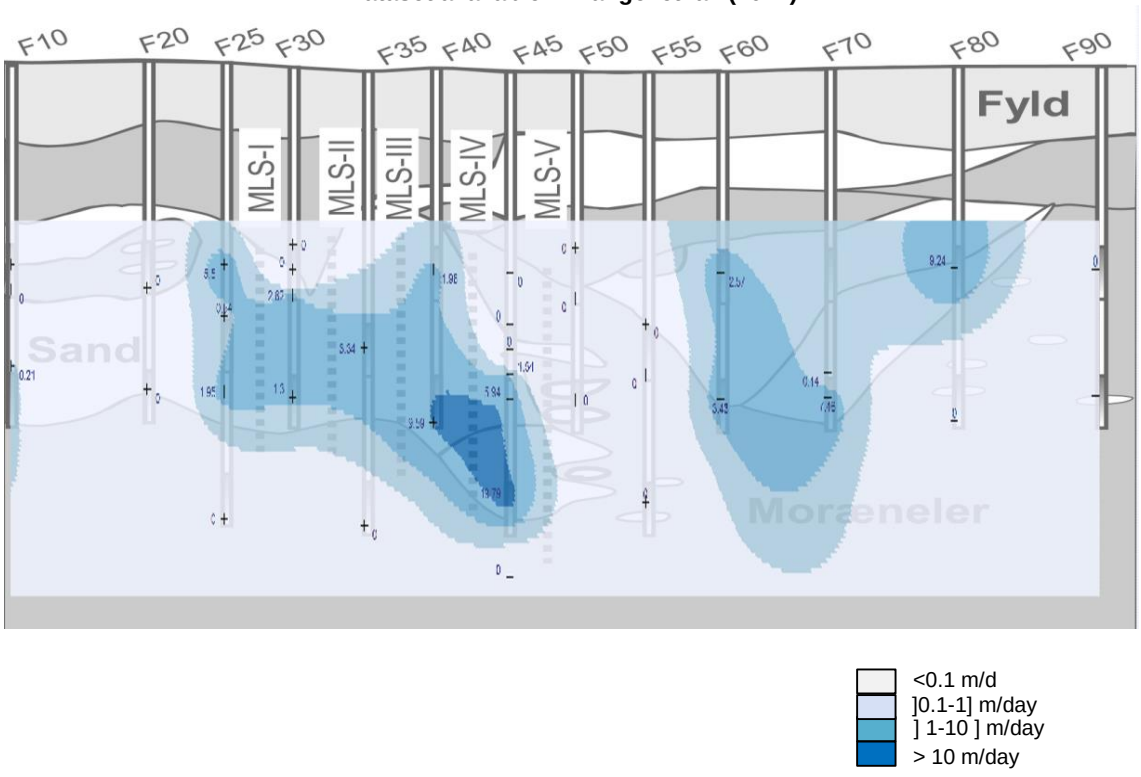

Interpolation of concentration data

Each compound and time step was interpolated separately, as variations were expected to happen due to the modification of spatial distribution (section 5). The variograms for each of the dataset were automatically assessed by use of the geostatistical package under R software and with constraint of constant anisotropic ratio (r=0.35, selected from manual trial). As a boundary condition, the concentration was assumed equal to zero at an elevation of XX m. corresponding roughly to points above water table. Some validation cases are present in the following figures, e.g. PCE eq. with some selected dates and all compounds at one particular measurement period.

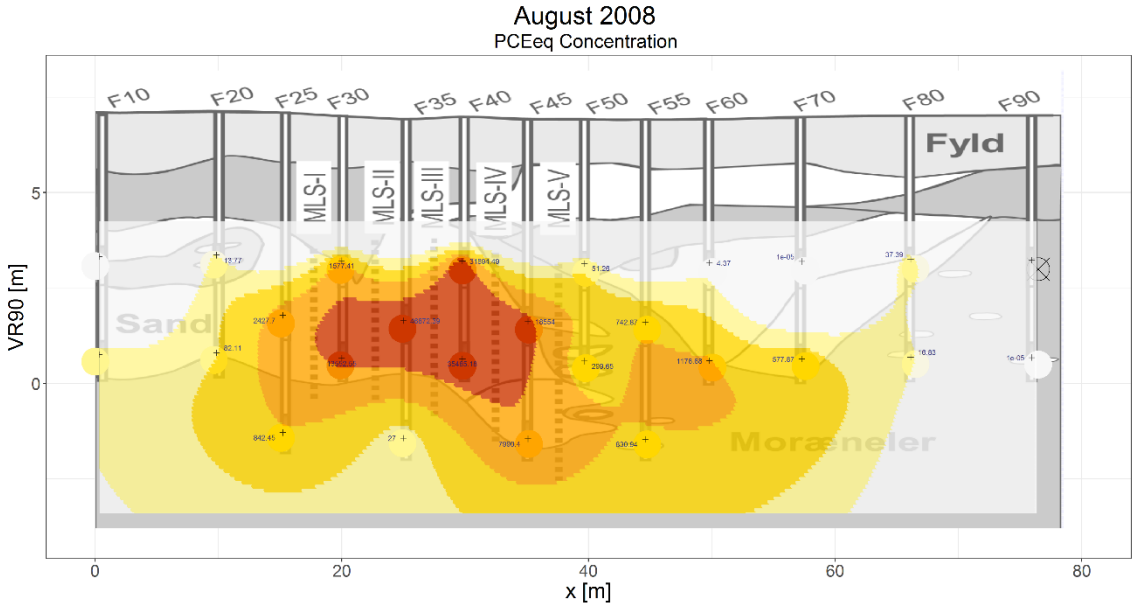

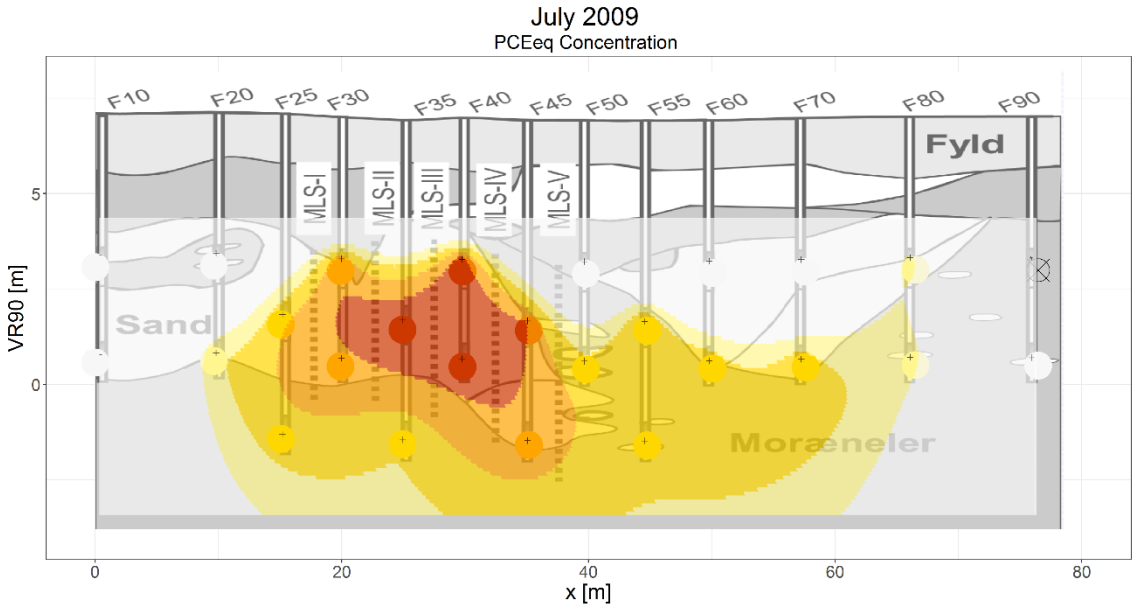

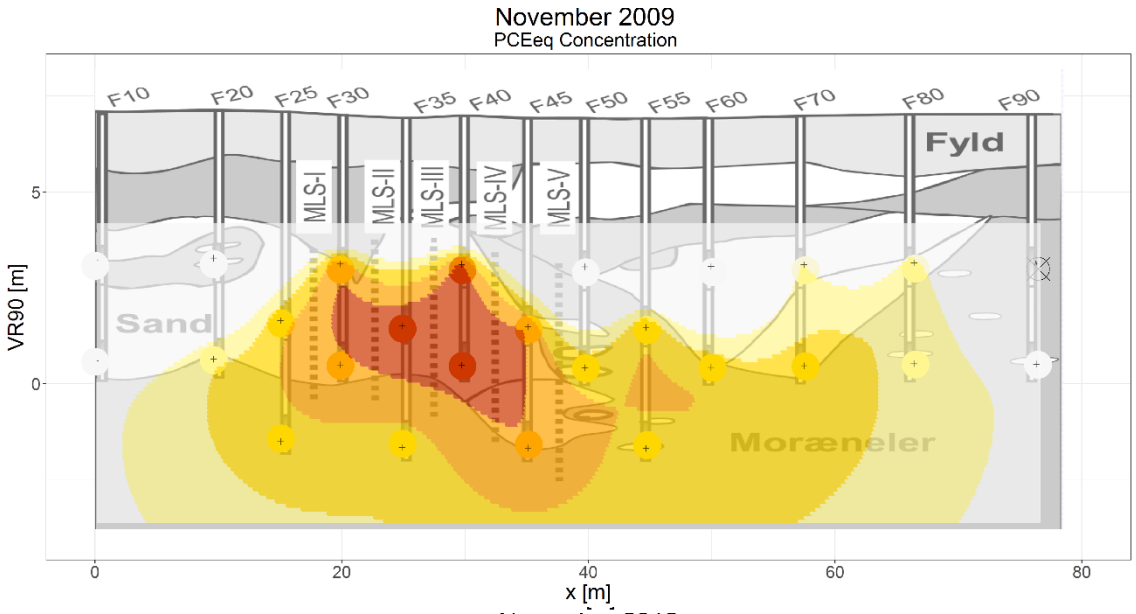
November 2009
PCEeq Concentration
F10
F20
F25
F30
F35
F40
F45
F50
F55
F60
F70
F80
F90
MLS-I
MLS-II
MLS-III
MLS-IV
MLS-V
Fyld
Sand
Moræneler
VR90 [m]
5
0
0
20
40
60
80
x [m]

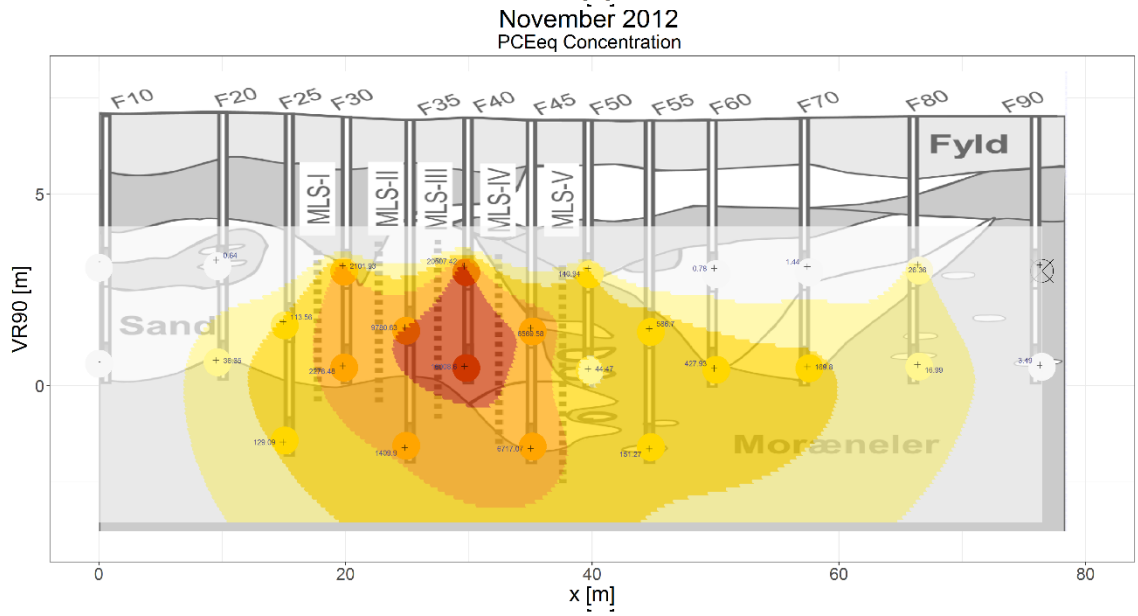
November 2012
PCEeq Concentration
F10
F20
F25
F30
F35
F40
F45
F50
F55
F60
F70
F80
F90
MLS-I
MLS-II
MLS-III
MLS-IV
MLS-V
Fyld
Sand
Moræneler
VR90 [m]
5
0
0
20
40
60
80
x [m]

January 2015
PCEeq Concentration

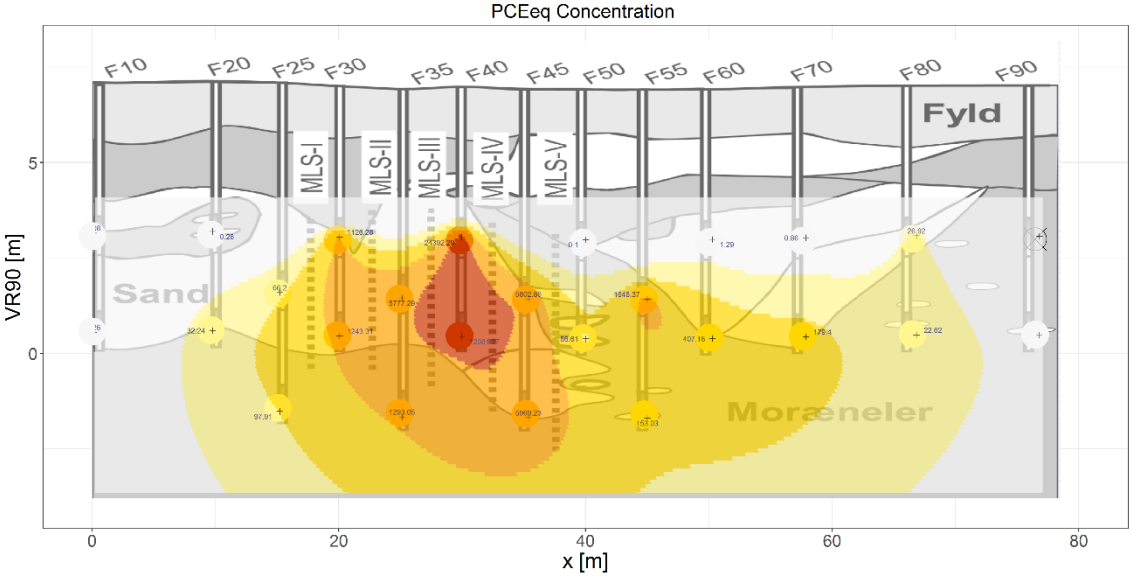

February 2016
PCEeq Concentration

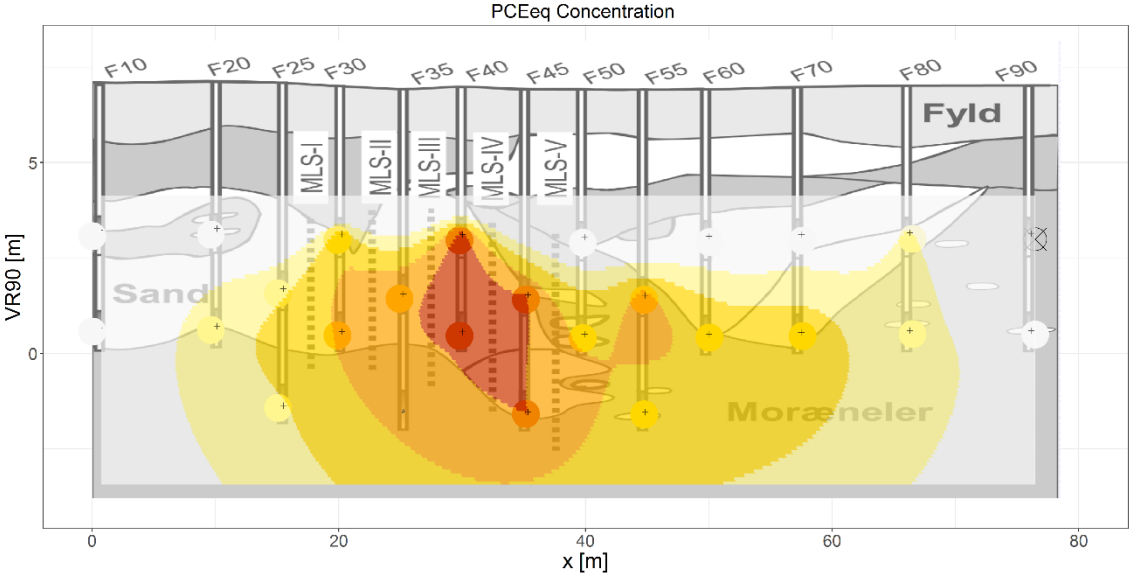

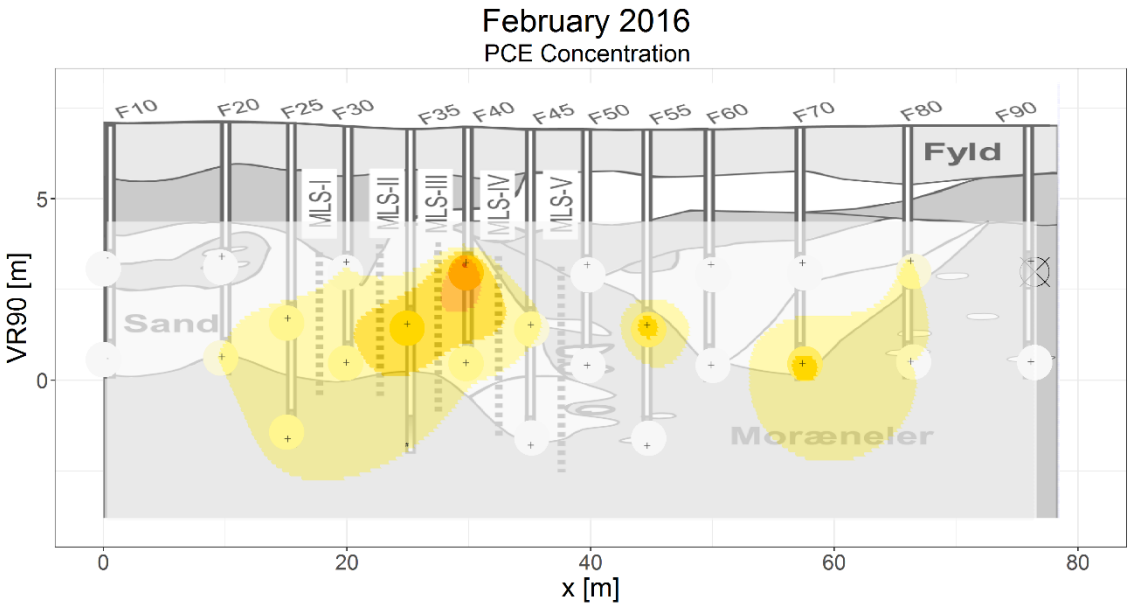
February 2016
PCE Concentration
F10
F20
F25
F30
F35
F40
F45
F50
F55
F60
F70
F80
F90
MLS-I
MLS-II
MLS-III
MLS-IV
MLS-V
Fyld
Sand
Moræneler
VR90 [m]
5
0
0
20
40
60
80
x [m]

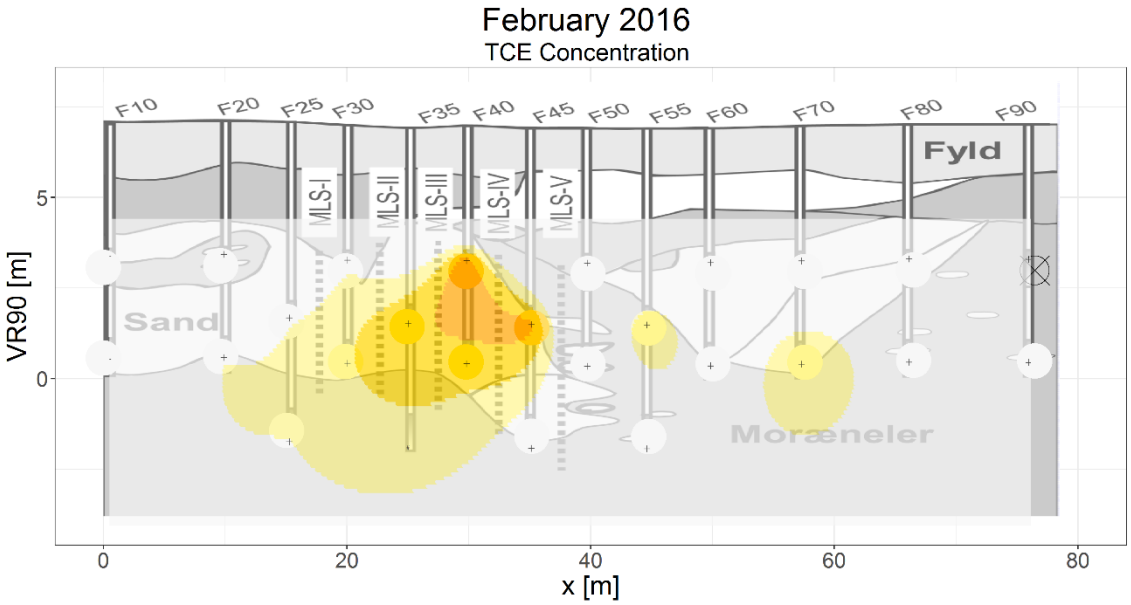
February 2016
TCE Concentration
F10
F20
F25
F30
F35
F40
F45
F50
F55
F60
F70
F80
F90
MLS-I
MLS-II
MLS-III
MLS-IV
MLS-V
Fyld
Sand
Moræneler
VR90 [m]
5
0
0
20
40
60
80
x [m]

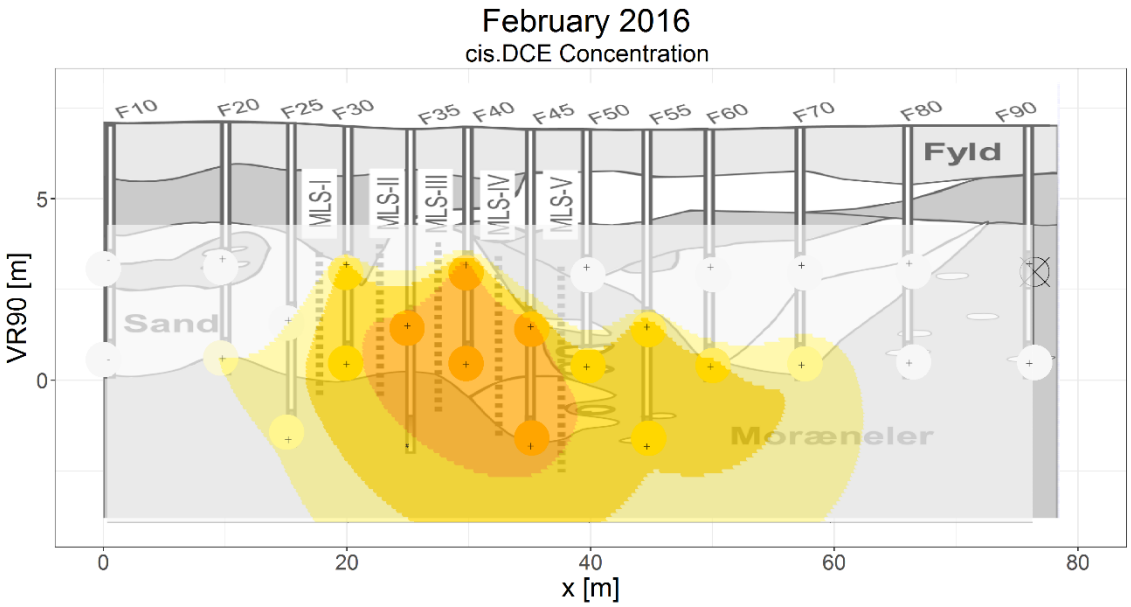
February 2016
cis.DCE Concentration
F10
F20
F25
F30
F35
F40
F45
F50
F55
F60
F70
F80
F90
MLS-I
MLS-II
MLS-III
MLS-IV
MLS-V
Fyld
Sand
Moræneler
VR90 [m]
5
0
0
20
40
60
80
x [m]

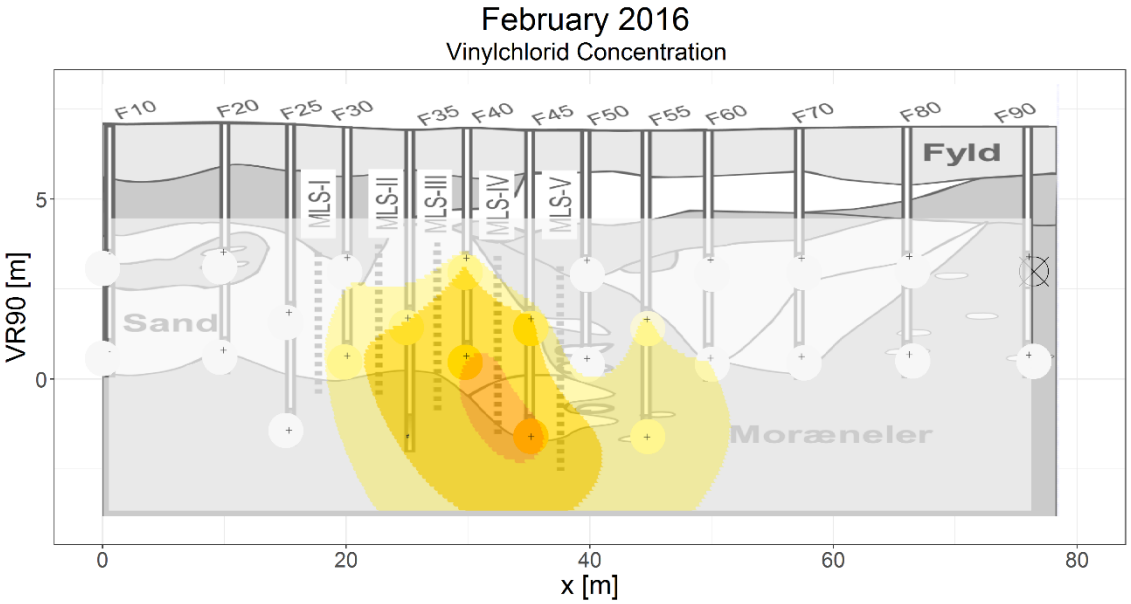
February 2016
Vinylchlorid Concentration
F10
F20
F25
F30
F35
F40
F45
F50
F55
F60
F70
F80
F90
MLS-I
MLS-II
MLS-III
MLS-IV
MLS-V
Fyld
Sand
Moræneler
VR90 [m]
5
0
0
20
40
60
80
x [m]

G Contaminant mass discharge estimation

G.1. Result per compound, method 1

Period	2008			2009			2012	2015		2016
	Jul	Aug	Dec	Mar	Jul	Nov	Nov	Jan	Sep	Feb
PCE [kg/y]	0.80	0.80	0.99	0.94	0.78	0.43	0.21	0.29	0.29	0.26
TCE [kg/y]	0.99	1.29	1.04	1.03	1.07	0.69	0.08	0.15	0.13	0.17
cisDCE [kg/y]	0.99	1.32	1.20	1.18	1.10	1.15	0.82	0.59	0.56	0.61
VC [kg/y]	0.03	0.03	0.02	0.03	0.02	0.02	0.08	0.06	0.1	0.11

Period	2008			2009			2012	2015		2016
	Jul	Aug	Dec	Mar	Jul	Nov	Nov	Jan	Sep	Feb
PCE [kg/y]	/	/	/	0.80	0.71	/	/	/	0.22	0.20
TCE [kg/y]	/	/	/	0.76	0.90	/	/	/	0.10	0.14
cisDCE [kg/y]	/	/	/	1.01	1.04	/	/	/	0.57	0.55
VC [kg/y]	/	/	/	0.02	0.02	/	/	/	0.09	0.09

G.2. Result per compound, method 2 – data interpolation

Period	2008			2009			2012	2015		2016
	Jul	Aug	Dec	Mar	Jul	Nov	Nov	Jan	Sep	Feb
PCE [kg/y]	0.56	0.36	0.48	0.44	0.34	0.15	0.01	0.03	0.01	0.02
TCE [kg/y]	0.72	0.86	0.60	0.58	0.57	0.41	0.02	0.06	0.02	0.05
cisDCE [kg/y]	0.83	1.07	1.02	0.97	1.04	1.16	0.82	0.68	0.56	0.79
VC [kg/y]	0.03	0.02	0.007	0.02	0.02	0.01	0.07	0.06	0.12	0.15

Period	2008			2009			2012	2015		2016
	Jul	Aug	Dec	Mar	Jul	Nov	Nov	Jan	Sep	Feb
PCE [kg/y]	/	/	/	0.99	0.75	/	/	/	0.04	0.05
TCE [kg/y]	/	/	/	0.83	1.02	/	/	/	0.03	0.05
cisDCE [kg/y]	/	/	/	0.83	0.94	/	/	/	0.60	0.54
VC [kg/y]	/	/	/	0.02	0.01	/	/	/	0.12	0.1

H Residence time estimation from hotspot I to edge of source area

The evaluation of the transport time between the hotspot I and the observation wells was carried out using the following methodology:

- The groundwater seepage velocity was estimated between 10 and 20 m/year in the source area (NIRAS, 2016B). A seepage groundwater velocity distribution is constructed using these values. It is assumed the velocities values are normally distributed, with a 95% interval confidence over the given velocity range:
  .

$$v_s = N(\mu = 15, \sigma = 5/1.96)$$

- In order to estimate the retardation factor, values of sorption coefficient are required. The sorption coefficient is estimated based on following formulae:

$$K_d = f_{oc} * K_{oc}$$
With $logK_{oc} = 1.04 * logK_{ow} - 0.84$

The carbon content f_{oc} is evaluated from the measurement performed by Lange. et al. (2011) in the transect. Only the values in the aquifers are considered and assumed to be representative of the carbon content properties of the upper aquifer in the source area as well. A log normal distribution is used to fit the variation of carbon content and estimate a distribution of retardation factor.

$f_{oc} \sim lnN(\mu = -2, \sigma = 0.65)$, distribution fit to data f_{oc}
and $R = 1 + f_{oc} * K_{oc} * \rho_b/\epsilon$

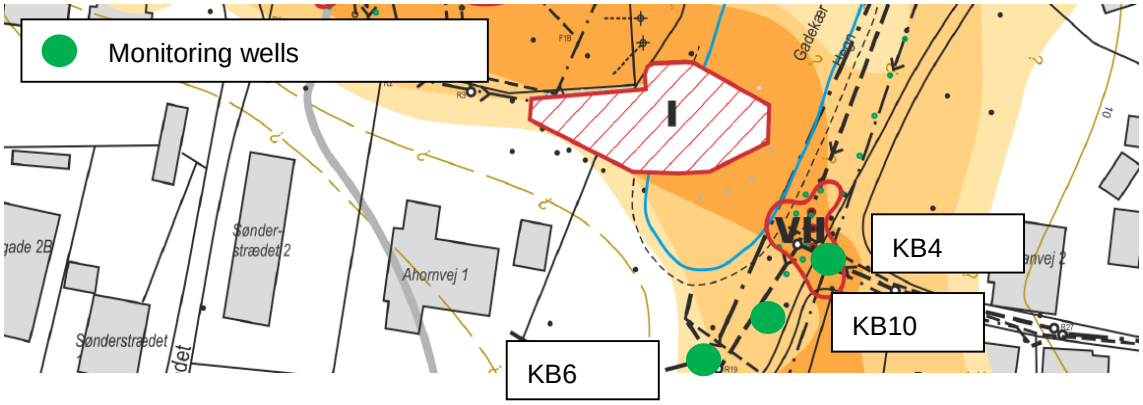

- The distance between hotspot I and the observation wells varies between approximately 10 and 30 m depending on which extremity of the hotspot is considered.

- A Monte Carlo simulation (n=10000 events) is run using the velocity distribution, a uniform range of distance to estimate the transportation time, and the distribution of retardation factor as expressed below:

$$t = \frac{dist}{(v_s/R)} \text{ with } dist = U(10,20)$$

- Histogram of time distribution is presented below in F for PCE and the degradation compounds, as well as the corresponding cumulative density function

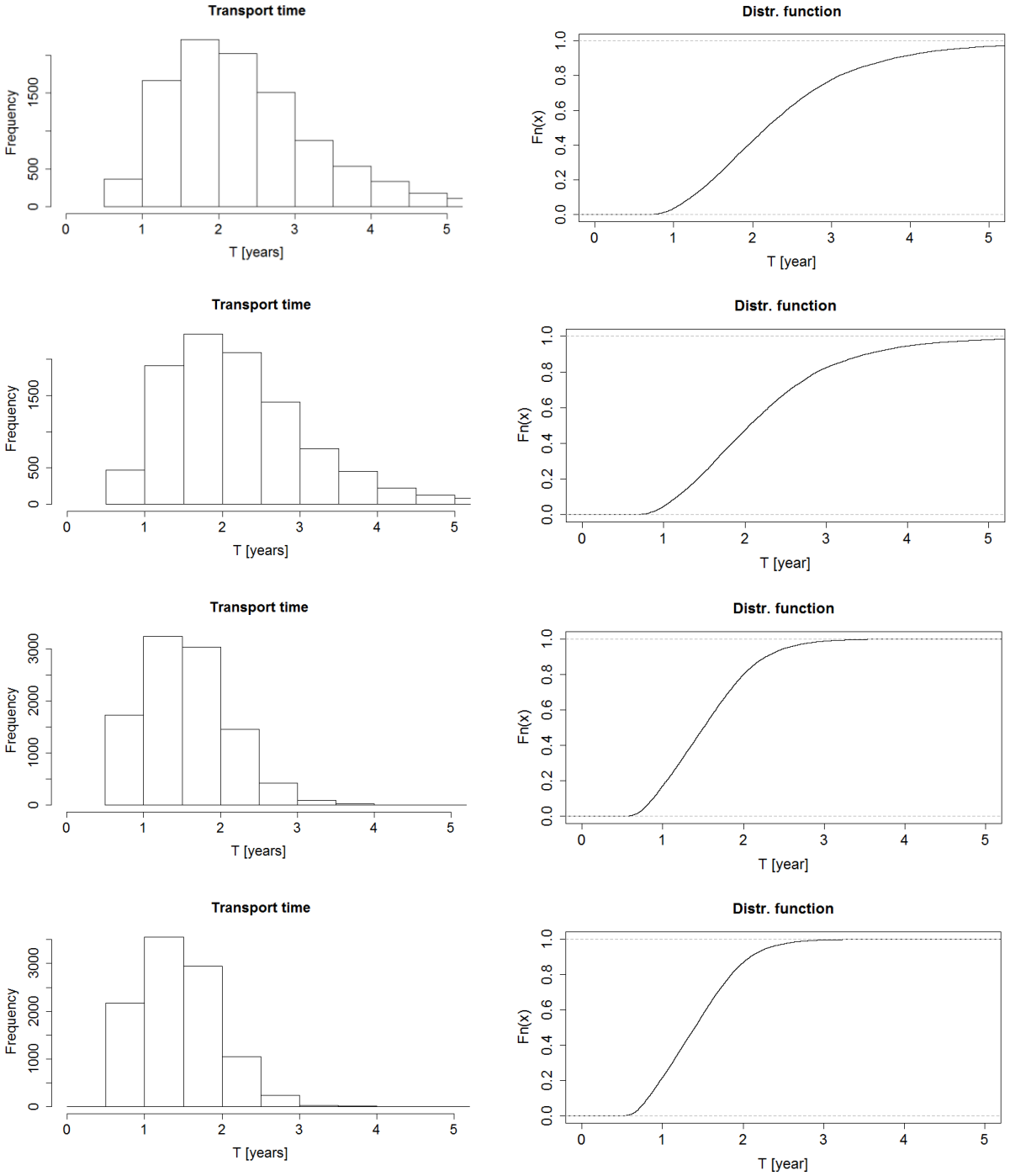

Figure 27. Evaluation of Transport time between observation wells and hotspot I
Result from Monte Carlo simulation (n=10000) and cumulative distribution function
From top to bottom: PCE/TCE/cisCE/VC

The average transportation time is approximately 1.4 years. 95% of all estimated transportation time lies in the interval [0.65-2.4] years (2.5 and 97.5% quantile values) for PCE.

I Transport time estimation from hotspot I to transect

A procedure similar to the one performed in Appendix H is carried out to get an estimate of the residence time between hotspot I and the Østergade transect.

- The groundwater seepage velocity was estimated from the PVP measurement performed in the transect (NIRAS, 2016a). A seepage groundwater velocity distribution is constructed using these values and a distribution fitting based on maximum likelihood estimation.

  .

- Retardation factor is estimated as previously done in Appendix I, i.e. from a distribution estimate of organic carbon content and sorption coefficient assessment.

- Distance from the hotspot I to the transect ranges from 70 to 100 m, depending on the point considered in the hotspot.

$$dist = U(70{,}100)$$

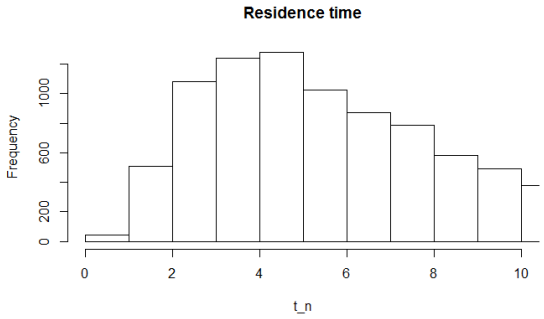

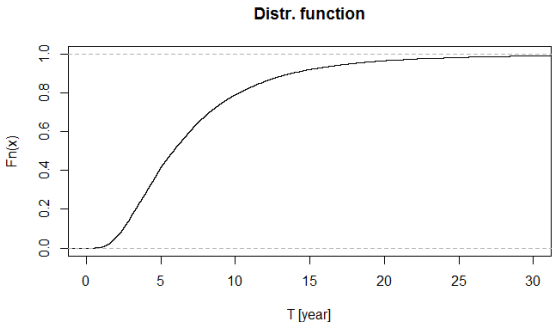

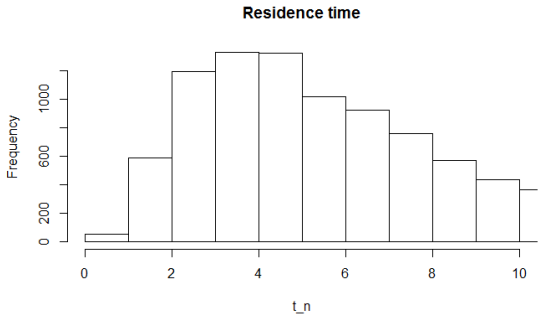

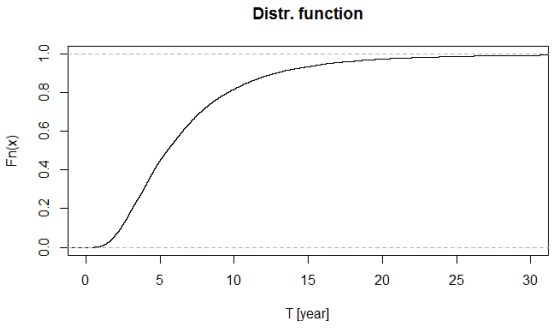

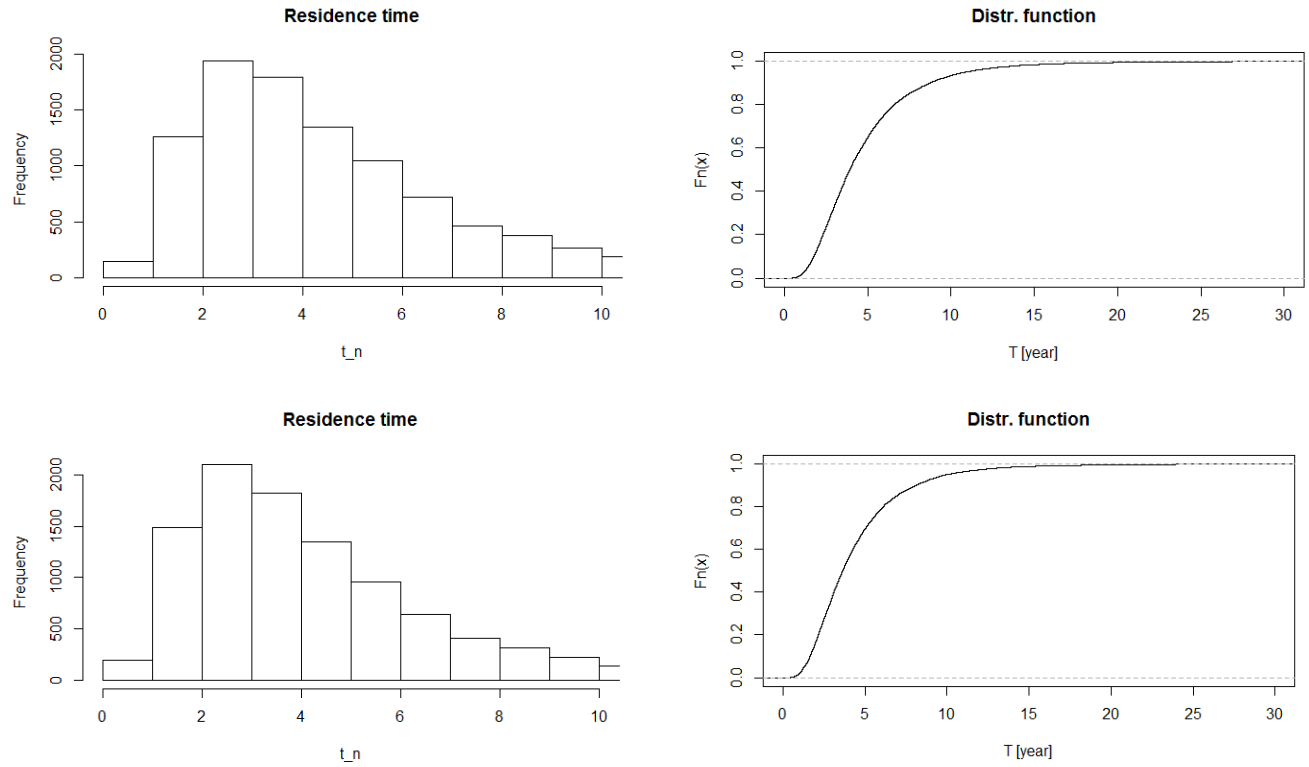

Evaluation of Transport time between Østergade transect and hotspot I
Result from Monte Carlo simulation (n=10000) and cumulative distribution function
From top to bottom: PCE/TCE/cisCE/VC

Table 19. Basic statistical quantities for the MC simulation and the evaluation of transport time between Østergade transect and hotspot I (expressed in years).

	Average	5% quantile	50% quantile	95% quantile
PCE	7.3	1.9	5.8	17.5
TCE	6.8	1.8	5.4	16.2
cisDCE	4.7	1.4	3.9	10.8
VC	4.4	1.3	3.6	9.9